



Agenzia Nazionale per le Nuove Tecnologie,
l'Energia e lo Sviluppo Economico Sostenibile



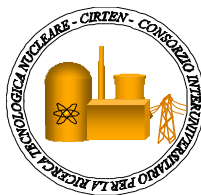
Ministero dello Sviluppo Economico

RICERCA DI SISTEMA ELETTRICO

SIET 01 572 ST09

Two-phase flow measurement for SPES3 facility: spool piece mathematical correlations

A. Achilli, M. Greco



TWO-PHASE FLOW MEASUREMENT FOR SPES3 FACILITY: SPOOL PIECE MATHEMATICAL
CORRELATIONS

A. Achilli, M. Greco

Settembre 2010

Report Ricerca di Sistema Elettrico

Accordo di Programma Ministero dello Sviluppo Economico – ENEA

Area: Produzione e fonti energetiche

Tema: Nuovo Nucleare da Fissione

Responsabile Tema: Stefano Monti, ENEA

Titolo

**Two-phase flow measurement for SPES3 facility:
Spool piece mathematical correlations**

Ente emittente: SIET

PAGINA DI GUARDIA

Descrittori

Tipologia del documento: Rapporto tecnico/Technical Report
Collocazione contrattuale: Accordo di programma ENEA-MSE: tema di ricerca "Nuovo nucleare da fissione"
Argomenti trattati: Reattori ad acqua leggera/Light Water Reactors

Sommario

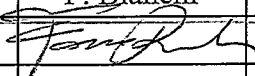
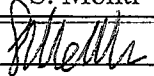
This report has been issued in the frame of the second research programme of the ENEA and MSE (Economic Development Ministry) agreement and it is one of the deliverables of the Task C "IRIS integral testing – special instrumentation selection" of the work-programme 2 "Evolutionary INTD (International Near Term Deployment) Reactors" of the research theme on "Nuovo Nucleare da Fissione"

The document deals with the activity performed at theoretical level for identifying spool pieces consisting of two or three instrument to be used in the SPES3 facility for the measurement of two-phase mass flow rate or other important thermal-hydraulic parameters, as quality, gas and liquid velocities.

Note

Copia n.

In carico a:

2			NOME			
			FIRMA			
1			NOME			
			FIRMA			
0	EMISSIONE	28/09/2010	NOME	F. Bianchi		S. Monti
			FIRMA			
REV.	DESCRIZIONE	DATA		CONVALIDA	VISTO	APPROVAZIONE



Società Informazioni Esperienze Termoidrauliche
Via Nino Bixio, 27 - 29100 Piacenza (I)

EMITTENTE
issued by
Unità di Produzione
Production Unit

CLIENTE: ENEA
Client :

COMMESSA: 1PN000CA90245
job:

DISCO: CA90245/1
disk:

PAGINA: 1 **DI:** 127
page: of

IDENTIFICATIVO: 01 572 RT 09
document:

Classe Ris.:
Confidential:



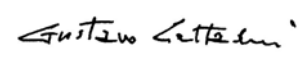
ALLEGATI:
Enclosures:

TITOLO: TWO-PHASE FLOW MEASUREMENT FOR SPES3 FACILITY:
Title: **SPOOL PIECE MATHEMATICAL CORRELATIONS**

REDATTORI: A. Achilli, M. Greco
prepared by:

LISTA DI DISTRIBUZIONE
distribution list

ENEA	Renato Tinti
ENEA	Fosco Bianchi
SIET S.p.A.	Andrea Achilli
SIET S.p.A.	Gustavo Cattadori
SIET S.p.A.	Stefano Gandolfi
SIET S.p.A.	Matteo Greco
SIET S.p.A.	Roberta Ferri
SIET S.p.A.	Gaetano Tortora
SIET S.p.A.	Cinzia Congiu

Rev.0	14/07/2010	Emissione	A. Achilli  M. Greco 	G.Cattadori 
REV. Rev.	DATA date	DESCRIZIONE description	REDAZIONE prepared by	APPROVAZIONE approved by

Informazioni strettamente riservate di proprietà SIET SpA - Da non utilizzare per scopi diversi da quelli per cui sono state fornite.
Confidential information property of SIET SpA - Not to be used for any purpose other than those for which it is supplied.

CONTENTS

LIST OF TABLES.....	5
LIST OF FIGURES	8
LIST OF ACRONYMS.....	12
1 SCOPE.....	13
2 INTRODUCTION.....	14
3 BREAK POSITIONS	16
4 ANALYTICAL EXPRESSIONS OF THE SPOOL PIECE	27
4.1 Drag Disk flowmeter (DD)	27
4.2 Turbine Flowmeter (T).....	29
4.2.1 Rouhani model	30
4.2.2 Aya model	31
4.2.3 Volumetric model.....	32
4.3 Void Fraction Detector (Void).....	32
4.4 Venturi meter.....	33
5 Mathematical models	35
5.1 Drag Disk and Void Fraction Detector.....	46
5.2 Drag Disk and Turbine Flowmeter.....	50
5.2.1 Rouhani model	50
5.2.2 Aya Model	51
5.2.3 Volumetric Model.....	52
5.3 Void Fraction Detector and Turbine Flowmeter.....	54
5.3.1 Rouhani Model	54
5.3.2 Aya Model	55
5.3.3 Volumetric Model.....	57
5.4 Preliminary analytical considerations	58
5.5 Synthesis on the analytical models	62
6 MASS FLOW RATE DATA REDUCTION FOR SPECIFIED TRANSIENTS.....	63
6.1 Determination of the mass flow rate with two instruments	63
6.1.1 DVI TEST	64
6.1.1.1 DVI SPLIT break line.....	64
6.1.1.2 ADS Stage-I ST.....	70
6.1.1.3 ADS Stage-I DT.....	74
6.1.2 EBT TEST	78
6.1.2.1 EBT SPLIT break line.....	78

6.1.2.2	ADS Stage-I ST	82
6.1.2.3	ADS Stage-I DT	85
6.1.3	ADS TEST	88
6.1.3.1	ADS SPLIT break line	88
6.1.3.2	ADS Stage-I DT	92
6.1.4	Synthesis on two instrument spool piece	96
6.2	Determination of the mass flow rate with three instruments	97
6.2.1	Rouhani model	97
6.2.2	Aya Model	99
6.2.3	Volumetric model	100
6.2.4	Synthesis on three instrument spool piece	101
7	HOMOGENEOUS MODEL	102
7.1	DVI break test	104
7.1.1	DVI SPLIT break line	104
7.1.2	ADS Stage-I ST line	105
7.2	EBT break test	106
7.2.1	EBT SPLIT break line	106
7.3	Synthesis on the homogeneous model	107
8	TWIN VENTURI METER	108
9	CONCLUSIONS	126

LIST OF TABLES

Table 3.1: Base cases for the SPES3 break transients	16
Table 3.2: Positions of the spool piece to measure two-phase flow in SPES3	17
Table 3.3: DVI SPLIT break line – Thermal-hydraulic variables and flow regimes	17
Table 3.5: EBT SPLIT break line – Thermal-hydraulic variables and flow regimes	18
Table 3.6: ADS Stage-I ST SPLIT break line – Thermal-hydraulic variables and flow regimes.....	18
Table 3.7: ADS Stage-I ST line – Thermal-hydraulic variables and flow regimes.....	18
Table 3.8: ADS Stage-I line DT– Thermal-hydraulic variables and flow regimes	19
Table 3.9: DVI SPLIT break line – geometrical dimensions and nodalization volumes	20
Table 3.10: EBT SPLIT break line – geometrical dimensions and nodalization volumes	20
Table 3.12: ADS Stage-I ST SPLIT break line – geometrical dimensions and nodalization volumes	20
Table 3.13: ADS Stage-I ST line – geometrical dimensions and nodalization volumes.....	21
Table 3.15: ADS Stage-I DT line – geometrical dimensions and nodalization volumes	21
Table 3.16: List of the involved lines and spool pieces for each test.....	26
Table 4.1: Minimum and maximum values of the momentum flux.....	29
Table 4.2: Minimum and maximum values of the mixture velocity theoretically measured by a Turbine Flowmeter (T) – ROUHANI MODEL – in each line for each test.	30
Table 4.3: Minimum and maximum values of the mixture velocity theoretically measured by a Turbine Flowmeter (T) – AYA MODEL – in each line for each test.....	31
Table 4.4: Minimum and maximum values of the mixture velocity theoretically measured by a Turbine Flowmeter (T) – VOLUMETRIC MODEL – in each line for each test.	32
Table 5.1: List of the conventional numbers used in the graphs to indicate whether the flow is critical or not and the flow regimes	40
Table 5.2: Reference conditions for the preliminary calculation of the mass flow rate	58
Table 5.3: Errors per cent vs pressure and slip ratio change for various instrument couplings.....	59
Table 5.4: Best and worst couplings with different slip ratios and qualities	62
Table 6.1: Errors per cent between the RELAP5 mass flow and the Spool Piece mass flow - Rouhani model - DVI SPLIT line, DVI break test	64
Table 6.2: Errors per cent between the RELAP5 mass flow and the Spool Piece mass flow - Aya model - DVI SPLIT line, DVI break test.....	66
Table 6.3: Errors per cent between the RELAP5 mass flow and the Spool Piece mass flow - Volumetric model - DVI SPLIT line, DVI break test.....	68
Table 6.4: Errors per cent between the RELAP5 mass flow and the Spool Piece mass flow - Rouhani model - ADS Stage-I ST line, DVI break test.....	70

Table 6.5: Errors per cent between the RELAP5 mass flow and the Spool Piece mass flow - Aya model - ADS Stage-I ST line, DVI break test	72
Table 6.6: Errors per cent between the RELAP5 mass flow and the Spool Piece mass flow - Volumetric model - ADS ST (stage I) line, DVI break test	73
Table 6.7: Errors per cent between the RELAP5 mass flow and the Spool Piece mass flow - Rouhani model - ADS DT (stage I) line, DVI break test.....	74
Table 6.8: Errors per cent between the RELAP5 mass flow and the Spool Piece mass flow - Aya model - ADS Stage-I DT line, DVI break test.....	76
Table 6.9: Errors per cent between the RELAP5 mass flow and the Spool Piece mass flow - Volumetric model - ADS Stage-I DT line, DVI break test.....	77
Table 6.10: Errors per cent between the RELAP5 mass flow and the Spool Piece mass flow - Rouhani model - EBT SPLIT line, EBT break test	78
Table 6.11: Errors per cent between the RELAP5 mass flow and the Spool Piece mass flow - Aya model - EBT SPLIT line, EBT break test.....	80
Table 6.12: Errors per cent between the RELAP5 mass flow and the Spool Piece mass flow - Volumetric model - EBT SPLIT line, EBT break test.....	81
Table 6.13: Errors per cent between the RELAP5 mass flow and the Spool Piece mass flow - Rouhani model - ADS Stage-I ST line, EBT break test.....	82
Table 6.14: Errors per cent between the RELAP5 mass flow and the Spool Piece mass flow - Aya model - ADS Stage-I ST line, EBT break test	83
Table 6.15: Errors per cent between the RELAP5 mass flow and the Spool Piece mass flow - Volumetric model - ADS ST (stage I) line, EBT break test	84
Table 6.16: Errors per cent between the RELAP5 mass flow and the Spool Piece mass flow - Rouhani model - ADS Stage-I DT line, EBT break test	85
Table 6.17: Errors per cent between the RELAP5 mass flow and the Spool Piece mass flow - Aya model - ADS Stage-I DT line, EBT break test	86
Table 6.18: Errors per cent between the RELAP5 mass flow and the Spool Piece mass flow - Volumetric model - ADS Stage-I DT line, EBT break test.....	87
Table 6.19: Errors per cent between the RELAP5 mass flow and the Spool Piece mass flow - Rouhani model - ADS SPLIT line, ADS break test	88
Table 6.20: Errors per cent between the RELAP5 mass flow and the Spool Piece mass flow - Aya model - ADS SPLIT line, ADS break test.....	90
Table 6.21: Errors per cent between the RELAP5 mass flow and the Spool Piece mass flow - Volumetric model - ADS SPLIT line, ADS break test.....	91
Table 6.22: Errors per cent between the RELAP5 mass flow and the Spool Piece mass flow - Rouhani model - ADS Stage-I DT line, ADS break test.....	92

Table 6.23: Errors per cent between the RELAP5 mass flow and the Spool Piece mass flow - Aya model – ADS Stage-I DT line, ADS break test.....	94
Table 6.24: Errors per cent between the RELAP5 mass flow and the Spool Piece mass flow - Volumetric model - ADS Stage-I DT line, ADS break test	95
Table 8.1: List of variables derived by [4] upstream and downstream of the break.....	108
Table 8.2: Different case analysed for the determination of the relationships between the density ratio and the other thermal-hydraulic variables	112

LIST OF FIGURES

Figure 3.1: SPES3 DVI-B break line nodalization	22
Figure 3.2: SPES3 EBT-B break line nodalization	23
Figure 3.3: SPES3 ADS ST and ADS Stage-I ST break line nodalization (top view)	24
Figure 3.4: SPES3 ADS Stage-I DT nodalization (top view).....	25
Figure 5.1: Comparison between the RELAP5 and theoretical mass flow, void fraction and quality in DVI SPLIT break line, DVI Test.....	36
Figure 5.2: Comparison between the RELAP5 and theoretical mass flow, void fraction and quality in ADS Stage-I ST line, DVI Test	36
Figure 5.3: Comparison between the RELAP5 and theoretical mass flow, void fraction and quality in ADS Stage-I DT line, DVI Test.....	37
Figure 5.4: Comparison between the RELAP5 and theoretical mass flow, void fraction and quality in EBT SPLIT break line, EBT Test.....	37
Figure 5.5: Comparison between the RELAP5 and theoretical mass flow, void fraction and quality in ADS Stage-I ST line, EBT Test	38
Figure 5.6: Comparison between the RELAP5 and theoretical mass flow, void fraction and quality in ADS Stage-I DT line, EBT Test.....	38
Figure 5.7: Comparison between the RELAP5 and theoretical mass flow, void fraction and quality in ADS SPLIT break line, ADS Test.....	39
Figure 5.8: Comparison between the RELAP5 and theoretical mass flow, void fraction and quality in ADS Stage-I DT line, ADS Test	39
Figure 5.9: Comparison between the RELAP5 and theoretical mass flow, flow regimes and presence of critical flow in DVI SPLIT beak line, DVI Test	40
Figure 5.10: Comparison between the RELAP5 and theoretical mass flow, flow regimes and presence of critical flow in ADS ST stage I line, DVI Test	41
Figure 5.11: Comparison between the RELAP5 and theoretical mass flow, flow regimes and presence of critical flow in ADS DT stage I line, DVI Test	41
Figure 5.12: Comparison between the RELAP5 and theoretical mass flow, flow regimes and presence of critical flow in EBT SPLIT beak line, EBT Test	42
Figure 5.13: Comparison between the RELAP5 and theoretical mass flow, flow regimes and presence of critical flow in ADS Stage-I ST line, EBT Test.....	42
Figure 5.14: Comparison between the RELAP5 and theoretical mass flow, flow regimes and presence of critical flow in ADS Stage-I DT line, EBT Test	43
Figure 5.15: Comparison between the RELAP5 and theoretical mass flow, flow regimes and presence of critical flow in ADS SPLIT beak line, ADS Test.....	43

Figure 5.16: Comparison between the RELAP5 and theoretical mass flow, flow regimes and presence of critical flow in ADS Stage-I DT line, ADS Test	44
Figure 5.17: Comparison between the mass flow rate obtained by the coupling of two instruments (DD + Void) and the RELAP5 mass flow rate in the DVI SPLIT line, DVI break test	48
Figure 5.18: Errors per cent function of the slip ratio at 7 bars with quality set to 0.7.....	60
Figure 5.19: Errors per cent function of the slip ratio at 7 bars with quality set to 0.97.....	61
Figure 5.20: Errors per cent function of the slip ratio at 7 bars with quality set to 0.997.....	61
Figure 6.1: Comparison between the RELAP5 mass flow and the Spool Piece mass flow - Rouhani model -DVI SPLIT line, DVI break test.....	64
Figure 6.2: Comparison between the RELAP5 mass flow and the Spool Piece mass flow - Aya model - DVI SPLIT line, DVI break test.....	66
Figure 6.3: Comparison between the RELAP5 mass flow and the Spool Piece mass flow - Volumetric model - DVI SPLIT line, DVI break test.....	68
Figure 6.4: Comparison between the RELAP5 mass flow and the Spool Piece mass flow - Rouhani model - ADS Stage-I ST line, DVI break test	70
Figure 6.5: Comparison between the RELAP5 mass flow and the Spool Piece mass flow - Aya model - ADS Stage-I ST line, DVI break test	72
Figure 6.6: Comparison between the RELAP5 mass flow and the Spool Piece mass flow - Volumetric model - ADS Stage-I ST line, DVI break test	73
Figure 6.7: Comparison between the RELAP5 mass flow and the Spool Piece mass flow - Rouhani model - ADS Stage-I DT line, DVI break test.....	74
Figure 6.8: Comparison between the RELAP5 mass flow and the Spool Piece mass flow - Aya model - ADS DT (stage I) line, DVI break test	76
Figure 6.9: Comparison between the RELAP5 mass flow and the Spool Piece mass flow - Volumetric model - ADS Stage-I DT line, DVI break test.....	77
Figure 6.10: Comparison between the RELAP5 mass flow and the Spool Piece mass flow - Rouhani model - EBT SPLIT line, EBT break test	79
Figure 6.11: Comparison between the RELAP5 mass flow and the Spool Piece mass flow - Aya model - EBT SPLIT line, EBT break test.....	80
Figure 6.12: Comparison between the RELAP5 mass flow and the Spool Piece mass flow - Volumetric model - EBT SPLIT line, EBT break test.....	81
Figure 6.13: Comparison between the RELAP5 mass flow and the Spool Piece mass flow - Rouhani model - ADS Stage-I ST line, EBT break test.....	82
Figure 6.14: Comparison between the RELAP5 mass flow and the Spool Piece mass flow - Aya model – ADS Stage-I ST line, EBT break test	83
Figure 6.15: Comparison between the RELAP5 mass flow and the Spool Piece mass flow - Volumetric model - ADS Stage-I ST line, EBT break test	84

Figure 6.16: Comparison between the RELAP5 mass flow and the Spool Piece mass flow - Rouhani model - ADS Stage-I DT line, EBT break test	85
Figure 6.17: Comparison between the RELAP5 mass flow and the Spool Piece mass flow - Aya model – ADS Stage-I DT line, EBT break test	86
Figure 6.18: Comparison between the RELAP5 mass flow and the Spool Piece mass flow - Volumetric model – ADS Stage-I DT line, EBT break test	87
Figure 6.19: Comparison between the RELAP5 mass flow and the Spool Piece mass flow - Rouhani model - ADS SPLIT line, ADS break test	89
Figure 6.20: Comparison between the RELAP5 mass flow and the Spool Piece mass flow - Aya model - ADS SPLIT line, ADS break test.....	90
Figure 6.21: Comparison between the RELAP5 mass flow and the Spool Piece mass flow - Volumetric model - ADS SPLIT line, ADS break test.....	91
Figure 6.22: Comparison between the RELAP5 mass flow and the Spool Piece mass flow - Rouhani model - ADS Stage-I ST line, ADS break test	92
Figure 6.23: Comparison between the RELAP5 mass flow and the Spool Piece mass flow - Aya model - ADS Stage-I DT line, ADS break test	94
Figure 6.24: Comparison between the RELAP5 mass flow and the Spool Piece mass flow - Volumetric model - ADS Stage-I DT line, ADS break test	95
Figure 7.1: Comparison between the RELAP5 quality and void fraction in volume 667030000 versus the quality and void fraction obtained by the homogenous model, DVI SPLIT break line, DVI break test.	104
Figure 7.2: Comparison between the RELAP5 quality and void fraction in volume 134010000 versus the quality and void fraction obtained by the homogenous model, ADS Stage-I ST line, DVI break test.	105
Figure 7.3: Comparison between the RELAP5 quality and void fraction in volume 644030000 versus the quality and void fraction obtained by the homogenous model, EBT SPLIT break line, EBT break test.	106
Figure 8.1: Upstream void fraction versus the ratio between the upstream and downstream mixture density in CASE 1.....	113
Figure 8.2: Upstream quality versus the ratio between the upstream and downstream mixture density in CASE 1.....	113
Figure 8.3: Upstream mixture density versus the ratio between the upstream and downstream mixture density in CASE 1.	114
Figure 8.4: Downstream void fraction versus the ratio between the upstream and downstream mixture density in CASE 1.	114
Figure 8.5: Downstream quality versus the ratio between the upstream and downstream mixture density in CASE 1.....	115

Figure 8.6: Downstream mixture density versus the ratio between the upstream and downstream mixture density in CASE 1.	115
Figure 8.7: Upstream Void Fraction versus the ratio between the upstream and downstream mixture density in CASE 2.	116
Figure 8.8: Upstream Quality versus the ratio between the upstream and downstream mixture density in CASE 2.	116
Figure 8.9: Upstream Mixture Density versus the ratio between the upstream and downstream mixture density in CASE 2.	117
Figure 8.10: Downstream Void Fraction versus the ratio between the upstream and downstream mixture density in CASE 2.	117
Figure 8.11: Downstream Quality versus the ratio between the upstream and downstream mixture density in CASE 2.	118
Figure 8.12: Downstream Mixture Density versus the ratio between the upstream and downstream mixture density in CASE 2.	118
Figure 8.13: Upstream and downstream pressure and mass flow in the DVI SPLIT break line, DVI break test.	120
Figure 8.14: Comparison between the RELAP5 quality and the calculated quality downstream of the break during the DVI break test in the DVI SPLIT line.	121
Figure 8.15: Comparison between the RELAP5 quality and the calculated quality downstream of the break during the DVI break test in the DVI SPLIT line.	121
Figure 8.16: Upstream and downstream pressure and mass flow in the EBT SPLIT break line, EBT break test.	123
Figure 8.17: Comparison between the RELAP5 quality and the calculated quality downstream of the break during the EBT break test in the EBT SPLIT line.	124
Figure 8.18: Comparison between the RELAP5 quality and the calculated quality downstream of the break during the EBT break test in the EBT SPLIT line.	124

LIST OF ACRONYMS

ADS	Automatic Depressurization System
Aya	Aya model for the Turbine flowmeter velocity
CHF	Critical Heat Flux
DEG	Double Ended Guillotine
DD	Drag Disk
DT	Double Train
DVI	Direct Vessel Injection
EBT	Emergency Boration Tank
FL	Feedwater line
IRIS	International Reactor Innovative and Secure
LOCA	Loss Of Coolant Accident
LWR	Light Water Reactor
Rou	Rouhani model for the Turbine flowmeter velocity
SBLOCA	Small Break Loss Of Coolant Accident
SL	Steam line
SPES	Simulatore Pressurizzato per Esperienze di Sicurezza
ST	Single Train
T	Turbine Flowmeter
Void	Void Fraction Detector
Vol	Volumetric model for the Turbine flowmeter velocity
WMS	Wire Mesh Sensor

1 SCOPE

In the frame of the SPES3 facility design activities, an important item is related to the identification of the possible instrument set for the two-phase mass flow measurement.

In particular, the activity has been primarily aimed at evaluating the performance of the suitable instruments for the indirect determination of the two-phase mass flow by developing a mathematical model for a spool piece consisting of a Turbine Flowmeter, a Drag Disk and a Void Fraction Detector, during specified SPES3 transients.

The mathematical model has been tested versus the RELAP5 simulation results of accidental transients with a reverse process where calculated variables, like void fraction, quality and slip ratio, have been given as input data to a specifically developed program to get back the mass flow.

The analytical results, verified versus different break transients, well agree with the RELAP5 mass flowrate, so demonstrating the feasibility of this kind of measurement through the envisaged spool piece.

2 INTRODUCTION

The SPES-3 facility is an integral simulator of the IRIS reactor, suitable to test the plant response to postulated design basis accidents and to provide experimental data for code validation and IRIS plant safety analyses [1].

The IRIS reactor is an advanced medium size nuclear reactor, based on the proven technology of Pressurized (Light) Water Reactors with an innovative integral configuration and safety features suitable to cope with Loss of Coolant Accidents through a dynamic coupling of the primary and containment systems. It is under design in the frame of an international consortium led by Westinghouse including industries, universities and research centres.

All the primary, secondary and containment systems are simulated in SPES3 with 1:100 volume and power scaling, 1:1 elevation scaling and the fluid at IRIS pressure and temperature nominal conditions [2].

A test matrix establishes the simulation of a series of SBLOCAs and secondary breaks which data will be fundamental for the certification process that IRIS is going to undergo by the US-NRC [1].

The SBLOCA tests and the secondary side breaks foresee two-phase flow conditions in the pipes simulating the break flow paths, in critical flow during the early phases of the transients and driven by differential pressure in the later phases.

An accurate accident analysis requires the measurement of the mass flow rate of a non-homogeneous mixture occurring in a Loss of Coolant Accidents (LOCA), when a piping break occurs at elevated temperature and pressure.

The two-phase mass flow rate cannot be directly measured by conventional instruments, e.g. Coriolis or Venturi meters, which are usually utilized in single-phase flow conditions. The need to limit intrusive measures and the occurrence of different flow regimes require special instrumentation, typically a set up of two or more instruments.

Because of the severe thermal-hydraulic conditions present during the blow-down phase, like high velocity, high void fraction and different flow regimes, only few instrument types have gained widespread acceptance. This has led to evaluate the use of heterogeneous instruments to realize a Spool Piece device generally consisting of a fluid thermocouple, an absolute pressure measure, a Turbine Flowmeter for volumetric flow or velocity, a Drag Disk for momentum flux and a Void Fraction Detector (gammadensitometer, conductive or inductive sensor) for the measure of chordal average density of the fluid.

The main activity reported in this document is the analysis of the theoretical responses of the instruments in order to obtain the two-phase mass flow and the other thermal-hydraulic parameters during the break tests. In particular, the possibility to predict the two-phase mass flow by coupling only two of the three instruments described above (Drag Disk, Turbine Flowmeter and Void Fraction Detector), has been evaluated. A mathematical model and appropriate numerical programs, describing the analytic response of the different instruments and the couplings of two or more devices, have been developed.

The data obtained by the SPES3 facility simulation of Design Basis Accident transients, [4], with the RELAP5 thermal-hydraulic code, [3], have provided the reference conditions to define the main

thermal-hydraulic parameter ranges and the set of instruments suitable to measure them and to derive the required quantities. Document [5] describes the lines involved in the two-phase mass flow measurements, the range of the main thermal-hydraulic variables and also a preliminary choice of the available instruments.

The analytic evaluation of any possible instrument combination has been carried-out substituting the symbolic expression of the instrument data reduction formulas with the thermal-hydraulic parameters obtained by the RELAP5 pre-test analyses of the LOCA and break transients [4] in order to obtain the theoretical responses (mixture density, turbine velocity and momentum flux). The choice of the commercial instruments and the problems related to the actual responses will be tasks of a future activity.

In the analytic evaluation, the instrument value outputs are considered as theoretical values, i.e. not affected by different flow regimes, pressure and temperature of the fluid, overall uncertainty and linearity bias.

The outputs of the instruments have been combined to obtain the mass flow rate, coupling two or three instruments.

The combination of signals coming from two or three instruments and the comparison of the calculated mass flows with the corresponding RELAP5 mass flows has allowed to identify the best instrument combination.

A further important activity described in this document is the evaluation of the possibility to obtain other important thermal-hydraulic parameters (as the quality, the gas and liquid velocities) by the responses of two or three instruments combination, other than to obtain the mass flow.

Three different models to estimate the turbine velocity (Aya [6], Rouhani [7] and volumetric model [8]) have been taken into consideration and the analytic results have been presented. Anyway they need to be validated against experimental data and to identify which better adapts to the different conditions of the two-phase flow.

The effectiveness of the homogenous model has also been studied and compared to the other models.

The possibility to obtain information about the two-phase mass flows and the other thermal-hydraulic parameters using a coupling of two Venturi meters, upstream and downstream of the rupture, has been considered and compared to the other solutions.

3 BREAK POSITIONS

Five base transient case simulations have been utilized to study the two-phase flow occurrence in the break lines. Such transients have been chosen according to what specified in the test matrix [1] and reported in [4]. The five investigated base cases are shown in Table 3.1 .

Table 3.1: Base cases for the SPES3 break transients

RELAP base case number	Case name	Description
SPES 89	DVI break	Double Ended Guillotine break of the Direct Vessel Injection Line B
SPES 90	EBT break	Double Ended Guillotine break of the top connection between the Emergency Boration Tank B and the Reactor Vessel
SPES 91	ADS break	Double Ended Guillotine break of the Automatic Depressurization System Single Train Line
SPES 92	SL break	Double Ended Guillotine break of the Steam Line B
SPES 93	FL break	Double Ended Guillotine break of the Feed Line B

The investigated cases cover the main primary system LOCAs and secondary system breaks and the ADS lines are involved in the studied transients.

For each case, the Double Ended Guillotine (DEG) break is simulated, representing a complete severance of the pipe.

During a break transient, it is important to keep under control the mass and enthalpy balances of the system, measuring the mass flow and the quality at the break.

The analysis of the main thermal-hydraulic parameters obtained by the SPES3 facility simulation with the use of RELAP5 thermal-hydraulic code [3] [4] and the work reported in [5] have allowed the selection of those break lines in which two-phase mass flow is foreseen and needs to be measured.

The thermal-hydraulic conditions ensuing from the five ruptures, chosen among the fourteen possible locations, require the use of special instrumentation, namely a spool piece. Table 3.2 shows the spool piece positioning .

Such spool piece will be arranged with three different instruments including: a Turbine Flowmeter, for volumetric flow or velocity, a Drag Disk, for the momentum flux, and a Void Fraction Detector, as a gammadensitometer, a conductive or inductive sensor, for the chordal average density of the fluid.

Table 3.2: Positions of the spool piece to measure two-phase flow in SPES3

DVI SPLIT line downstream of the break valve
EBT SPLIT line downstream of the break valve
ADS Stage-I ST SPLIT line downstream of the break valve
ADS Stage-I ST downstream of the valve
ADS Stage-I DT downstream of the valve

Table 3.3, Table 3.4, Table 3.5, Table 3.6 and Table 3.7 present the envelope of minimum and maximum values of the main thermal-hydraulic variables during the whole transient, extracted from the RELAP5 pre-test results described in [4], in particular:

- temperature,
- liquid velocity,
- gas velocity,
- pressure,
- void fraction,
- quality,
- mass flow rate.

Such values have been extracted for each line from the volume where the special instrumentation is supposed to be installed, as reported in [5].

It is worth underlining that there is not correspondence between the instant at which a generic variable reaches the minimum or maximum value and the others, i.e. as during the DVI break test in the DVI split line the minimum value of pressure is 0.102 MPa, at the same instant the temperature can be different from the minimum value of 37.51 °C as well as the gas and liquid velocities can reach the maximum value in different moments.

Table 3.3: DVI SPLIT break line – Thermal-hydraulic variables and flow regimes

Flow regimes		Annular mist, bubbly, horizontal stratified						
Fluid conditions:	Pressure [MPa]	Temp. [°C]	Mass Flow [kg/s]	Quality	Liquid Vel. [m/s]	Gas Vel. [m/s]	Void Fraction	Calculated Volumetric Flow [m³/s]
MIN.	0.102	37.51	-0.13	-0.0025	-5.398	-0.922	0**	-0.002
MAX.	0.690	164.42	1.33	0.9997	55.492	187.888	1	0.464

** The void fraction reaches this minimum value just at the end of the transient, when the safety system starts to operate. For our measurement range of interest, the minimum void fraction is 0.6256.

Table 3.4: EBT SPLIT break line – Thermal-hydraulic variables and flow regimes

Flow regimes		Annular mist, mist pre-CHF, horizontal stratified						
Fluid conditions:	Pressure [MPa]	Temp. [°C]	Mass Flow [kg/s]	Quality	Liquid Vel. [m/s]	Gas Vel. [m/s]	Void Fraction	Calculated Volumetric Flow [m³/s]
MIN.	0.1024	128.73	-0.020	0.199	-5.691	-5.928	0.978	-0.006
MAX.	1.391	203.96	4.67	1.04	189.771	258.755	1	0.250

Table 3.5: ADS Stage-I ST SPLIT break line – Thermal-hydraulic variables and flow regimes

Flow regimes		Annular mist, mist pre-CHF, horizontal stratified						
Fluid conditions:	Pressure [MPa]	Temp. [°C]	Mass Flow [kg/s]	Quality	Liquid Vel. [m/s]	Gas Vel. [m/s]	Void Fraction	Calculated Volumetric Flow [m³/s]
MIN.	0.1024	90	-0.044	0.435	-2.928	-2.928	0.993	-0.014
MAX.	0.795	216	4.51	1.076	205.687	405.115	1	1.930

Table 3.6: ADS Stage-I ST line – Thermal-hydraulic variables and flow regimes

Flow regimes		Annular mist, mist pre-CHF, horizontal stratified, bubbly						
Fluid conditions:	Pressure [MPa]	Temp. [°C]	Mass Flow [kg/s]	Quality	Liquid Vel. [m/s]	Gas Vel. [m/s]	Void Fraction	Calculated Volumetric Flow [m³/s]
MIN.	0.1024	36.8	-0.269	-0.0002	-2.9735	-2.9735	0**	-0.003
MAX.	2.0505	216.2	0.9577	1.0533	25.6128	66.3613	1	0.075

** The void fraction reaches this minimum value due to the reflux of water sucked from the quench tank. For the measure of our interest the minimum void fraction is 0.9471.

Table 3.7: ADS Stage-I line DT– Thermal-hydraulic variables and flow regimes

Flow regimes		Annular mist, mist pre-CHF, horizontal stratified						
Fluid conditions:	Pressure [MPa]	Temp. [°C]	Mass Flow [kg/s]	Quality	Liquid Vel. [m/s]	Gas Vel. [m/s]	Void Fraction	Calculated Volumetric Flow [m³/s]
MIN.	0.1024	38.2	-0.016	0.3281	-2.4829	-2.4829	0.94893	-0.008
MAX.	1.8419	216	3.1324	1.0695	32.8595	96.2626	1	0.261

The above tables report also the maximum and minimum values of the volumetric flow rate, obtained by the formula:

$$Q = A \cdot [V_L \cdot (1 - \alpha) + V_G \cdot \alpha] \quad (3.1)$$

where

- Q is the volumetric flow rate in m³/s
- A is the cross section of the pipe in m²
- V_L, V_G are the liquid and gas velocity in m/s
- α is the cross-sectional void fraction defined as

$$\alpha = \frac{A_G}{A} \quad (3.2)$$

where

- A_G is the cross section occupied by the gas phase in m².

The indications of the different flow regimes the fluid experiments during the blow-down are also reported in the above-mentioned Tables.

The spool pieces will be located downstream the break valves, or actuation valves for ADS Stage-I, with horizontal orientation, as indicated in [5]. The geometrical dimensions of the pipe and the corresponding volume of the nodalization described in [4] are reported in Table 3.8, Table 3.9, Table 3.10,

Table 3.11, Table 3.12 and in

Figure 3.1, Figure 3.2, Figure 3.3 and Figure 3.4.

Table 3.8: DVI SPLIT break line – geometrical dimensions and nodalization volumes

Test line	Control volume	Pipe size	Pipe inner diameter
Upstream	665010000	½" Sch. 80	13.8 mm
Downstream	667090000	2" ½ Sch. 40	62.7 mm
Break:			
	Valve junction	666000000	
	Valve	IV10	
	Orifice	4.28 mm	

Table 3.9: EBT SPLIT break line – geometrical dimensions and nodalization volumes

Test line	Control volume	Pipe size	Pipe inner diameter
Upstream	622010000	¾" Sch. 80	18.9 mm
Downstream	644030000	1" ¼ Sch. 40	35.1 mm
Break:			
	Valve junction	643000000	
	Valve	IV13	
	Orifice	8.73 mm	

Table 3.10: ADS Stage-I ST SPLIT break line – geometrical dimensions and nodalization volumes

Test line	Control volume	Pipe size	Pipe inner diameter
Upstream	157010000	1" ½ Sch. 80	38.1 mm
Downstream	133040000	3" Sch. 40	77.9 mm

Break:	Valve junction	158000000
	Valve	IV19
	Orifice	13.18 mm

Table 3.11: ADS Stage-I ST line – geometrical dimensions and nodalization volumes

Test line	Control volume	Pipe size	Pipe inner diameter
Upstream	152030000	1" ½ Sch. 80	38.1 mm
Downstream	134010000	1"½ Sch. 40	40.9 mm
Break:	Valve junction	153000000	
	Valve	IV17	
	Orifice	13.18 mm	

Table 3.12: ADS Stage-I DT line – geometrical dimensions and nodalization volumes

Test line	Control volume	Pipe size	Pipe inner diameter
Upstream	142080000	2" ½ Sch. 80	59.0 mm
Downstream	1310100000	2"½ Sch. 40	62.7 mm
Break:	Valve junction	143000000	
	Valve	IV15	
	Orifice	18.64 mm	

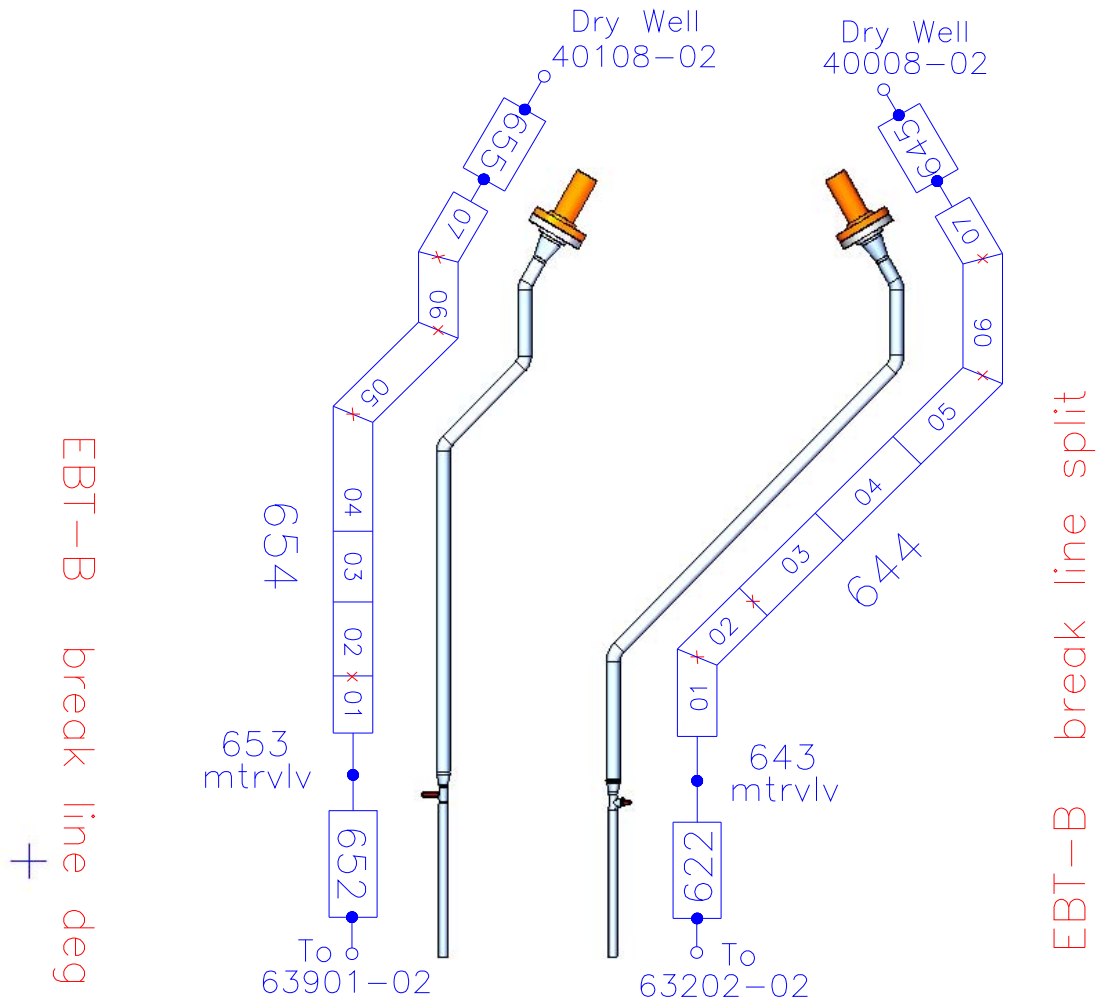


Figure 3.2: SPES3 EBT-B break line nodalization

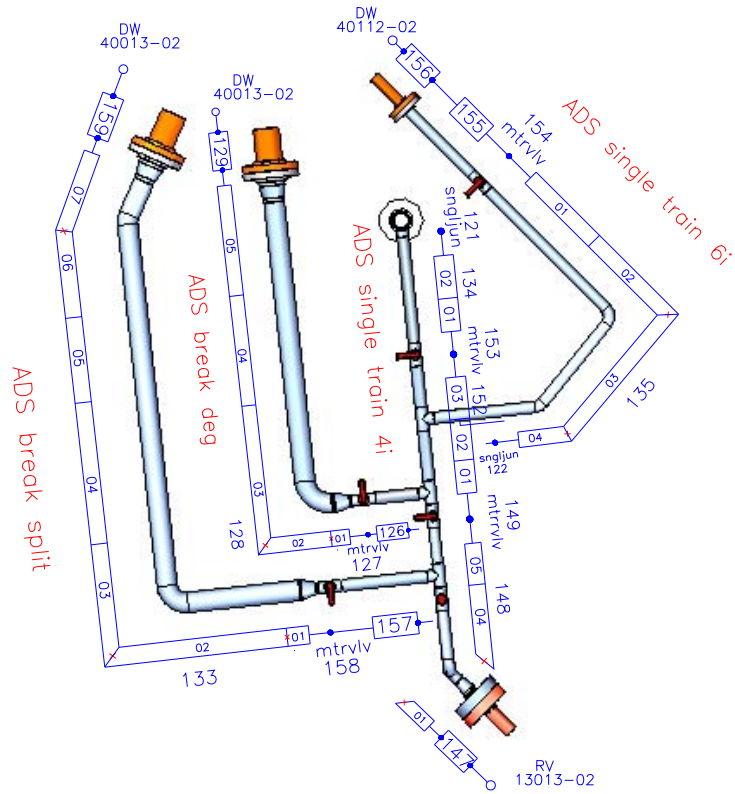


Figure 3.3: SPES3 ADS ST and ADS Stage-I ST break line nodalization (top view)

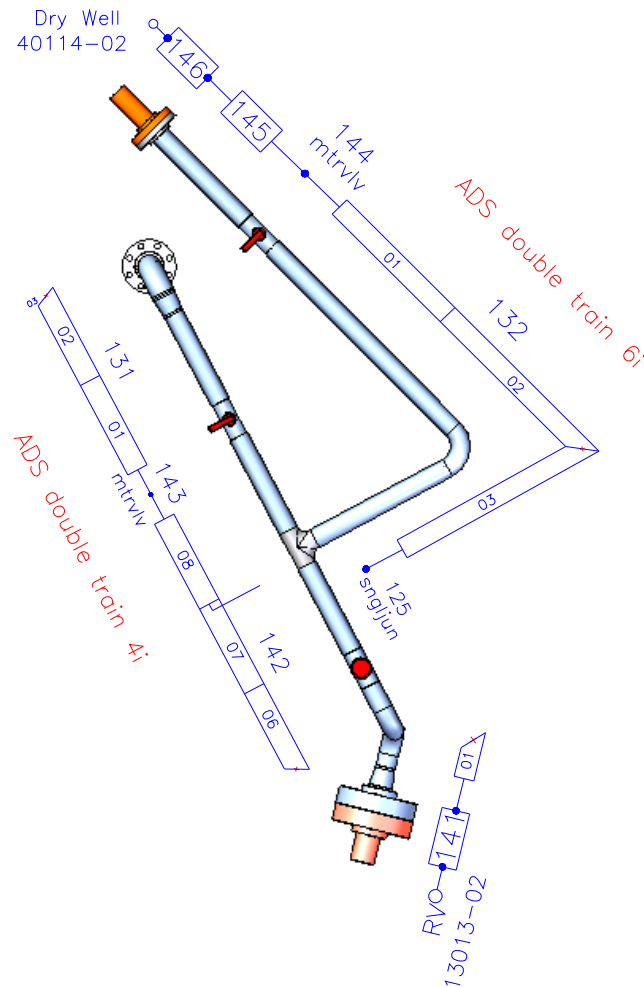


Figure 3.4: SPES3 ADS Stage-I DT nodalization (top view)

Turbine Flowmeters and Drag Disks shall be bidirectional, since the flow direction changes during the blowdown, as reported in [5].

The analysis of the spool piece design, the availability of commercial devices, the repeatability of the measures, the calibrations are beyond the scope of this document. Anyway, on the basis of what described in [9] [10] [11], the instruments have to be as less intrusive as possible, not to largely affect the flow regime. The reciprocal location of the instruments is also important. Generally the device that less affects the two-phase flow (usually the Void Fraction Detector) is placed upstream while the device that more influences (usually the Drag Disk, but it depends on the plate dimensions) is placed downstream. The different components of the spool piece have to stay close because of the unsteadiness and non-homogeneous nature of two-phase flow.

The DVI SPLIT line, the EBT SPLIT line and the ADS SPLIT line experiment two-phase mass flow just in the related transients, i.e. DVI break test, EBT break test and ADS break test. The situation of the ADS stage-I ST and DT lines is different, because the ADS Stage-I valves are actuated

whenever a high containment pressure signal occurs contemporarily to a low pressurizer pressure signal, events present in the above said LOCA transients. Therefore, the spool pieces located in the ADS stage-I ST and DT will operate during the DVI and EBT break test, while during the ADS break test just the ADS Stage-I DT will work, as the ST is lost for the break. During the SL and FL break tests the intervention of the ADS lines is not foreseen.

This document describes also the theoretical behaviour of five spool pieces, located in the interested lines characterized by different diameters and different extreme conditions (mixture velocity, mixture momentum flux and void fraction).

The spool piece placed downstream of the ADS Stage-I ST actuation valve will operate during two transients, while the spool piece placed downstream of the ADS Stage-I DT actuation valve will operate during three transients, for a total of eight spool piece theoretical responses, as indicated in Table 3.13.

Table 3.13: List of the involved lines and spool pieces for each test

Test	Involved line and spool piece	Initials
DVI break test	DVI SPLIT	DVI SPLIT
	ADS Stage-I ST	DVI ADS ST
	ADS Stage-I DT	DVI ADS DT
EBT break test	EBT SPLIT	EBT SPLIT
	ADS Stage-I ST	EBT ADS ST
	ADS Stage-I DT	EBT ADS DT
ADS break test	ADS SPLIT	ADS SPLIT
	ADS Stage-I DT	ADS ADS DT

The procedure followed to complete this activity is summarized in the following points:

- write the analytical expressions of the instrument governing equations;
- substitute the required variables, obtained from the RELAP5 results of the five transients [4], to the analytical expressions of the different devices to simulate the spool piece theoretical responses;
- combine the different instruments outputs with the appropriate mathematical model to achieve the mass flow rate and steam quality;
- compare the mass flow rate and steam quality values to those derived from the transients [4].

The comparison demonstrates the correctness of the mathematical model and also the feasibility of the mass flow derivation using only two instruments instead of three.

The same data are used to investigate the suitability of the homogenous model and the feasibility of the coupling of two Venturi meters.

4 ANALYTICAL EXPRESSIONS OF THE SPOOL PIECE

In this section the governing equations of the main devices are presented as well as the main hypotheses of the computation models used to determine the analytical outputs.

The devices taken into consideration are:

- Drag Disk flowmeter (momentum flux ρV^2)
- Turbine Flowmeter (turbine velocity V_T)
- Void Fraction Detector (mixture density ρ_{AV})
- Venturi meter (pressure drop ΔP)

The main assumptions are:

- gas and liquid phases at same temperature in the pipe portion occupied by the spool piece,
- no variation of void fraction, quality, temperature and pressure in the pipe portion occupied by the spool piece
- fully developed flow,
- no influence of the different flow regimes on the instrument outputs.

4.1 Drag Disk flowmeter (DD)

A Drag Disk (DD) is designed to measure the bidirectional average momentum flux passing through a duct.

The measure is performed by disposing a drag body or target in the flow stream and by measuring the drag force exerted on the body by the fluid flow.

The movement of the body, detected by strain gauges, is proportional to the drag force, which varies with the square of the velocity of the two phases and thus provides a measure of the average momentum flux of the flow.

The drag disk determines an abrupt change of section of the duct. That leads to have a concentrated head loss, which can be measured by a differential pressure instrument.

The output I_D [Pa] returned by a Drag Disk can be expressed as:

$$I_D = \frac{F_D}{A} \quad (4.1)$$

Where

A is the cross-sectional area of the pipe in m^2

F_D is the drag force in N, which is defined as:

$$F_D = \frac{1}{2} C_D A (\rho V^2) \quad (4.2)$$

Where

C_D is the non-dimensional drag coefficient, that should be taken from calibration tests for the instrument

ρV^2 is the momentum flux in Pa, which is analytically expressed by

$$(\rho V^2) = \alpha \rho_G V_G^2 + (1 - \alpha) \rho_L V_L^2 = V_L^2 (\alpha \rho_G S^2 + (1 - \alpha) \rho_L) \quad (4.3)$$

Where

ρ_G is the density of the gas phase in kg/m^3

ρ_L is the density of the liquid phase in kg/m^3

S is the slip ratio, defined as

$$S = \frac{V_G}{V_L} \quad (4.4)$$

The pressure drop ΔP [Pa] at the instrument can be described by:

$$\Delta P = K (\rho V^2) \quad (4.5)$$

Where

K is a proportional factor that depends on the calibration, the shape of the disk and the flow conditions.

In this analysis, the K and C_D terms will not be considered because calibration tests are not available and the terms can be neglected in the reduction formula.

In order to individuate the possible working condition of the Drag Disks in each of the five lines, the theoretical maximum and minimum values of the momentum flux have been calculated using the RELAP5 data for each investigated break line in the volume indicated in Table 3.8, Table 3.9, Table 3.10,

Table 3.11 and Table 3.12.

The RELAP5 results are described in detail in [5] and the theoretical maximum and minimum values of the momentum flux theoretically measured by a Drag Disk (DD) in each line for each test are reported in Table 4.1.

Table 4.1: Minimum and maximum values of the momentum flux

Test	Involved line and spool piece	DRAG DISK	
		Minimum value [Pa]	Maximum value [Pa]
DVI break test	DVI SPLIT	0	34820
	ADS ST (stage I)	0	29724
	ADS DT (stage I)	0	25855
EBT break test	EBT SPLIT	0	900796
	ADS ST (stage I)	0	29532
	ADS DT (stage I)	0	25414
ADS break test	ADS SPLIT	0	259194
	ADS DT (stage I)	0	36749

4.2 Turbine Flowmeter (T)

A Turbine Flowmeter is an instrument designed to measure the bidirectional average velocity of a fluid flow.

This instrument consists of a pipe containing a bladed rotor coaxial to the fluid flow.

The rotor spins as the liquid passes through the blades. The rotational speed is a direct function of volumetric flow rate and can be sensed by magnetic pick-up, photoelectric cell, or gears. Electrical pulses can be counted and totalized.

In the two-phase flow regimes the instrument output signal is proportional to the combination of both the gas fraction velocity and the liquid fraction velocity.

In two-phase conditions there is no agreement about which analytical expression better matches the turbine outputs. The presence of the slip between the two phases, the different flow regimes, the influence of the gas flow rate and of the liquid flow rate strongly affect the Turbine Flowmeter.

Three analytical models generally describe the turbine velocity, based on different assumptions: the Rouhani model, the Aya model and the volumetric model [6], [7], and [8].

The comparison of the velocities predicted by the above-mentioned models is beyond the purpose of this document, because it requires experimental tests.

The RELAP5 transient data are used to calculate the turbine velocities according to the three models, waiting for experimental calibration tests to discover which model better represents the mixture velocity.

The

Table 3.3, Table 3.4, Table 3.5, Table 3.6 and Table 3.7 indicate high gas mass flow rate, high void fraction, high slip ratio but also very low velocities and low qualities (i.e.: the flow experiments at least three different flow regimes). These conditions lead to exclude the use of a unique model during a whole transient. An experimental investigation should be done to find the model combination that better match the foreseen thermal-hydraulic conditions.

In order to find the possible working condition of the Turbine Flowmeters for the five lines, the theoretical maximum and minimum values of the turbine velocities, according to the three models, have been calculated using the RELAP5 data for each investigated break [5] and they are reported in Table 4.2, Table 4.3 and Table 4.4.

4.2.1 Rouhani model

Table 4.2: Minimum and maximum values of the mixture velocity theoretically measured by a Turbine Flowmeter (T) – ROUHANI MODEL – in each line for each test.

Test ROUHANI MODEL	Involved line and spool piece	TURBINE METER Minimum value [m/s]	TURBINE METER Maximum value [m/s]
DVI break test	DVI SPLIT	-0.6227	81.4205
	ADS ST (stage I)	-18.1372	59.8180
	ADS DT (stage I)	-2.4828	68.6738
EBT break test	EBT SPLIT	-5.928	248.05
	ADS ST (stage I)	-5.1256	57.8376
	ADS DT (stage I)	-0.4353	59.7891
ADS break test	ADS SPLIT	-2.928	374.517
	ADS DT (stage I)	-1.3163	77.1020

This model is based on the assumption that the change in momentum (impulse) of the Turbine Flowmeter blades, due to the flow stream, is negligible as follows:

$$\alpha V_G \rho_G (V_G - V_T) - (1 - \alpha) V_L \rho_L (V_L - V_T) = 0 \quad (4.6)$$

The turbine velocity according to Rouhani can be expressed as:

$$V_T = \frac{\alpha \rho_G V_G^2 + (1 - \alpha) \rho_L V_L^2}{\alpha \rho_G V_G + (1 - \alpha) \rho_L V_L} = V_L \frac{\alpha \rho_G S^2 + (1 - \alpha) \rho_L}{\alpha \rho_G S + (1 - \alpha) \rho_L} \quad (4.7)$$

4.2.2 Aya model

This model is based on a momentum balance on a turbine blade due to velocity differences between the two phases and the turbine blade.

It typically describes dispersed flow with gas velocity higher than the liquid one.

$$\alpha \rho_G C_{TG} (V_G - V_T)^2 = (1 - \alpha) \rho_L C_{TL} (V_T - V_L)^2 \quad (4.8)$$

Where the coefficients C_{TG} and C_{TL} are the drag coefficients of a turbine blade for the gas and liquid phases respectively, that should come out of calibration tests. They are set to unity in this work. Therefore, the turbine velocity according to Aya can be expressed by:

$$V_T = \frac{V_L \sqrt{\rho_L (1 - \alpha)} + V_G \sqrt{\rho_G \alpha}}{\sqrt{\rho_L (1 - \alpha)} + \sqrt{\rho_G \alpha}} = V_L \frac{\sqrt{\rho_L (1 - \alpha)} + S \sqrt{\rho_G \alpha}}{\sqrt{\rho_L (1 - \alpha)} + \sqrt{\rho_G \alpha}} \quad (4.9)$$

Table 4.3: Minimum and maximum values of the mixture velocity theoretically measured by a Turbine Flowmeter (T) – AYA MODEL – in each line for each test.

.Test AYA MODEL	Involved line and spool piece	TURBINE METER	
		Minimum value [m/s]	Maximum value [m/s]
DVI break test	DVI SPLIT	-0.4195	75.4401
	ADS ST (stage I)	-2.9735	50.4865
	ADS DT (stage I)	-2.4828	55.1215
EBT break test	EBT SPLIT	-5.924	236.10

	ADS ST (stage I)	-0.9532	48.890
	ADS DT (stage I)	-0.4353	52.9210
ADS break test	ADS SPLIT	-2.928	330.528
	ADS DT (stage I)	-1.3163	51.7121

4.2.3 Volumetric model

This model assumes that the measured velocity V_T represents the volumetric flow rate per unit flow area, which gives:

$$Q = A(\alpha V_G + (1 - \alpha)V_L) \quad (4.10)$$

That yields

$$V_T = \frac{Q}{A} = \alpha V_G + (1 - \alpha)V_L = V_L (\mathcal{S}\alpha + (1 - \alpha)) \quad (4.11)$$

Table 4.4: Minimum and maximum values of the mixture velocity theoretically measured by a Turbine Flowmeter (T) – VOLUMETRIC MODEL – in each line for each test.

Test	Involved line and spool piece	TURBINE METER	
		Minimum value [m/s]	Maximum value [m/s]
DVI break test	DVI SPLIT	-0.6237	150.4414
	ADS ST (stage I)	-2.9734	65.5983
	ADS DT (stage I)	-2.4828	76.4041
EBT break test	EBT SPLIT	-5.928	258.568
	ADS ST (stage I)	-0.9645	61.6219
	ADS DT (stage I)	-0.4353	62.8894
ADS break test	ADS SPLIT	-2.928	405.005
	ADS DT (stage I)	-1.3163	95.5422

4.3 Void Fraction Detector (Void)

The third instrument necessary to measure the two-phase mass flow rate in a spool piece is the Void Fraction Detector. This device represents one of the most critical points of the method,

because commonly a gamma densitometer is chosen for the determination of the average chordal density, involving high costs and radiation protection problems. Other possibilities have been considered to obtain the mixture density: impedance methods, as conductive needle probes [12] or electrical capacitance tomography [13], ultrasonic methods [14] and recently the wire mesh sensors, based on a local measurement of electrical conductivity of the fluid within the cross-section by means of a mesh of crossing electrodes [15].

The feasibility of these measurements and the availability of the relative instruments are beyond the scope of this report.

A generic Void Fraction Detector is considered for measuring the mass flow rate with a spool piece. This device gives the mixture density, function of cross sectional void fraction and pressure, according to the expression:

$$\rho_{AV} = \alpha\rho_G + (1 - \alpha)\rho_L \quad (4.12)$$

Where ρ_{AV} is the mixture density.

The difficulties in measuring the void fraction, the required high speed record rate, the issues involved in the use of gamma rays (gamma densitometer), the lack of experimental experiences about the other techniques, the reliance of the results on the flow regimes and finally the costs, imply an effort to avoid the use of this device and to restrict the spool piece to two instruments (Drag Disk and Turbine Flowmeter). The comparison between the results obtained using two and three instruments are presented in section {6}. Despite the attempt of avoiding the Void Fraction Detector, the analytical analysis considers also its coupling with the Turbine Flowmeter or with the Drag Disk flowmeter to identify which additional information on the flow parameters becomes available

4.4 Venturi meter

A Venturi meter is a tube with a restricted throat that increases velocity and decreases pressure. It is used for measuring the flowrate of compressible and incompressible fluids in pipeline using the pressure drop along the conduit, according to the formula:

$$\dot{m} = \gamma \cdot A \sqrt{\rho \cdot \Delta P} \quad (4.13)$$

Where

\dot{m} is the mass flowrate in kg/s

- ρ is the density of the fluid, that can be the average density in case of two-phase flow in Kg/m^3
- ΔP is the pressure drop along the Venturi meter in Pa
- γ is a flow coefficient depending on the flow regime, the Reynolds number and the geometry of the instrument.

The coupling of a Venturi meter with a Void Fraction Detector for the measurement of the mixture density may return directly the mass flow rate. However the output signal of the instruments is not proportional to the mass flow rate when the flow presents two separated phases, but it is affected by the flow regimes, the slip ratio, and the different acceleration of the gas phase. Experimental data are required to evaluate the correlation of the outputs with the thermal-hydraulic variables.

In order to avoid the use of a Void Fraction Detector, an attempt to use two coupled Venturi meters (the former upstream, the latter downstream of the rupture) has been done to derive the mixture density as described in section {8}

5 Mathematical models

The theoretical model has been drawn for a spool piece device that consists of a Drag Disk (DD), a Turbine Flowmeter (T) and a Void Fraction Detector (Void). The signal outputs of these three instruments have been combined in order to obtain a data reduction mathematical model for the two-phase mass flow rate and quality. The mass flow rate analysis has been performed using the following instruments coupling:

- Turbine Flowmeter + Drag Disk (T+DD)
- Turbine Flowmeter + Void Fraction Detector (T+Void)
- Drag Disk + Void Fraction Detector (DD+Void)
- Turbine Flowmeter + Drag Disk + Void Fraction Detector (DD+T+Void)

For each coupling a mathematical model has been derived. Regarding to the Turbine Flowmeter, the three different models – Aya, Rouhani and Volumetric model – have been taken into consideration. The analyses and the comparison between the different models are presented in the next section and the analytical techniques have been tested using the RELAP5 data results [4], [5].

From the RELAP5 data the mass flow rate at the investigated junction is available at each time step. In the same time, the main thermal-hydraulic variables necessary to obtain the spool piece response have been extracted in the volume where the devices are foreseen.

The mass flow rate can be expressed by the formula:

$$\dot{m} = A[\alpha\rho_G V_G + (1-\alpha)\rho_L V_L] \quad (5.1)$$

Using the void fraction, the liquid and gas velocity, the liquid and gas density from RELAP5, the mass flow rate has been calculated and compared with the corresponding RELAP5 mass flow rate at the junction. Figure 5.1, Figure 5.2, Figure 5.3, Figure 5.4, Figure 5.5, Figure 5.6, Figure 5.7 and Figure 5.8 show the comparison between the calculated mass flow rate according to [5.1] and the RELAP5 data. The agreement is absolute.

The void fraction and quality trends are also plotted in the same graphs, because such information can be useful to set the spool piece, as indicated in [5].

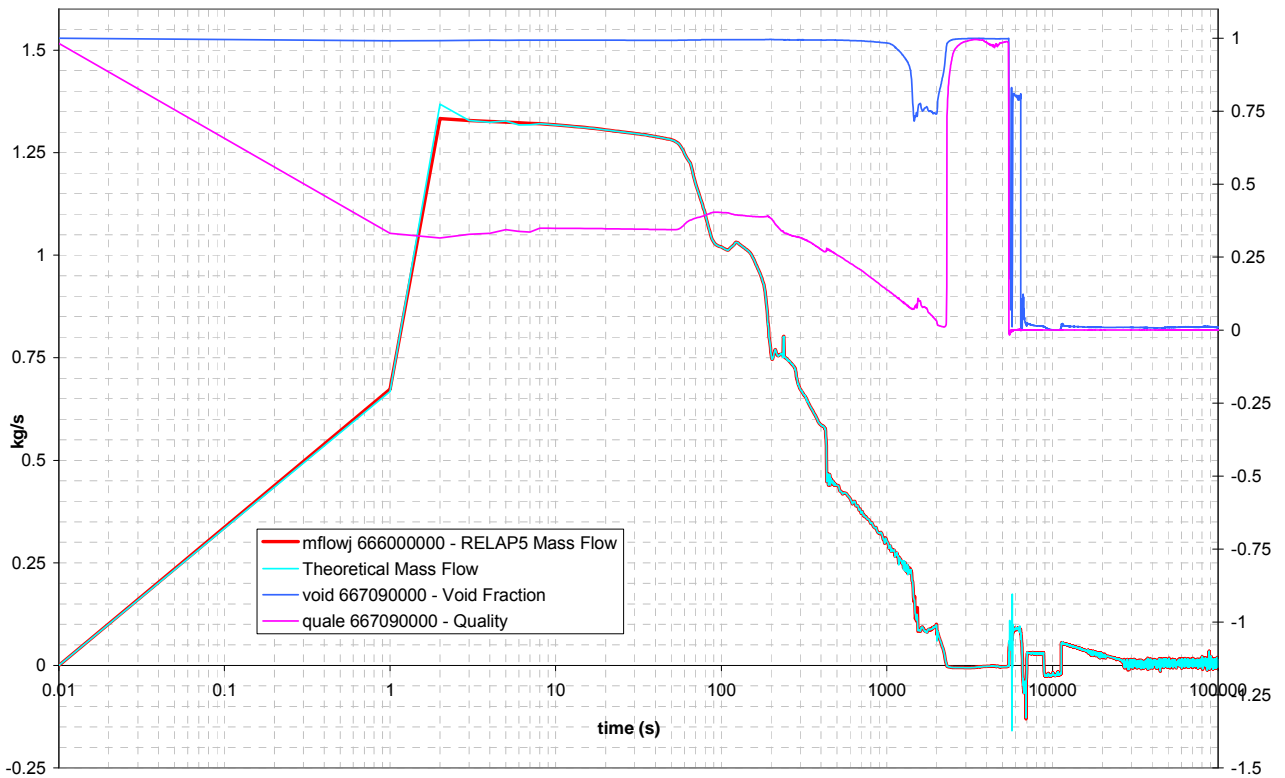


Figure 5.1: Comparison between the RELAP5 and theoretical mass flow, void fraction and quality in DVI SPLIT break line, DVI Test

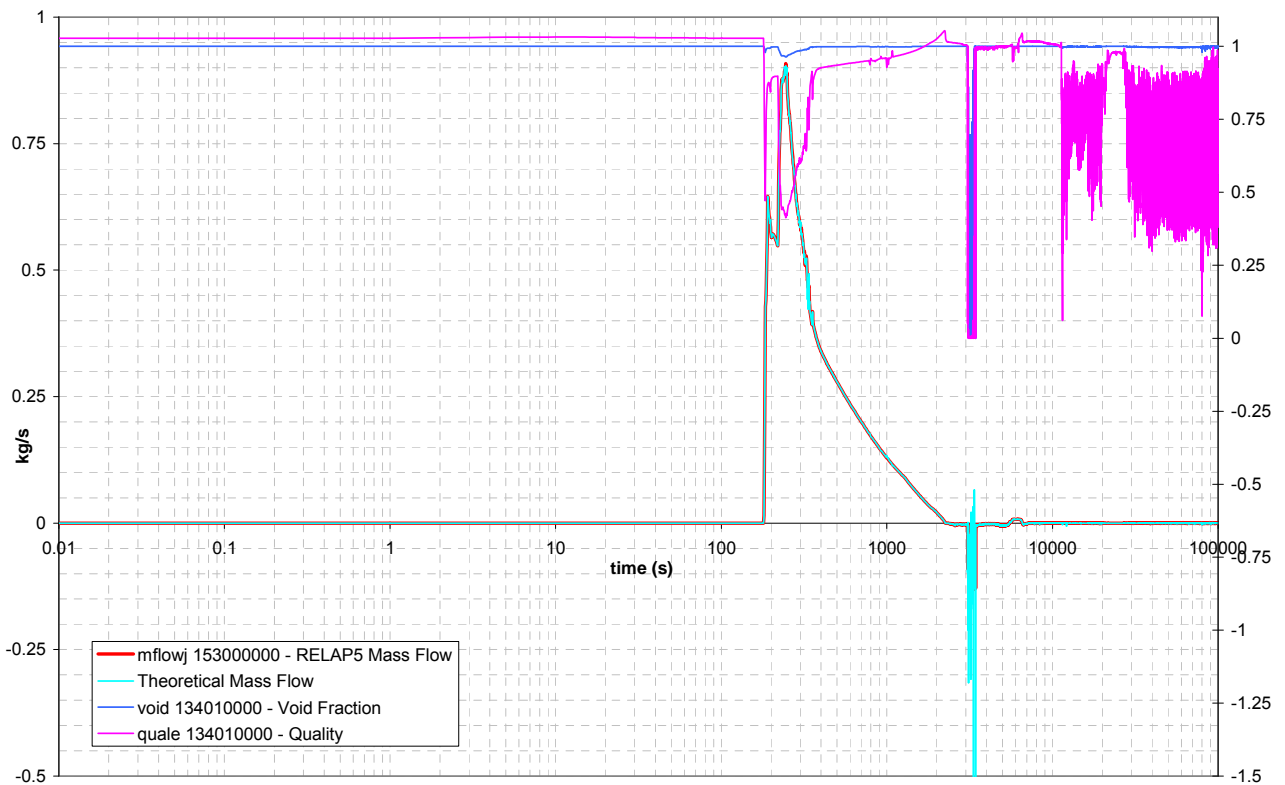


Figure 5.2: Comparison between the RELAP5 and theoretical mass flow, void fraction and quality in ADS Stage-I ST line, DVI Test

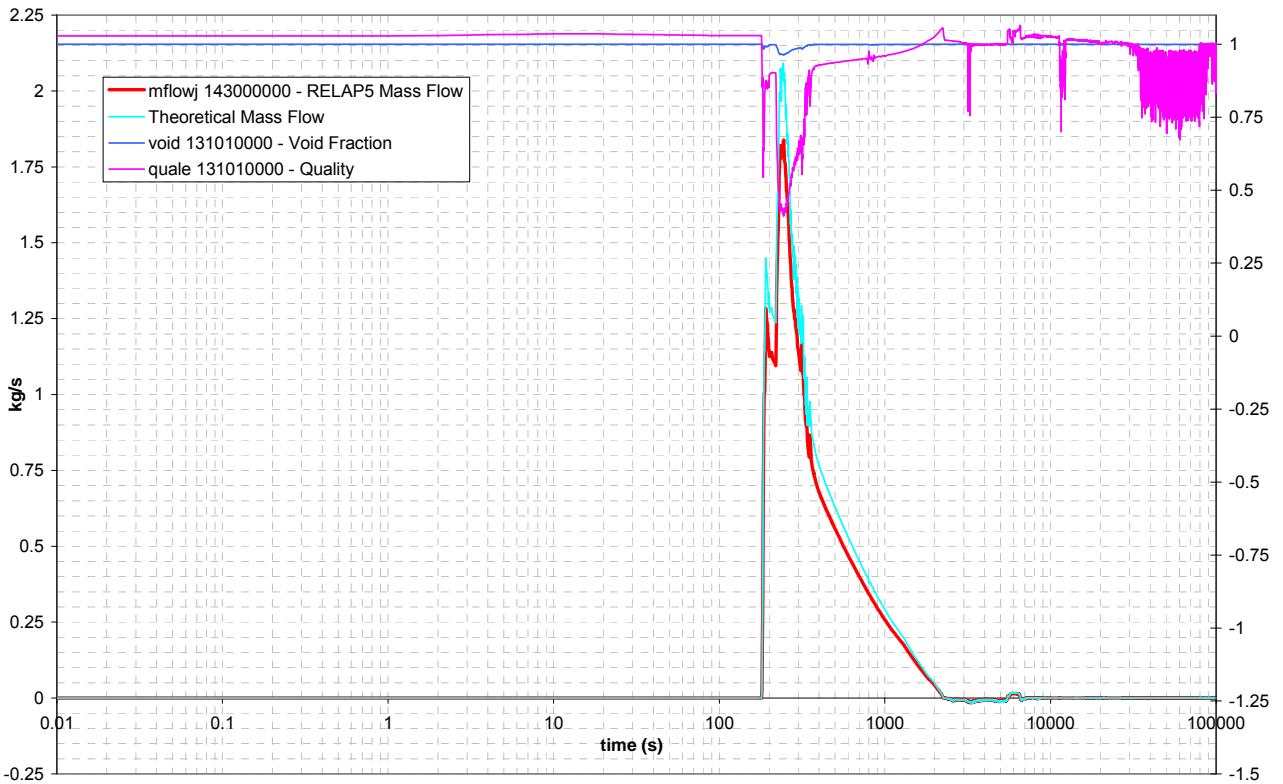


Figure 5.3: Comparison between the RELAP5 and theoretical mass flow, void fraction and quality in ADS Stage-I DT line, DVI Test

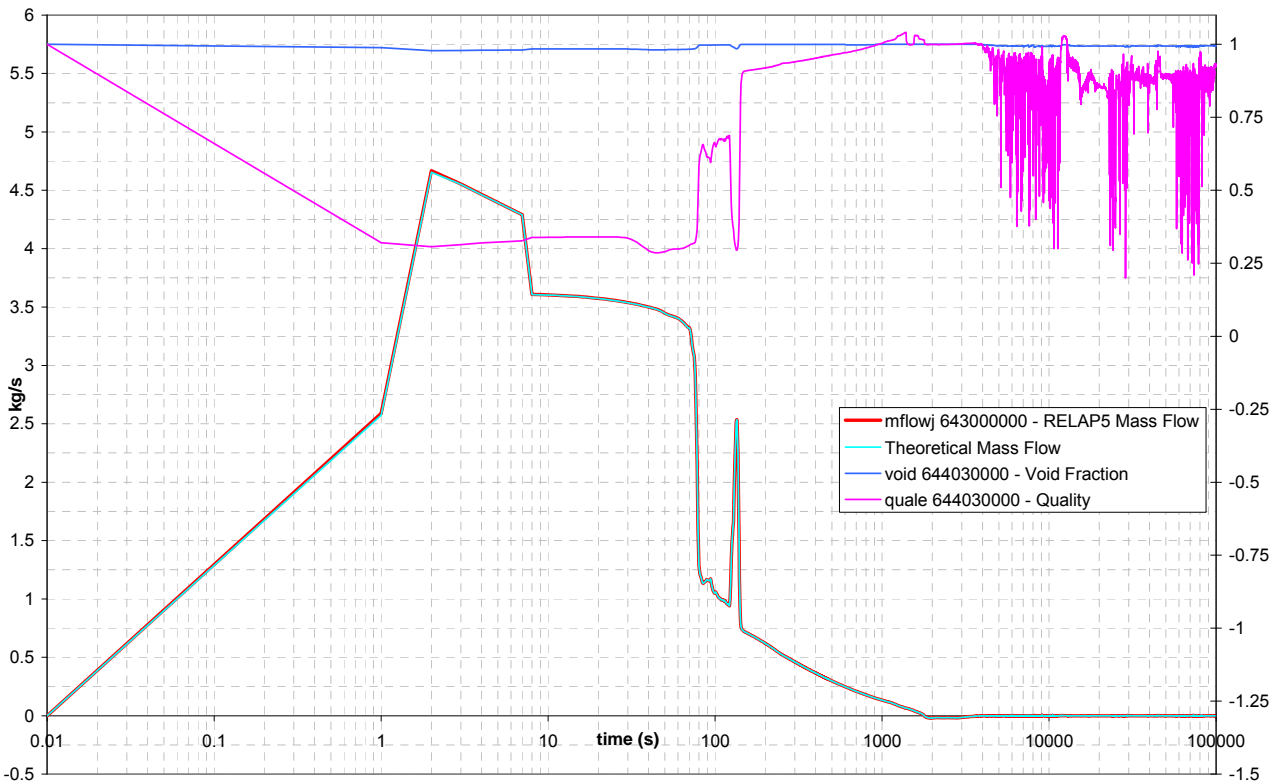


Figure 5.4: Comparison between the RELAP5 and theoretical mass flow, void fraction and quality in EBT SPLIT break line, EBT Test

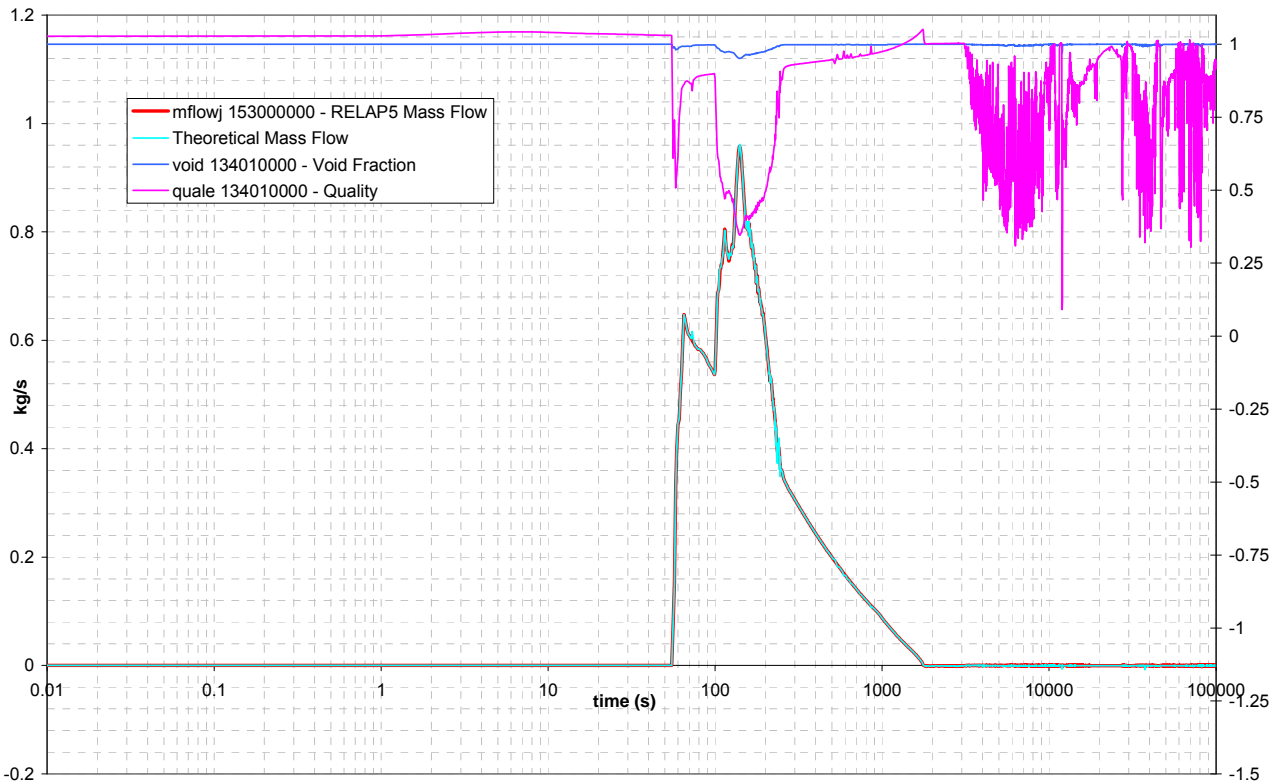


Figure 5.5: Comparison between the RELAP5 and theoretical mass flow, void fraction and quality in ADS Stage-I ST line, EBT Test

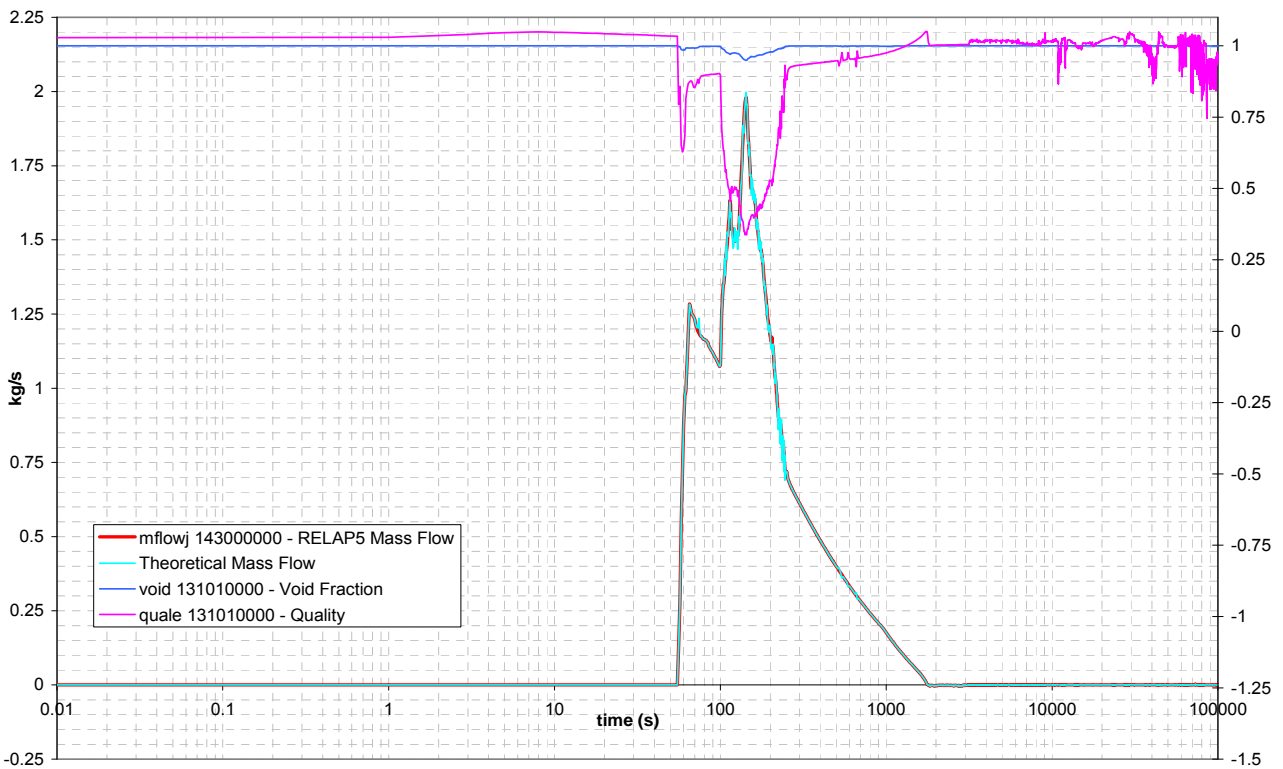


Figure 5.6: Comparison between the RELAP5 and theoretical mass flow, void fraction and quality in ADS Stage-I DT line, EBT Test

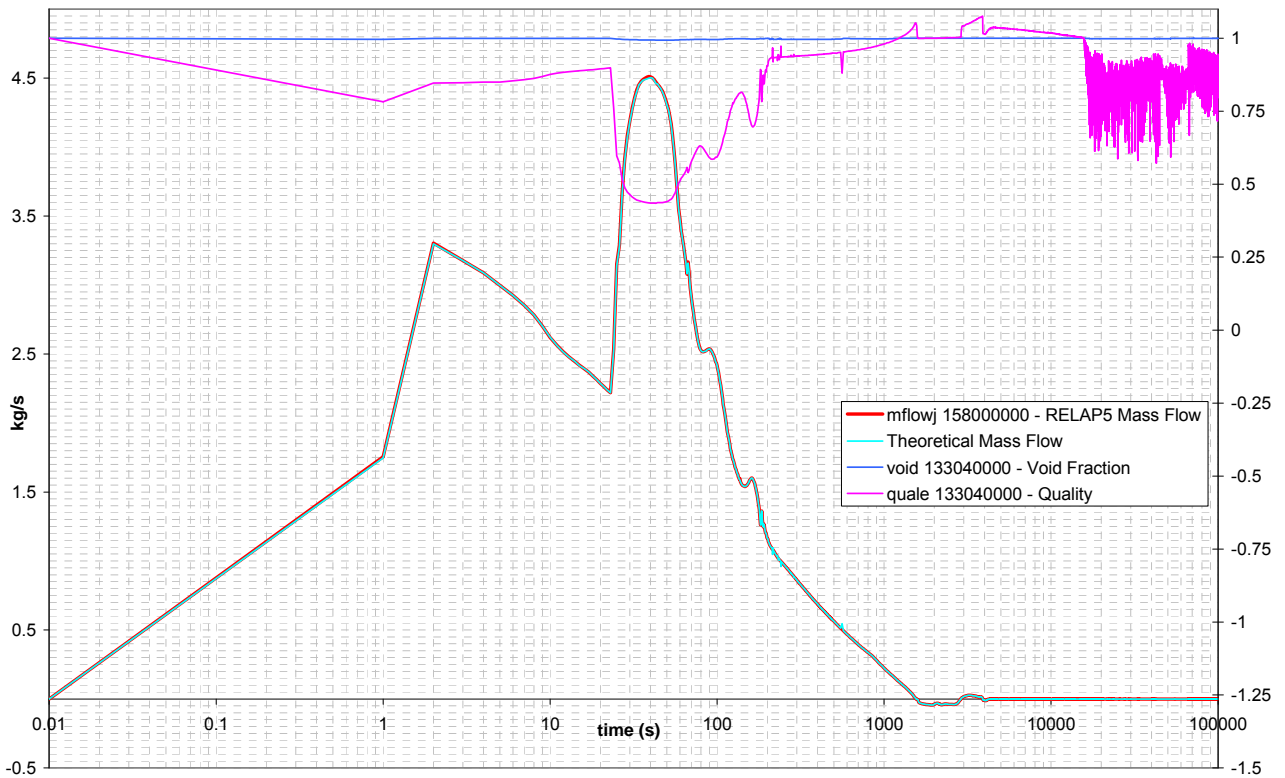


Figure 5.7: Comparison between the RELAP5 and theoretical mass flow, void fraction and quality in ADS SPLIT break line, ADS Test

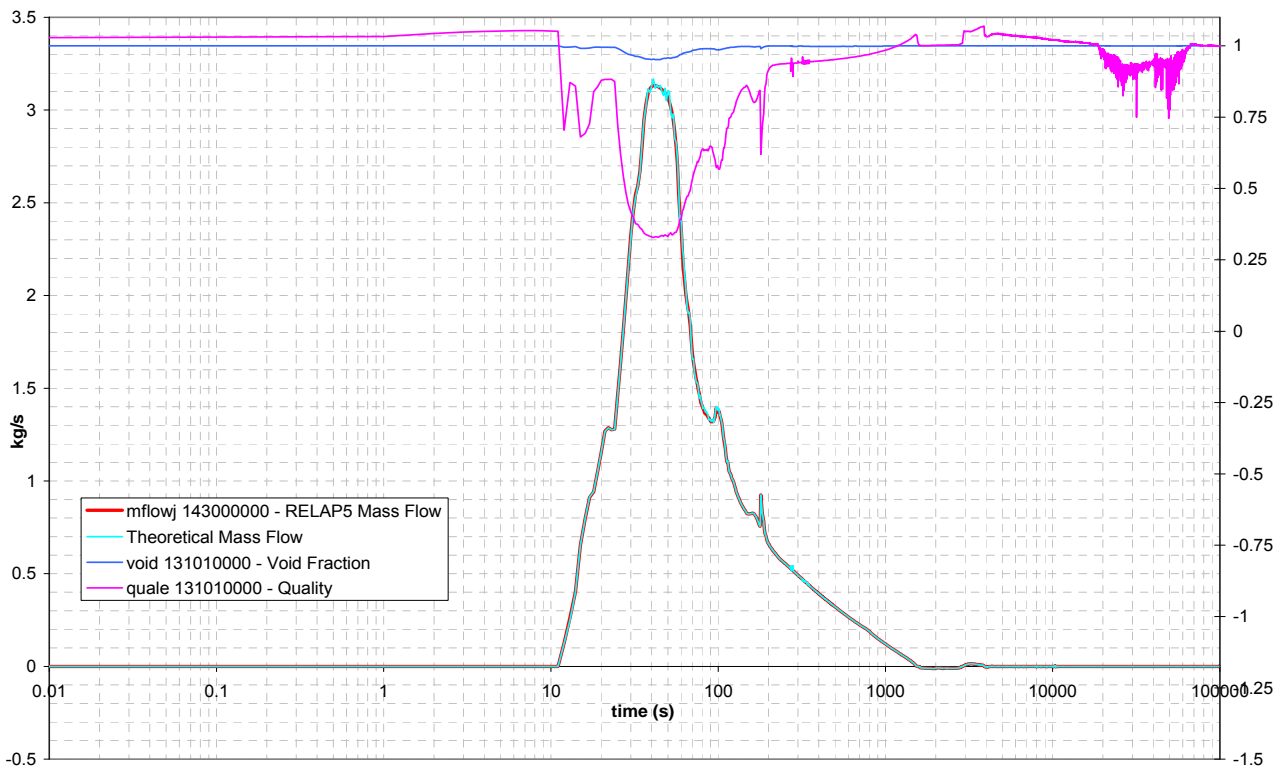


Figure 5.8: Comparison between the RELAP5 and theoretical mass flow, void fraction and quality in ADS Stage-I DT line, ADS Test

The Figure 5.9, Figure 5.10, Figure 5.11, Figure 5.12, Figure 5.13, Figure 5.14, Figure 5.15 and Figure 5.16 show the comparison of the calculated and RELAP5 mass flow rates, besides the information on the flow regimes and the presence of choked flow at the rupture orifice (not in the instrumented volume, in which the flow is always not critical). The information about the flow regimes is useful for a correct determination of the Drag Disk shape and for the Turbine Flowmeter models.

The Table 5.1 lists the conventional numbers used in the graph to indicate whether the flow is critical or not and the flow regimes.

Table 5.1: List of the conventional numbers used in the graphs to indicate whether the flow is critical or not and the flow regimes

Choked Flow		Flow Regimes	
Value	Description	Value	Description
0	Not choked	0.4	Bubbly
1	choked	0.6	Annular Mist
		0.7	Mist pre-CHF
		1.2	Horizontal stratified

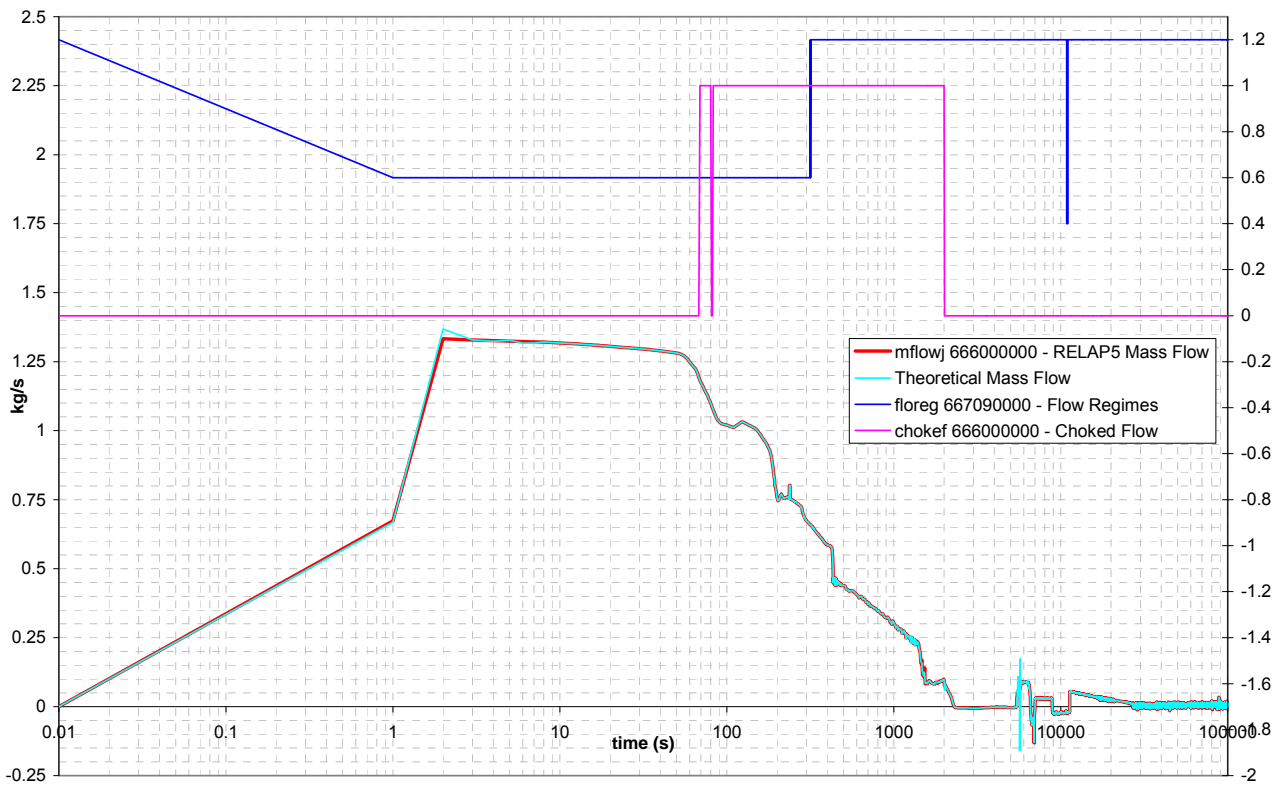


Figure 5.9: Comparison between the RELAP5 and theoretical mass flow, flow regimes and presence of critical flow in DVI SPLIT beak line, DVI Test

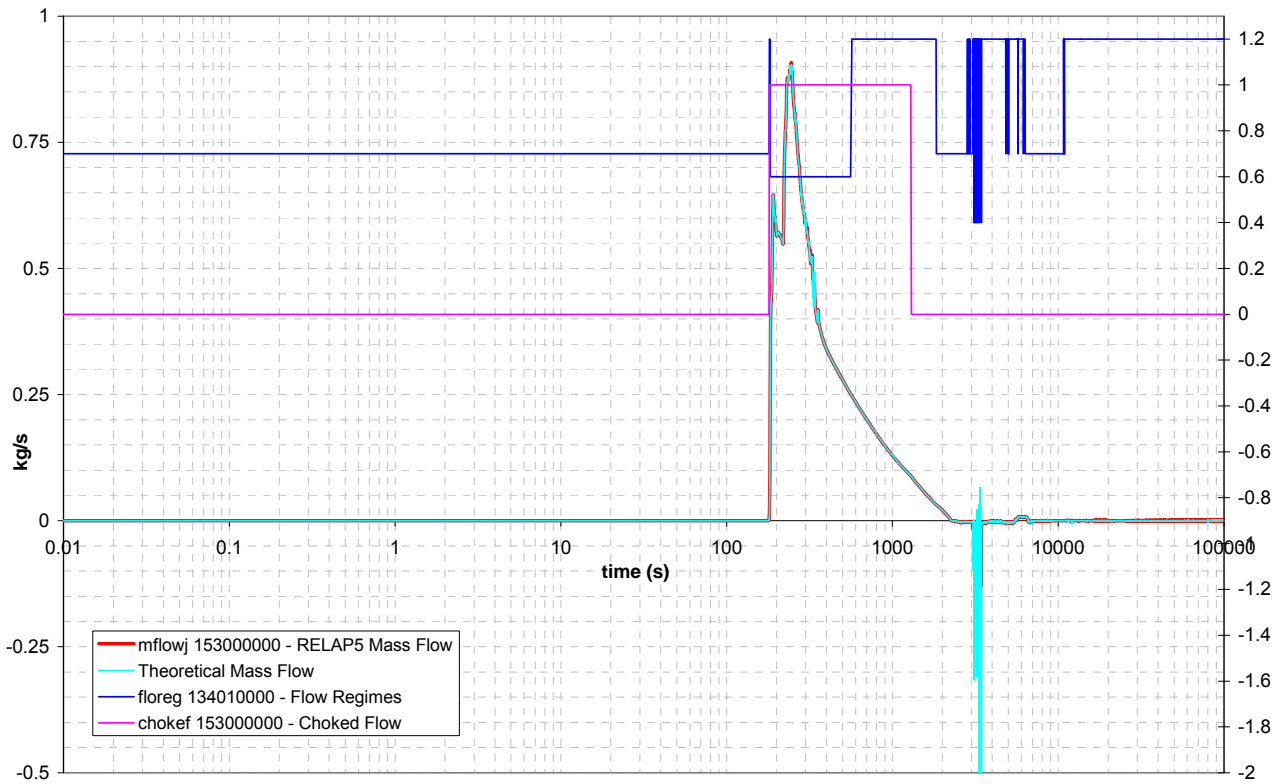


Figure 5.10: Comparison between the RELAP5 and theoretical mass flow, flow regimes and presence of critical flow in ADS ST stage I line, DVI Test

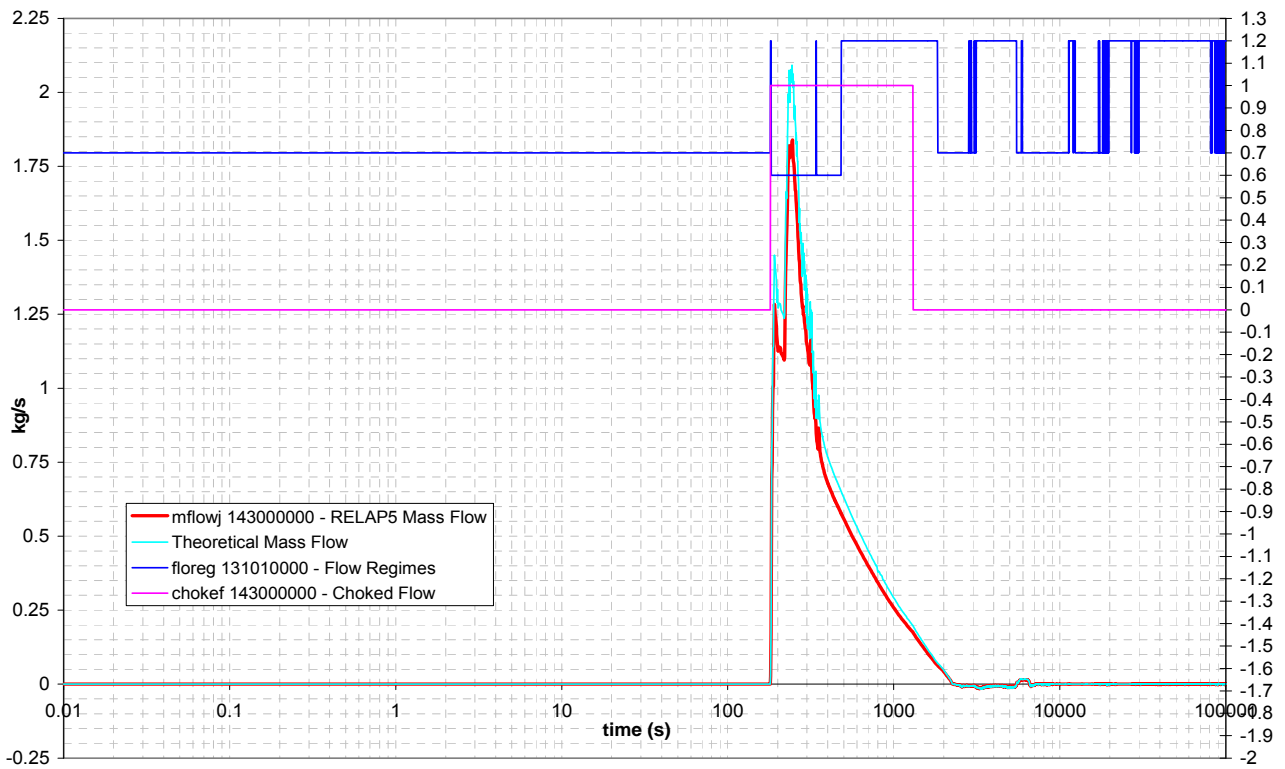


Figure 5.11: Comparison between the RELAP5 and theoretical mass flow, flow regimes and presence of critical flow in ADS DT stage I line, DVI Test

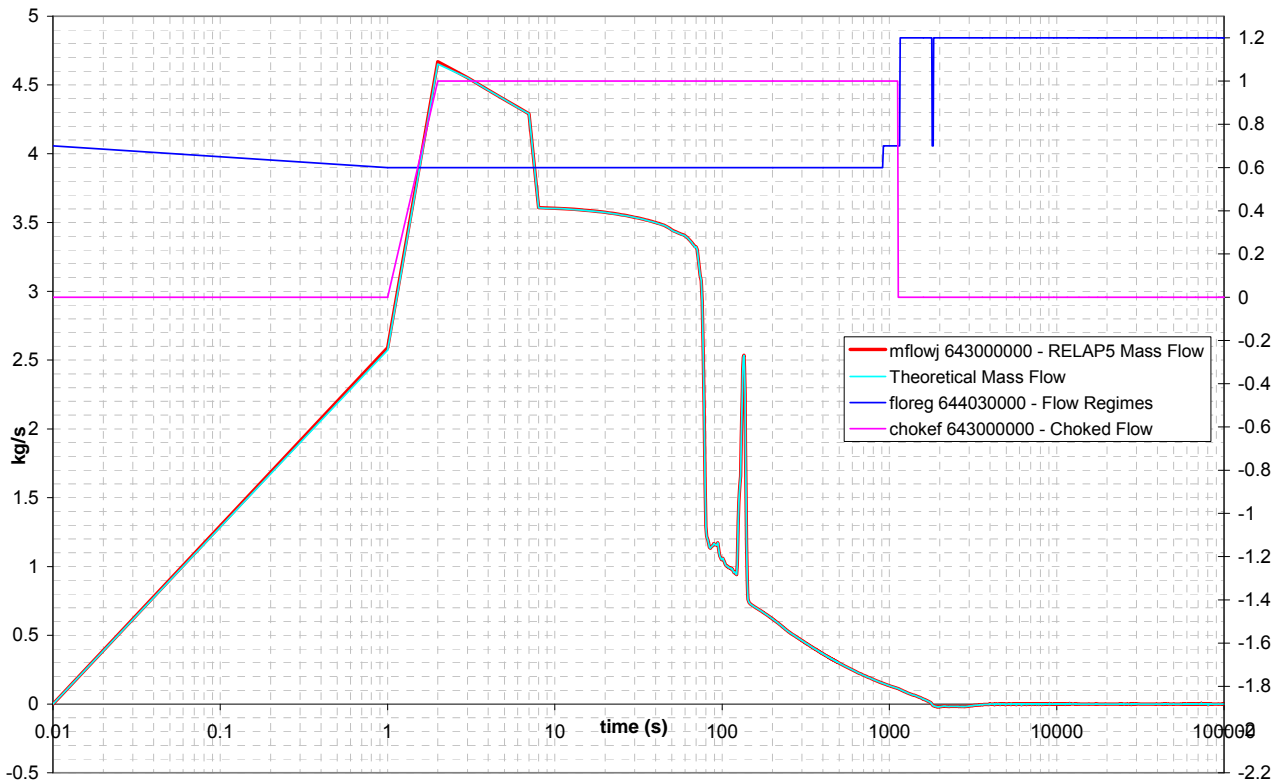


Figure 5.12: Comparison between the RELAP5 and theoretical mass flow, flow regimes and presence of critical flow in EBT SPLIT beak line, EBT Test

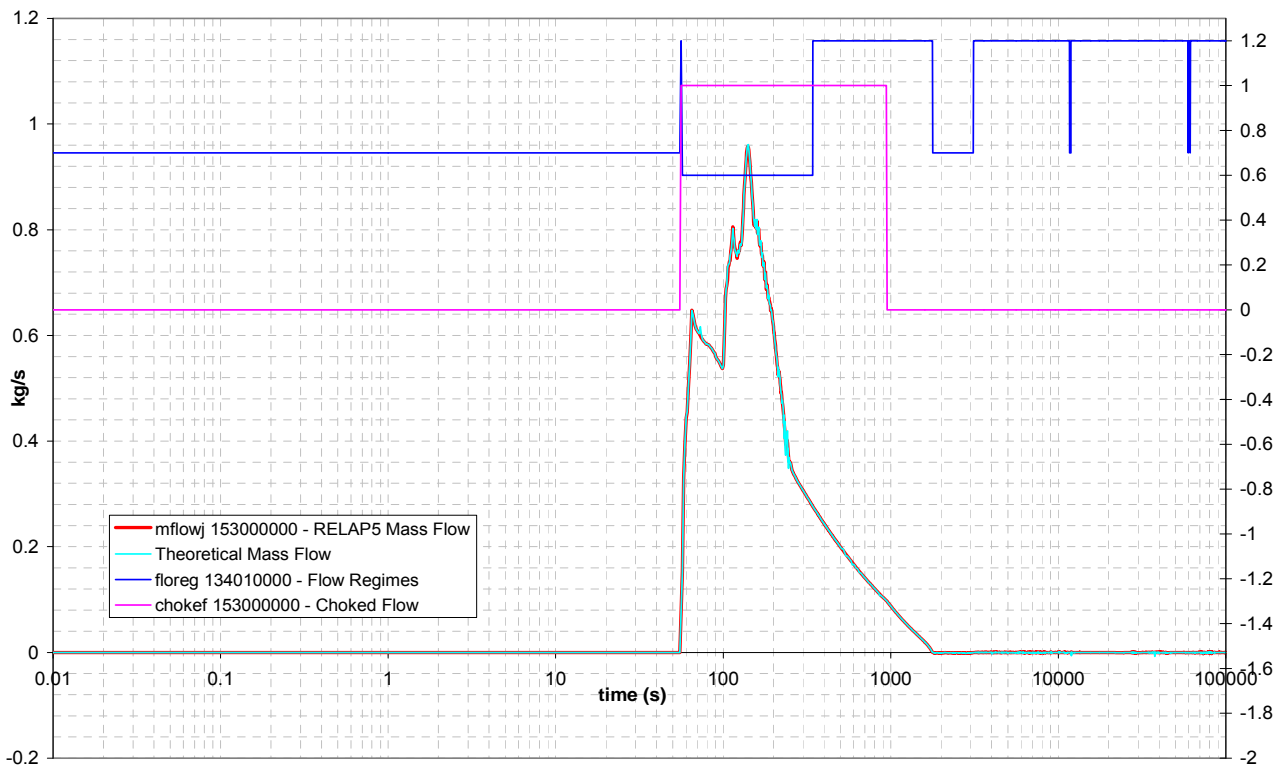


Figure 5.13: Comparison between the RELAP5 and theoretical mass flow, flow regimes and presence of critical flow in ADS Stage-I ST line, EBT Test

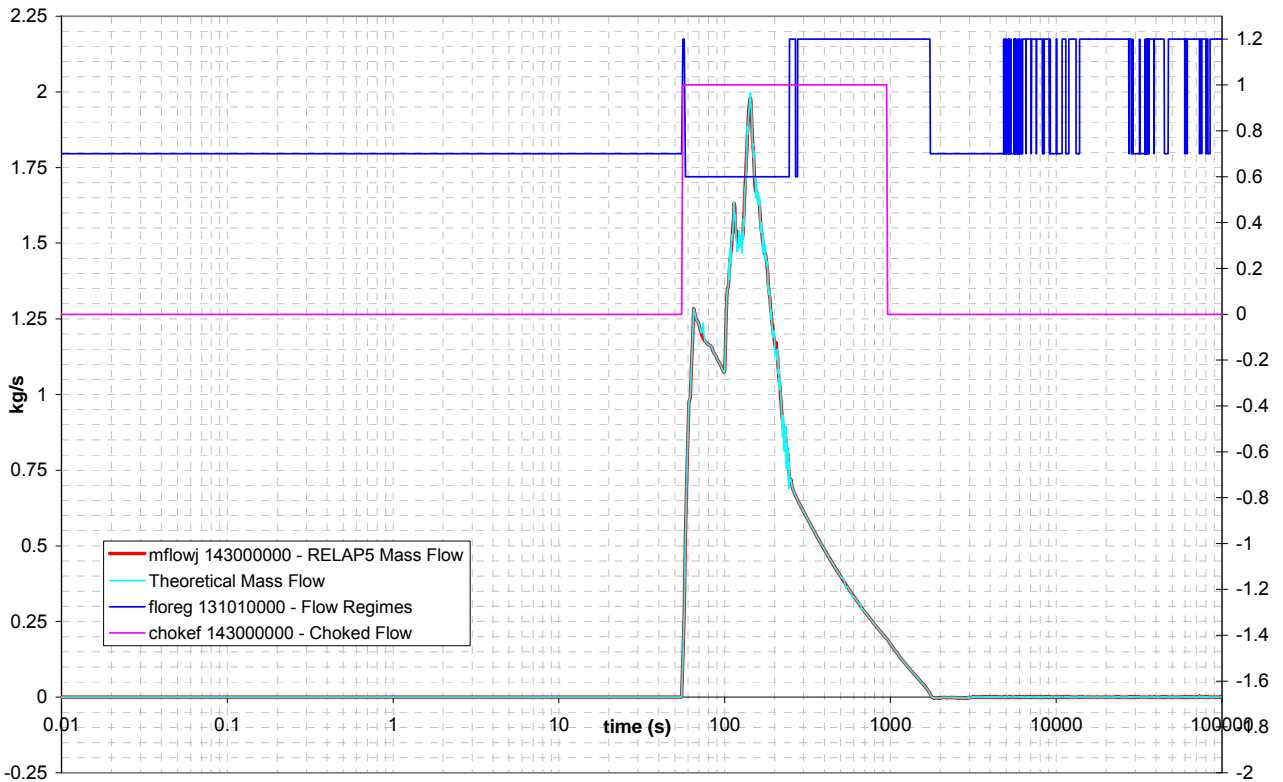


Figure 5.14: Comparison between the RELAP5 and theoretical mass flow, flow regimes and presence of critical flow in ADS Stage-I DT line, EBT Test

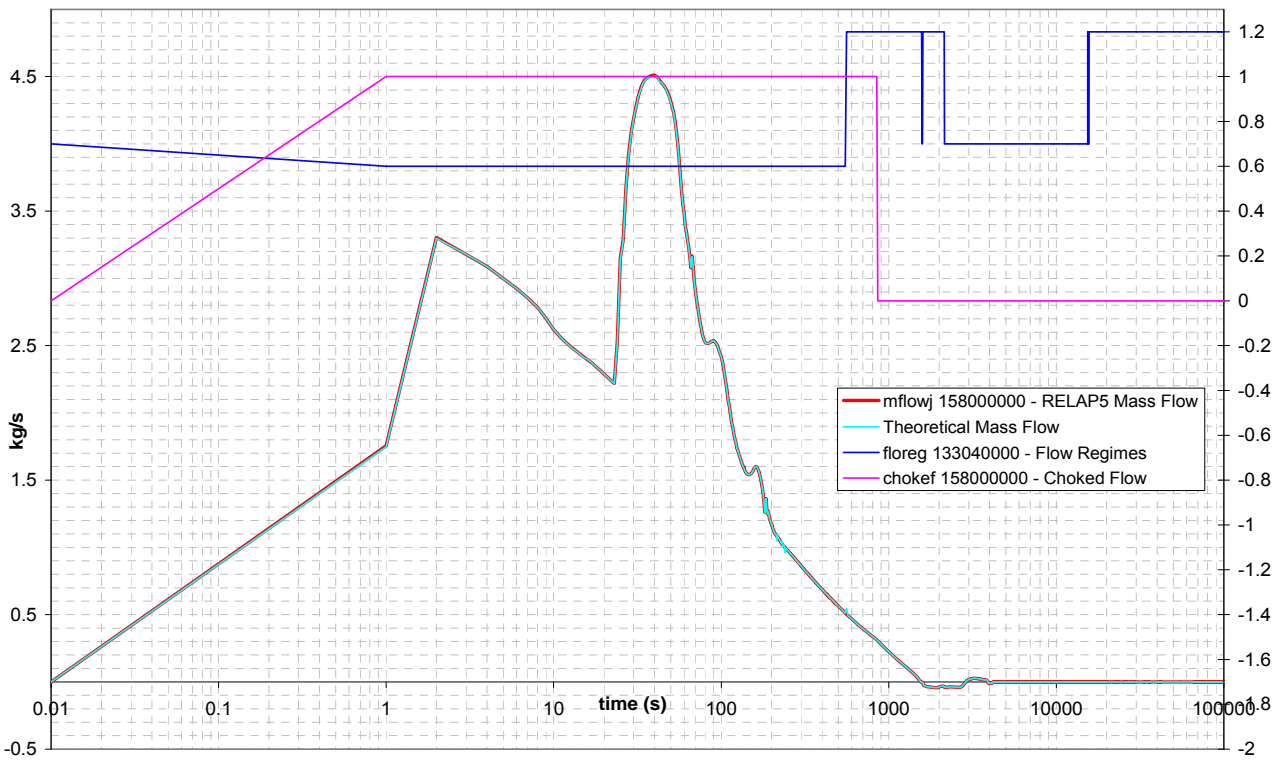


Figure 5.15: Comparison between the RELAP5 and theoretical mass flow, flow regimes and presence of critical flow in ADS SPLIT beak line, ADS Test

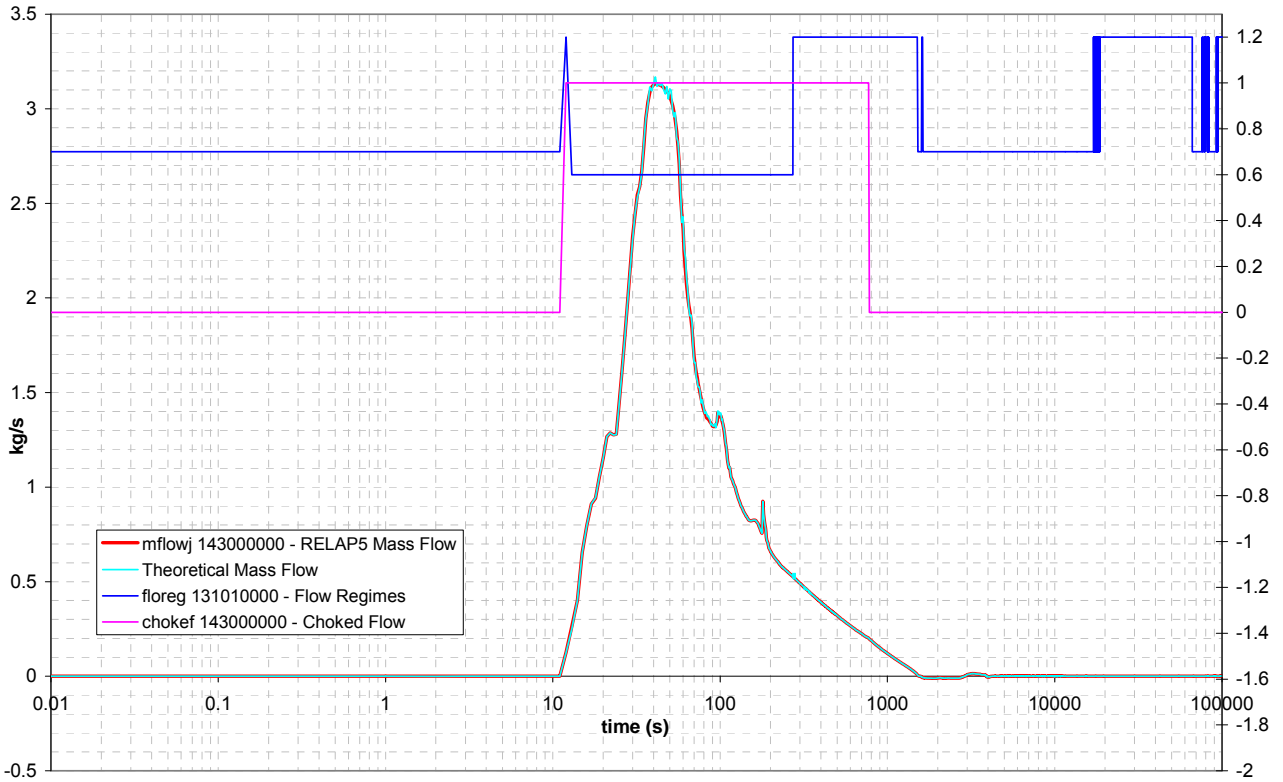


Figure 5.16: Comparison between the RELAP5 and theoretical mass flow, flow regimes and presence of critical flow in ADS Stage-I DT line, ADS Test

Slip ratio, void fraction and quality are related using the standard mass flow rates, as follows:

$$x = \frac{\dot{m}_G}{\dot{m}} = \frac{\dot{m}_G}{\dot{m}_G + \dot{m}_L} = \frac{\alpha \rho_G V_G}{\alpha \rho_G V_G + (1-\alpha) \rho_L V_L} = \frac{\frac{\alpha}{(1-\alpha)} \frac{\rho_G}{\rho_L} \frac{V_G}{V_L}}{\frac{\alpha}{(1-\alpha)} \frac{\rho_G}{\rho_L} \frac{V_G}{V_L} + 1} \quad (5.2)$$

$$x + \frac{\alpha}{(1-\alpha)} \frac{\rho_G}{\rho_L} S x = \frac{\alpha}{(1-\alpha)} \frac{\rho_G}{\rho_L} S \quad (5.3)$$

$$x = \frac{\alpha}{(1-\alpha)} \frac{\rho_G}{\rho_L} S (1-x) \quad (5.4)$$

$$S = \frac{(1-\alpha) \rho_L}{\alpha \rho_G} \frac{x}{(1-x)}, \quad (5.5)$$

in particular,

$$\frac{x}{(1-x)} = \frac{\alpha}{(1-\alpha)} \frac{\rho_G}{\rho_L} S, \quad (5.6)$$

Equation (5.6) can be useful to express the mass flow rate (5.1) in another form:

$$\dot{m} = A[\alpha\rho_G V_G + (1-\alpha)\rho_L V_L] = A\rho_L V_L(1-\alpha) \left[\frac{\alpha}{(1-\alpha)} \frac{\rho_G}{\rho_L} \frac{V_G}{V_L} + 1 \right] \quad (5.7)$$

$$\dot{m} = A\rho_L V_L(1-\alpha) \left[\frac{x}{1-x} + 1 \right] = A\rho_L V_L(1-\alpha) \left[\frac{1}{1-x} \right] = A\rho_L V_L \left[\frac{1-\alpha}{1-x} \right]. \quad (5.8)$$

A dimensional analysis shows that it's possible to determine the mass flow rate from two independent measured variables, according to the following expressions:

$$\dot{m}_{Void+DD} = A \cdot [\rho_{AV} \cdot (\rho V^2)]^{1/2} \quad \text{Drag Disk + Void Fraction Detector} \quad (5.9)$$

$$\dot{m}_{T+DD} = A \cdot \left[\frac{(\rho V^2)}{V_T} \right] \quad \text{Drag Disk + Turbine Flowmeter} \quad (5.10)$$

$$\dot{m}_{Void+T} = A \cdot \rho_{AV} \cdot V_T \quad \text{Void Fraction Detector + Turbine Flowmeter} \quad (5.11)$$

As two analytical expressions are enough to solve the equation system, it is possible to use the third expression as checker.

Since the Drag Disk returns the pressure drop in addition to the drag force, two expressions can be derived in order to determine the momentum flux:

$$(\rho V^2) = \frac{2F_D}{C_D A_S} \quad (5.12)$$

$$(\rho V^2) = \frac{\Delta P}{K}, \quad (5.13)$$

It is possible to arrive to 5 different formulations involving the couplings of the three instruments:

Drag Disk + Turbine Flowmeter

$$\dot{m} = A \cdot \left[\frac{(\rho V^2)}{V_T} \right] = A \cdot \left[\frac{2F_D}{C_D A_S} \frac{1}{V_T} \right] \quad \text{with Drag Force} \quad (5.14)$$

$$\dot{m} = A \cdot \left[\frac{(\rho V^2)}{V_T} \right] = A \cdot \left[\frac{\Delta P}{K} \frac{1}{V_T} \right] \quad \text{with Pressure Drop} \quad (5.15)$$

Drag Disk + Void Fraction Detector

$$\dot{m} = A \cdot [\rho_{AV} \cdot (\rho V^2)]^{1/2} = A \cdot \left[\rho_{AV} \cdot \frac{2F_D}{C_D A_S} \right]^{1/2} \quad \text{with Drag Force} \quad (5.16)$$

$$\dot{m} = A \cdot [\rho_{AV} \cdot (\rho V^2)]^{1/2} = A \cdot \left[\rho_{AV} \cdot \frac{\Delta P}{K} \right]^{1/2} \quad \text{with Pressure Drop} \quad (5.17)$$

Void Fraction Detector + Turbine Flowmeter

$$\dot{m} = A \cdot \rho_{AV} \cdot V_T \quad (5.18)$$

As both the pressure drop signal and the drag force signal are proportional to the momentum flux ρV^2 , only the equations (5.9), (5.10) and (5.11) are used for the data reduction analyses.

The next section presents the different couplings and the uncertainties related to the use of two or three instruments. When the Turbine Flowmeter is involved, the analysis is done for each velocity model.

5.1 Drag Disk and Void Fraction Detector

Coupling the momentum flux calculated according to (4.3) and the mixture density expressed by (4.12), the mass flow rate can be determined, (5.9), as follows

$$\dot{m}_{Void+DD} = A \cdot [\rho_{AV} \cdot (\rho V^2)]^{1/2} = A \cdot [(\alpha \rho_G + (1-\alpha)\rho_L) \cdot (V_L^2 (\alpha \rho_G S^2 + (1-\alpha)\rho_L))]^{1/2} \quad (5.19)$$

$$\dot{m}_{Void+DD} = A \cdot V_L [(\alpha \rho_G + (1-\alpha)\rho_L) \cdot (\alpha \rho_G S^2 + (1-\alpha)\rho_L)]^{1/2} \quad (5.20)$$

$$\dot{m}_{Void+DD} = A \cdot V_L \cdot \rho_L \left[\left(\alpha \frac{\rho_G}{\rho_L} + (1-\alpha) \right) \cdot \left(\alpha \frac{\rho_G}{\rho_L} S^2 + (1-\alpha) \right) \right]^{1/2} \quad (5.21)$$

$$\dot{m}_{Void+DD} = A \cdot V_L \cdot \rho_L (1-\alpha) \left[\left(\frac{\alpha}{(1-\alpha)} \frac{\rho_G}{\rho_L} + 1 \right) \cdot \left(\frac{\alpha}{(1-\alpha)} \frac{\rho_G}{\rho_L} S^2 + 1 \right) \right]^{1/2} \quad (5.22)$$

Using the (5.6),

$$\frac{\alpha}{(1-\alpha)} \frac{\rho_G}{\rho_L} = \frac{x}{(1-x)} \frac{1}{S} \quad (5.23)$$

and replacing in the former expression

$$\dot{m}_{Void+DD} = A \cdot V_L \cdot \rho_L (1-\alpha) \left[\left(\frac{x}{(1-x)} \frac{1}{S} + 1 \right) \cdot \left(\frac{x}{(1-x)} S + 1 \right) \right]^{\frac{1}{2}} \quad (5.24)$$

$$\dot{m}_{Void+DD} = A \cdot V_L \cdot \rho_L \frac{(1-\alpha)}{(1-x)} \left[\left(x \frac{1}{S} + 1 - x \right) \cdot (xS + 1 - x) \right]^{\frac{1}{2}} \quad (5.25)$$

$$\dot{m}_{Void+DD} = A \cdot V_L \cdot \rho_L \frac{(1-\alpha)}{(1-x)} \left[\left(\frac{x + (1-x)S}{S} \right) \cdot (xS + 1 - x) \right]^{\frac{1}{2}} \quad (5.26)$$

$$\dot{m}_{Void+DD} = A \cdot V_L \cdot \rho_L \frac{(1-\alpha)}{(1-x)} \left[(x + (1-x)S) \cdot \left(x + \frac{(1-x)}{S} \right) \right]^{\frac{1}{2}} \quad (5.27)$$

The comparison of the equation (5.27) with the equation (5.8) shows that the coupling of a Void Fraction Detector signal and a Drag Disk signal does not give the exact mass flow rate. The error is described by the factor K_s ,

$$K_s = \left((x + (1-x)S) \cdot \left(x + \frac{(1-x)}{S} \right) \right) \quad (5.28)$$

that depends on two thermal-hydraulic variables: the steam quality and the slip ratio. In order to determine the actual value of the mass flow rate, it is necessary to divide the combination of the two instrument outputs by $K_s^{1/2}$:

$$\dot{m} = \frac{\dot{m}_{Void+DD}}{K_s^{1/2}} = A \cdot \left[\frac{\rho_{AV} (\rho V^2)}{K_s} \right]^{\frac{1}{2}} \quad (5.29)$$

The Figure 5.17 show the comparison between the actual RELAP5 mass flow rate and the mass flow rate achieved with the Void Fraction Detector and the Drag Disk, according to (5.27), for the DVI SPLIT break line. The comparison for the other lines is illustrated in section {6}; here the DVI break line is given as an example.

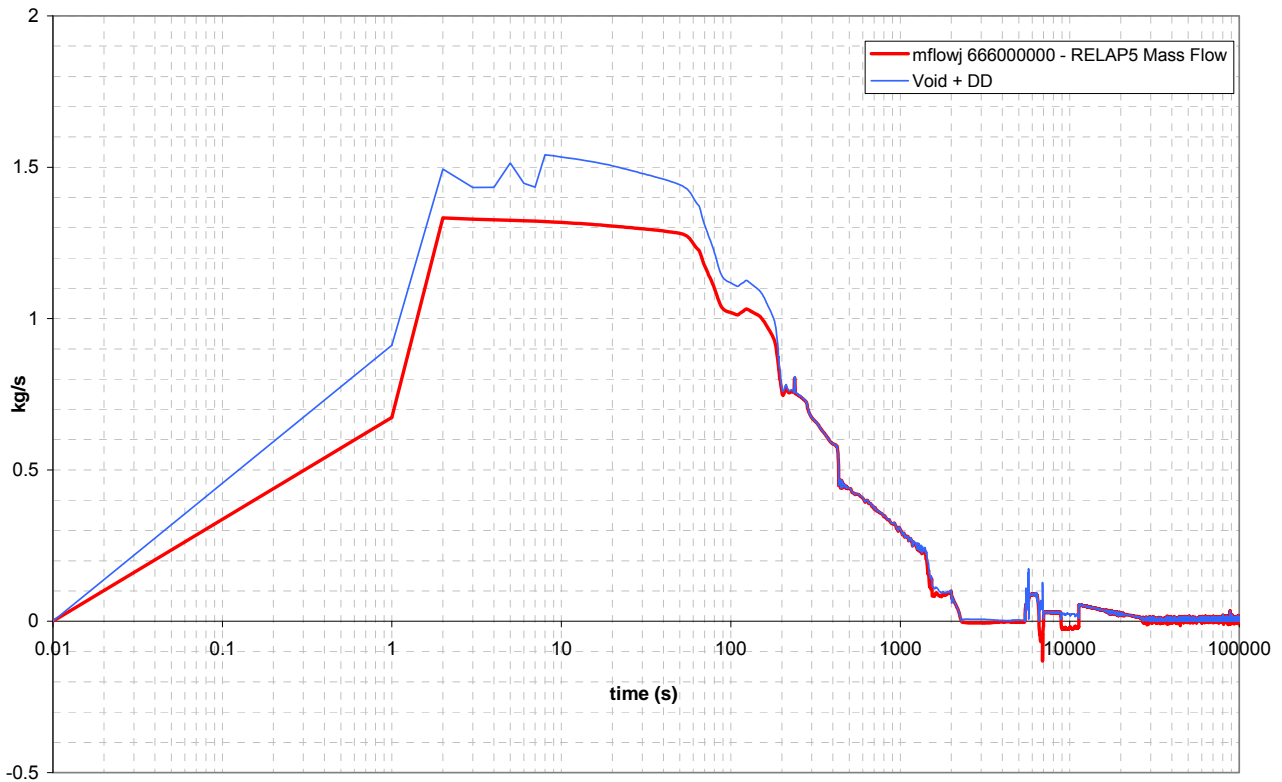


Figure 5.17: Comparison between the mass flow rate obtained by the coupling of two instruments (DD + Void) and the RELAP5 mass flow rate in the DVI SPLIT line, DVI break test

At any time step of the transient, the analytical responses of the two instruments have been calculated using the thermal-hydraulic variables extracted from the RELAP5 data and the outputs have been combined and multiplied for the cross-section area. The plot shows that the theoretical response of the spool piece (Void + DD) follows the same trend, but it is not equal to the mass flow rate, and the error is proportional to the absolute value. It is also not possible to reduce the gap to a constant factor, because it depends on the thermal-hydraulic conditions.

The steam quality and the slip ratio are linked to the void fraction by equation (5.4). Since the value of the void fraction during the transient is provided by the Void Fraction Detector, to have the exact value of K_s , it is necessary to know the quality or the slip ratio.

From the equations, the known variables and unknown terms are as follows:

- | | | |
|--|------------------|---|
| a) $\rho_{AV} = \alpha\rho_G + (1-\alpha)\rho_L$ | α | derived from the Void Fraction Detector |
| | ρ_G, ρ_L | function of the pressure |
| | ρ_{AV} | derived from the previous quantities |

b) $(\rho V^2) = V_L^2 (\alpha \rho_G S^2 + (1 - \alpha) \rho_L)$	S	unknown
	V_L	unknown
	ρV^2	derived from the Drag Disk
c) $s = \frac{(1 - \alpha) \rho_L}{\alpha \rho_G} \frac{x}{(1 - x)}$	x	unknown
d) $\dot{m} = A \cdot \left[\frac{\rho_{AV} (\rho V^2)}{(x + (1 - x)S) \cdot \left(x + \frac{(1 - x)}{S} \right)} \right]^{\frac{1}{2}}$	\dot{m}	unknown

Except for equation a), which is completely defined, the other three equations (b, c, d) involve four unknowns terms, which requires another equation.

The unique way to complete the mathematical system is to use the third instrument, which is the Turbine Flowmeter. The three models of the turbine, in which for convenience the liquid velocity is explicit, are presented below. Each of such velocity expressions completes the mathematical system and allows to solve it.

$$V_L = V_T \frac{\sqrt{\rho_L(1 - \alpha)} + \sqrt{\rho_G \alpha}}{\sqrt{\rho_L(1 - \alpha)} + S \sqrt{\rho_G \alpha}} \quad \text{Aya model} \quad (5.30)$$

$$V_L = V_T \frac{\alpha \rho_G S + (1 - \alpha) \rho_L}{\alpha \rho_G S^2 + (1 - \alpha) \rho_L} \quad \text{Rouhani model} \quad (5.31)$$

$$V_L = V_T \frac{1}{(S \alpha + (1 - \alpha))} \quad \text{Volumetric model} \quad (5.32)$$

The mathematical analysis shows that it is not possible to determine the exact mass flow rate using the Void Fraction Detector and the Drag Disk *only*, but the Turbine Flowmeter is necessary in order to reduce the result uncertainty. The three instrument spool piece can evaluate accurately the mass flow rate, the quality and the slip ratio during the transient.

5.2 Drag Disk and Turbine Flowmeter

The coupling of the Drag Disk with the Turbine Flowmeter is done considering the three Turbine models separately, since experimental data are not available to identify which one better describes the mixture velocity.

5.2.1 Rouhani model

Coupling the momentum flux calculated according to (4.3) and the Rouhani mixture velocity expressed by (4.7), the mass flow rate can be determined, (5.10), as follows

$$\dot{m}_{DD+T_Rou} = A \cdot \rho V^2 / V_T = A \cdot \frac{V_L^2 (\alpha \rho_G S^2 + (1-\alpha) \rho_L)}{V_L \frac{\alpha \rho_G S^2 + (1-\alpha) \rho_L}{\alpha \rho_G S + (1-\alpha) \rho_L}} \quad (5.33)$$

$$\dot{m}_{DD+T_Rou} = A \cdot V_L (\alpha \rho_G S + (1-\alpha) \rho_L) \quad (5.34)$$

$$\dot{m}_{DD+T_Rou} = A \cdot V_L \cdot \rho_L \cdot (1-\alpha) \left(\frac{\alpha}{(1-\alpha)} \frac{\rho_G}{\rho_L} S + 1 \right) \quad (5.35)$$

Using the (5.6),

$$\frac{\alpha}{(1-\alpha)} \frac{\rho_G}{\rho_L} S = \frac{x}{(1-x)} \quad (5.36)$$

and replacing in the former expression

$$\dot{m}_{DD+T_Rou} = A \cdot V_L \cdot \rho_L \cdot (1-\alpha) \left(\frac{x}{(1-x)} + 1 \right) \quad (5.37)$$

$$\dot{m}_{DD+T_Rou} = A \cdot V_L \cdot \rho_L \cdot (1-\alpha) \left(\frac{x+1-x}{(1-x)} \right) \quad (5.38)$$

$$\dot{m}_{DD+T_Rou} = A \cdot V_L \cdot \rho_L \cdot (1-\alpha) \left(\frac{1}{(1-x)} \right) = A \cdot V_L \cdot \rho_L \cdot \frac{(1-\alpha)}{(1-x)} \quad (5.39)$$

The coupling of a Drag Disk and a Turbine Flowmeter with the Rouhani model provide an expression for the mass flow (5.39) that is exactly the theoretical expression of mass flow (5.8).

This analytical result involves that, if the Rouhani model depicts the turbine behaviour correctly or with an acceptable error, the mass flow rate can be obtained avoiding the use of the Void Fraction Detector, which, as mentioned above, presents the biggest problems. Anyway, the use of these devices does not give any information about the quality, for which the third instrument is fundamental.

5.2.2 Aya Model

Coupling the momentum flux calculated according to (4.3) and the Aya mixture velocity expressed by (4.9), the mass flow rate can be determined, (5.10), as follows

$$\dot{m}_{DD+T_Aya} = A \cdot \rho V^2 \Big/ V_T = A \cdot \frac{V_L^2 (\alpha \rho_G S^2 + (1-\alpha) \rho_L)}{V_L \frac{\sqrt{\rho_L(1-\alpha)} + S \sqrt{\rho_G \alpha}}{\sqrt{\rho_L(1-\alpha)} + \sqrt{\rho_G \alpha}}} \quad (5.40)$$

$$\dot{m}_{DD+T_Aya} = A \cdot V_L \cdot \rho_L \cdot (1-\alpha) \frac{\left(\frac{\alpha}{(1-\alpha)} \frac{\rho_G}{\rho_L} S^2 + 1 \right)}{\frac{\sqrt{\rho_L(1-\alpha)} + S \sqrt{\rho_G \alpha}}{\sqrt{\rho_L(1-\alpha)} + \sqrt{\rho_G \alpha}}} \quad (5.41)$$

Using the (5.6),

$$\frac{\alpha}{(1-\alpha)} \frac{\rho_G}{\rho_L} S = \frac{x}{(1-x)} \quad (5.42)$$

and replacing in the former expression

$$\dot{m}_{DD+T_Aya} = A \cdot V_L \cdot \rho_L \cdot (1-\alpha) \frac{\left(\frac{x}{(1-x)} S + 1 \right)}{\frac{\sqrt{\rho_L(1-\alpha)} + S \sqrt{\rho_G \alpha}}{\sqrt{\rho_L(1-\alpha)} + \sqrt{\rho_G \alpha}}} \quad (5.43)$$

$$\dot{m}_{DD+T_Aya} = A \cdot V_L \cdot \rho_L \cdot (1-\alpha) \frac{\left(\frac{xS + 1 - x}{1-x} \right)}{\frac{\sqrt{\rho_L(1-\alpha)} + S \sqrt{\rho_G \alpha}}{\sqrt{\rho_L(1-\alpha)} + \sqrt{\rho_G \alpha}}} \quad (5.44)$$

$$\dot{m}_{DD+T_Aya} = A \cdot V_L \cdot \rho_L \cdot \frac{(1-\alpha)}{(1-x)} \left[\frac{1-x+xS}{\frac{\sqrt{\rho_L(1-\alpha)} + S\sqrt{\rho_G\alpha}}{\sqrt{\rho_L(1-\alpha)} + \sqrt{\rho_G\alpha}}} \right] \quad (5.45)$$

The comparison of the equation (5.45) with the equation (5.8) shows that the coupling of a turbine flowmeter and a Drag Disk does not give the exact mass flow rate, if the Aya model is used to calculate the mixture velocity. The error is described by the factor K_{M1} ,

$$K_{M1} = \frac{1-x+xS}{\frac{\sqrt{\rho_L(1-\alpha)} + S\sqrt{\rho_G\alpha}}{\sqrt{\rho_L(1-\alpha)} + \sqrt{\rho_G\alpha}}} \quad (5.46)$$

Such error term depends on three thermal-hydraulic variables: the steam quality, the slip ratio and the pressure. In order to determine the actual value of the mass flow rate, it is necessary to divide the combination of the two instrument outputs by K_{M1} :

$$\dot{m} = \frac{\dot{m}_{DD+T_Aya}}{K_{M1}} = A \cdot \frac{(\rho V^2) / V_T}{K_{M1}} \quad (5.47)$$

To obtain the value of K_{M1} the Void Fraction Detector is necessary. The considerations are the same of section {5.1} and the comparison for all the lines involved in the transients are shown in section {6}.

5.2.3 Volumetric Model

Coupling the momentum flux calculated according to (4.3) and the volumetric mixture velocity expressed by (4.11), the mass flow rate can be determined, (5.10), as follows

$$\dot{m}_{DD+T_Vol} = A \cdot \rho V^2 / V_T = A \cdot \frac{V_L^2 (\alpha \rho_G S^2 + (1-\alpha) \rho_L)}{V_L (S\alpha + (1-\alpha))} \quad (5.48)$$

$$\dot{m}_{DD+T_Vol} = A \cdot V_L \frac{(\alpha \rho_G S^2 + (1-\alpha) \rho_L)}{(S\alpha + (1-\alpha))} \quad (5.49)$$

$$\dot{m}_{DD+T_Vol} = A \cdot V_L \cdot \rho_L \cdot (1-\alpha) \frac{\left(\frac{\alpha}{(1-\alpha)} \frac{\rho_G}{\rho_L} S^2 + 1 \right)}{(1-\alpha + \alpha S)} \quad (5.50)$$

Using the (5.6),

$$\frac{\alpha}{(1-\alpha)} \frac{\rho_G}{\rho_L} S = \frac{x}{(1-x)} \quad (5.51)$$

and replacing in the former expression

$$\dot{m}_{DD+T_Vol} = A \cdot V_L \cdot \rho_L \cdot (1-\alpha) \frac{\left(\frac{x}{(1-x)} S + 1 \right)}{(1-\alpha + \alpha S)} \quad (5.52)$$

$$\dot{m}_{DD+T_Vol} = A \cdot V_L \cdot \rho_L \cdot (1-\alpha) \frac{\left(\frac{xS + 1 - x}{1-x} \right)}{(1-\alpha + \alpha S)} \quad (5.53)$$

$$\dot{m}_{DD+T_Vol} = A \cdot V_L \cdot \rho_L \cdot \frac{(1-\alpha)(1-x + xS)}{(1-x)(1-\alpha + \alpha S)} \quad (5.54)$$

The comparison of the equation (5.54) with the equation (5.8) shows that the coupling of a turbine flowmeter drawn by the volumetric model and a Drag Disk does not give the exact mass flow rate. The error is described by the factor K_{M2} ,

$$K_{M2} = \frac{(1-x + xS)}{(1-\alpha + \alpha S)} \quad (5.55)$$

Such error term depends on three thermal-hydraulic variables: the steam quality, the slip ratio and the void fraction. In order to determine the actual value of the mass flow rate, it is necessary to divide the combination of the two instrument outputs by K_{M2} :

$$\dot{m} = \frac{\dot{m}_{DD+T_Vol}}{K_{M2}} = A \cdot \frac{(\rho V^2) / V_T}{K_{M2}} \quad (5.56)$$

To obtain the value of K_{M2} the Void Fraction Detector, is necessary. The considerations are the same of section {5.1} and the comparison for all the lines involved in the transients are shown in section {6}.

5.3 Void Fraction Detector and Turbine Flowmeter

The coupling of the Void Fraction Detector with the Turbine Flowmeter has been done considering the three models separately, as experimental data are not available for the present configuration to identify which one describes better the mixture velocity.

5.3.1 Rouhani Model

Coupling the mixture density calculated according to (4.12) and the Rouhani mixture velocity expressed by (4.7), the mass flow rate can be determined, (5.11), as follows

$$\dot{m}_{Void+T_Rou} = A \cdot \rho_{AV} \cdot V_T = A \cdot (\alpha \rho_G + (1-\alpha) \rho_L) \cdot V_L \cdot \frac{\alpha \rho_G S^2 + (1-\alpha) \rho_L}{\alpha \rho_G S + (1-\alpha) \rho_L} \quad (5.57)$$

$$\dot{m}_{Void+T_Rou} = A \cdot \rho_L \cdot V_L (1-\alpha) \left(\frac{\alpha \rho_G}{(1-\alpha) \rho_L} + 1 \right) \frac{\frac{\alpha \rho_G}{(1-\alpha) \rho_L} S^2 + 1}{\frac{\alpha \rho_G}{(1-\alpha) \rho_L} S + 1} \quad (5.58)$$

$$\dot{m}_{Void+T_Rou} = A \cdot \rho_L \cdot V_L (1-\alpha) \left(\frac{\alpha \rho_G}{(1-\alpha) \rho_L} + 1 \right) \cdot \frac{\frac{\alpha \rho_G}{(1-\alpha) \rho_L} S^2 + 1}{\frac{\alpha \rho_G}{(1-\alpha) \rho_L} S + 1} \quad (5.59)$$

Using the (5.6),

$$\frac{\alpha \rho_G}{(1-\alpha) \rho_L} S = \frac{x}{(1-x)} \quad (5.60)$$

and replacing in the former expression

$$\dot{m}_{Void+T_Rou} = A \cdot \rho_L \cdot V_L (1-\alpha) \left(\frac{x}{(1-x) S} + 1 \right) \cdot \frac{\frac{x}{(1-x)} S + 1}{\left(\frac{x}{(1-x)} \right) + 1} \quad (5.61)$$

$$\dot{m}_{Void+T_Rou} = A \cdot \rho_L \cdot V_L (1-\alpha) \left(\frac{x+xS+S}{(1-x)S} \right) \cdot \frac{1-x+xS}{\frac{x+1-x}{(1-x)}} \quad (5.62)$$

$$\dot{m}_{Void+T_Rou} = A \cdot \rho_L \cdot V_L \frac{(1-\alpha)}{(1-x)} \left(\frac{x+xS+S}{S} \right) \cdot \frac{1-x+xS}{x+1-x} \quad (5.63)$$

$$\dot{m}_{Void+T_Rou} = A \cdot \rho_L \cdot V_L \frac{(1-\alpha)}{(1-x)} \left(\frac{x+xS+S}{S} \right) \cdot (1-x+xS) \quad (5.64)$$

$$\dot{m}_{Void+T_Rou} = A \cdot \rho_L \cdot V_L \frac{(1-\alpha)}{(1-x)} (x+S(1-x)) \cdot \left(\frac{(1-x)}{S} + x \right) \quad (5.65)$$

The comparison of equation (5.65) with equation (5.8) shows that the coupling of a Void Fraction Detector and a Turbine Flowmeter drawn by the Rouhani model does not give the exact mass flow rate. The error is described again by the factor K_S and the actual mass flow rate is given by:

$$\dot{m} = \frac{\dot{m}_{Void+T_Rou}}{K_s} = A \cdot \frac{(\rho V^2) / V_T}{K_s} \quad (5.66)$$

For the previous considerations, in order to have a perfect analytical measure of the mass flow rate a third instrument is necessary, in particular a Drag Disk. The mass flow rate output will be affected by an error using two devices, while the complete spool piece should return also the slip ratio and the quality. The comparison for all the lines involved in the transients will be presented in section {6}.

5.3.2 Aya Model

Coupling the mixture density calculated according to (4.12) and the Aya mixture velocity expressed by (4.9), the mass flow rate can be determined, (5.11), as follows

$$\dot{m}_{Void+T_Aya} = A \cdot \rho_{AV} \cdot V_T = A \cdot (\alpha \rho_G + (1-\alpha) \rho_L) \cdot V_L \cdot \frac{\sqrt{\rho_L(1-\alpha)} + S \sqrt{\rho_G \alpha}}{\sqrt{\rho_L(1-\alpha)} + \sqrt{\rho_G \alpha}} \quad (5.67)$$

$$\dot{m}_{Void+T_Aya} = A \cdot V_L \cdot \rho_L \cdot (1-\alpha) \left(\frac{\alpha}{(1-\alpha)} \frac{\rho_G}{\rho_L} + 1 \right) \cdot \frac{\sqrt{\rho_L(1-\alpha)} + S \sqrt{\rho_G \alpha}}{\sqrt{\rho_L(1-\alpha)} + \sqrt{\rho_G \alpha}} \quad (5.68)$$

Using the (5.6),

$$\frac{\alpha}{(1-\alpha)} \frac{\rho_G}{\rho_L} = \frac{x}{(1-x)S} \quad (5.69)$$

and replacing in the former expression

$$\dot{m}_{Void+T_Aya} = A \cdot V_L \cdot \rho_L \cdot (1-\alpha) \left(\frac{x}{(1-x)S} + 1 \right) \cdot \left(\frac{\sqrt{\rho_L(1-\alpha)} + S\sqrt{\rho_G\alpha}}{\sqrt{\rho_L(1-\alpha)} + \sqrt{\rho_G\alpha}} \right) \quad (5.70)$$

$$\dot{m}_{Void+T_Aya} = A \cdot V_L \cdot \rho_L \cdot (1-\alpha) \left(\frac{x+S-xS}{(1-x)S} \right) \cdot \left(\frac{\sqrt{\rho_L(1-\alpha)} + S\sqrt{\rho_G\alpha}}{\sqrt{\rho_L(1-\alpha)} + \sqrt{\rho_G\alpha}} \right) \quad (5.71)$$

$$\dot{m}_{Void+T_Aya} = A \cdot V_L \cdot \rho_L \cdot \frac{(1-\alpha)}{(1-x)} \left(\frac{x+S-xS}{S} \right) \cdot \left(\frac{\sqrt{\rho_L(1-\alpha)} + S\sqrt{\rho_G\alpha}}{\sqrt{\rho_L(1-\alpha)} + \sqrt{\rho_G\alpha}} \right) \quad (5.72)$$

The comparison of equation (5.72) with equation (5.8) shows that the coupling of a Void Fraction Detector and a Turbine Flowmeter drawn by the Aya Model does not give the exact mass flow rate. The error is described by the factor K_{M3} ,

$$K_{M3} = \left(\frac{x+S-xS}{S} \right) \cdot \left(\frac{\sqrt{\rho_L(1-\alpha)} + S\sqrt{\rho_G\alpha}}{\sqrt{\rho_L(1-\alpha)} + \sqrt{\rho_G\alpha}} \right) \quad (5.73)$$

that depends on three thermal-hydraulic variables, i.e. the steam quality, the slip ratio and the void fraction. In order to determine the actual value of the mass flow rate, it is necessary to divide the combination of the two instrument outputs by K_{M3} :

$$\dot{m} = \frac{\dot{m}_{Void+T_Aya}}{K_{M3}} = A \cdot \frac{(\rho V^2) / V_T}{K_{M3}} \quad (5.74)$$

To obtain the value of K_{M3} a third instrument, i.e. the Drag Disk is necessary. The considerations are the same of section {5.1} and the comparison for all the lines involved in the transients will be presented in section {6}.

5.3.3 Volumetric Model

Coupling the mixture density calculated according to (4.12) and the Volumetric mixture velocity expressed by (4.11), the mass flow rate can be determined, (5.11), as follows

$$\dot{m}_{Void+T_Vol} = A \cdot \rho_{AV} \cdot V_T = A \cdot (\alpha \rho_G + (1-\alpha) \rho_L) \cdot V_L (S\alpha + (1-\alpha)) \quad (5.75)$$

$$\dot{m}_{Void+T_Vol} = A \cdot \rho_{AV} \cdot V_T = A \cdot V_L \cdot \rho_L \cdot (1-\alpha) \left(\frac{\alpha}{(1-\alpha)} \frac{\rho_G}{\rho_L} + 1 \right) \cdot (S\alpha + (1-\alpha)) \quad (5.76)$$

Using the (5.6),

$$\frac{\alpha}{(1-\alpha)} \frac{\rho_G}{\rho_L} = \frac{x}{(1-x)} \frac{1}{S} \quad (5.77)$$

and replacing in the former expression

$$\dot{m}_{Void+T_Vol} = A \cdot \rho_{AV} \cdot V_T = A \cdot V_L \cdot \rho_L \cdot (1-\alpha) \left(\frac{x}{(1-x)} \frac{1}{S} + 1 \right) \cdot (S\alpha + (1-\alpha)) \quad (5.78)$$

$$\dot{m}_{Void+T_Vol} = A \cdot \rho_{AV} \cdot V_T = A \cdot V_L \cdot \rho_L \cdot (1-\alpha) \left(\frac{x+S-xS}{(1-x)S} \right) \cdot (S\alpha + (1-\alpha)) \quad (5.79)$$

$$\dot{m}_{Void+T_Vol} = A \cdot \rho_{AV} \cdot V_T = A \cdot V_L \cdot \rho_L \cdot \frac{(1-\alpha)}{(1-x)} \left(\frac{x+S-xS}{S} \right) \cdot (S\alpha + (1-\alpha)) \quad (5.80)$$

$$\dot{m}_{Void+T_Vol} = A \cdot \rho_{AV} \cdot V_T = A \cdot V_L \cdot \rho_L \cdot \frac{(1-\alpha)}{(1-x)} (x+S(1-x)) \cdot \left(\alpha + \frac{(1-\alpha)}{S} \right) \quad (5.81)$$

The comparison of equation (5.81) with equation (5.8) shows that the coupling of a Void Fraction Detector and a Turbine Flowmeter drawn by the Aya Model does not give the exact mass flow rate. The error is described by the factor K_{M4} ,

$$K_{M4} = (x+S(1-x)) \cdot \left(\alpha + \frac{(1-\alpha)}{S} \right) \quad (5.82)$$

Such error term depends on three thermal-hydraulic variables: the steam quality, the slip ratio and the void fraction. In order to determine the actual value of the mass flow rate, it is necessary to divide the combination of the two instrument outputs by K_{M4} :

$$\dot{m} = \frac{\dot{m}_{Void+T_Vol}}{K_{M4}} = A \cdot \frac{(\rho V^2) / V_T}{K_{M4}} \quad (5.83)$$

To obtain the value of K_{M4} a third instrument, i.e. the Drag Disk, is necessary. The considerations are the same of section {5.1} and the comparison for all the lines involved in the transients are shown in section {6}.

5.4 Preliminary analytical considerations

Before applying the different couplings and the various models to the break transients, the equations (5.9), (5.10) and (5.11) have been tested versus specified values as reported in Table 5.2.

Table 5.2: Reference conditions for the preliminary calculation of the mass flow rate

Pressure	2 bar		7 bar		14 bar	
Quality	0.7		0.97		0.997	
Slip Ratio	0.5	0.75	2	3	6*	

* Used only in the comparison between qualities.

The reference mass flow rate has been calculated using the liquid velocity, the gas velocity, the pressure and the quality. The liquid and gas densities have been obtained by pressure, while the void fraction has been derived from equation (5.5) with the quality and the slip ratio. Finally the various quantities have been substituted to equation (5.1) in order to get the mass flow rate.

The aim of this preliminary analysis is to evaluate the influence of the slip ratio, pressure and quality on the mass flow rate responses in the following couplings:

- Turbine Flowmeter + Drag Disk – Rouhani model (M_DD_Trou)
- Turbine Flowmeter + Drag Disk – Aya model (M_DD_Taya)
- Turbine Flowmeter + Drag Disk – Volumetric model (M_DD_Tvol)
- Drag Disk + Void Fraction Detector (M_DD_Void)
- Turbine Flowmeter + Void Fraction Detector – Rouhani model (M_V_Trou)
- Turbine Flowmeter + Void Fraction Detector – Aya model (M_V_Taya)
- Turbine Flowmeter + Void Fraction Detector – Volumetric model (M_V_Tvol)

The reference conditions are shown in Table 5.2. The Table 5.3 presents the errors per cent committed by the different couplings by varying the pressure and the slip ratio.

No method to analytically evaluate the influence of the various flow regimes has been found; experiments are required to link the instrument outputs to the different flow regimes: i.e. in case of annular or horizontal stratified flow the Turbine Flowmeter and the Drag Disk have to cover the complete cross section.

Table 5.3: Errors per cent vs pressure and slip ratio change for various instrument couplings

X = 0.997					
Slip Ratio =		0.5	0.75	2	3
P = 2 bar	Error DD_Trou	0.00	0.00	0.00	0.00
	Error DD_Taya	3.31	1.39	3.58	5.93
	Error DD_Tvol	0.30	0.10	0.15	0.20
	Error DD_V	0.07	0.01	0.07	0.20
	Error V_Trou	0.15	0.02	0.15	0.40
	Error V_Taya	3.58	1.44	3.31	5.22
	Error V_Tvol	0.15	0.07	0.30	0.60
P = 7 bar	Error DD_Trou	0.00	0.00	0.00	0.00
	Error DD_Taya	3.31	1.39	3.58	5.93
	Error DD_Tvol	0.30	0.10	0.15	0.20
	Error DD_V	0.07	0.01	0.07	0.20
	Error V_Trou	0.15	0.02	0.15	0.40
	Error V_Taya	3.58	1.44	3.31	5.22
	Error V_Tvol	0.15	0.07	0.30	0.60
P = 14 bar	Error DD_Trou	0.00	0.00	0.00	0.00
	Error DD_Taya	3.31	1.39	3.58	5.93
	Error DD_Tvol	0.30	0.10	0.15	0.19
	Error DD_V	0.07	0.01	0.07	0.20
	Error V_Trou	0.15	0.02	0.15	0.40
	Error V_Taya	3.58	1.44	3.31	5.22
	Error V_Tvol	0.15	0.07	0.30	0.59

The Table 5.3 shows that the influence of pressure is not significant on the measurements of the mass flow rate. As reported in section {5.2.1}, the combination of the Drag Disk with the Turbine Flowmeter, according to the Rouhani model for the mixture velocity, returns the exact rate. The condition of homogenous flow (slip ratio set to unity), is not presented, because all the models and the couplings would give the same and exact result. When the slip ratio moves away from the unity the errors become higher.

An error per cent has been defined based on the mass flow rate from Eq. (5.8) and the mass flow rates obtained by the different instrument couplings when the quality and the slip ratio vary, Figure 5.18, Figure 5.19 and Figure 5.20.

The coupling of the Drag Disk and the Turbine Flowmeter according to the Rouhani model is not reported, because the error is null. When the quality value increases, the combination of the Drag Disk and the Turbine Flowmeter, according to the Volumetric model, is the most accurate.

The couplings of the Void Fraction Detector with the Turbine Flowmeter according to the Rouhani model and the Volumetric model involve significant errors when the slip ratio and the quality are high, but the approximation is acceptable when the quality value is around unity for each slip ratio.

The coupling of the Drag Disk with the Turbine Flowmeter described by Aya gives the worst results.

The error related to the DD+Void combination is quite high. Such error term decreases at high quality values.

The Aya model applied to the coupling of the Void Fraction Detector and the Turbine Flowmeter is the unique solution where the error decreases when the quality decreases.

Table 5.4 summarizes the best and the worst couplings when the slip ratio is smaller or greater than 1 with the quality change.

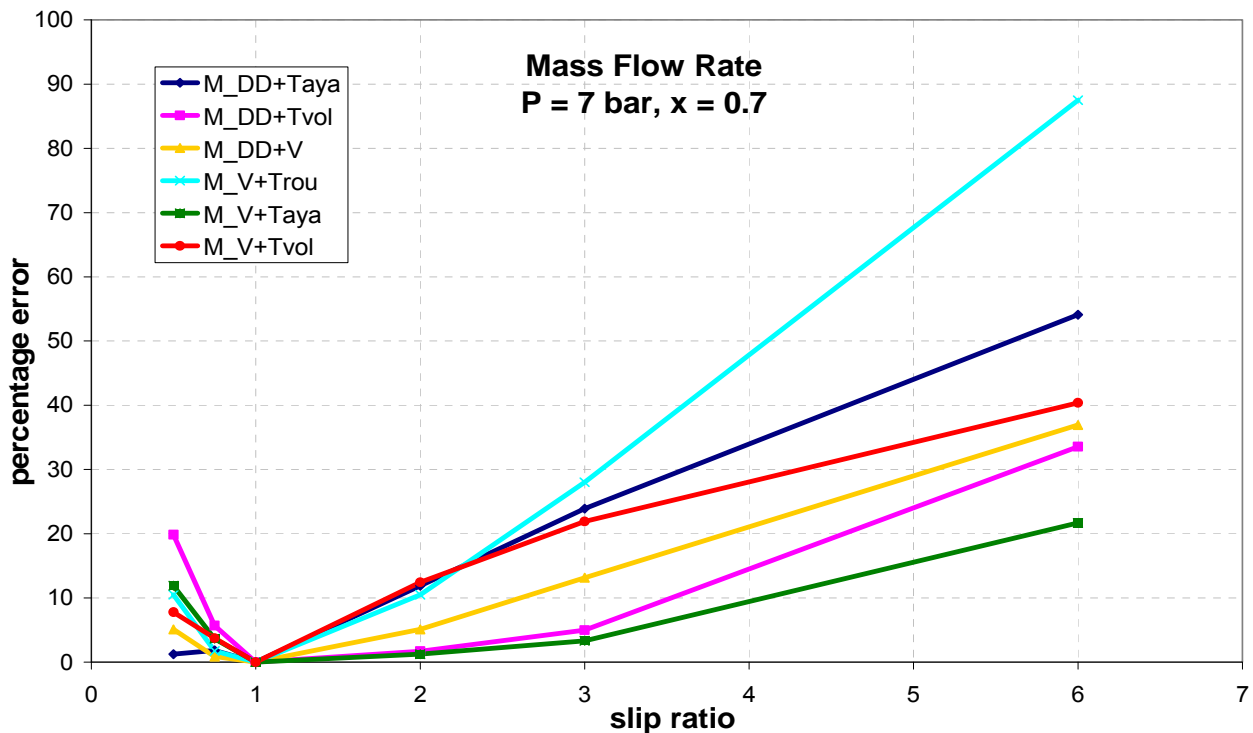


Figure 5.18: Errors per cent function of the slip ratio at 7 bars with quality set to 0.7

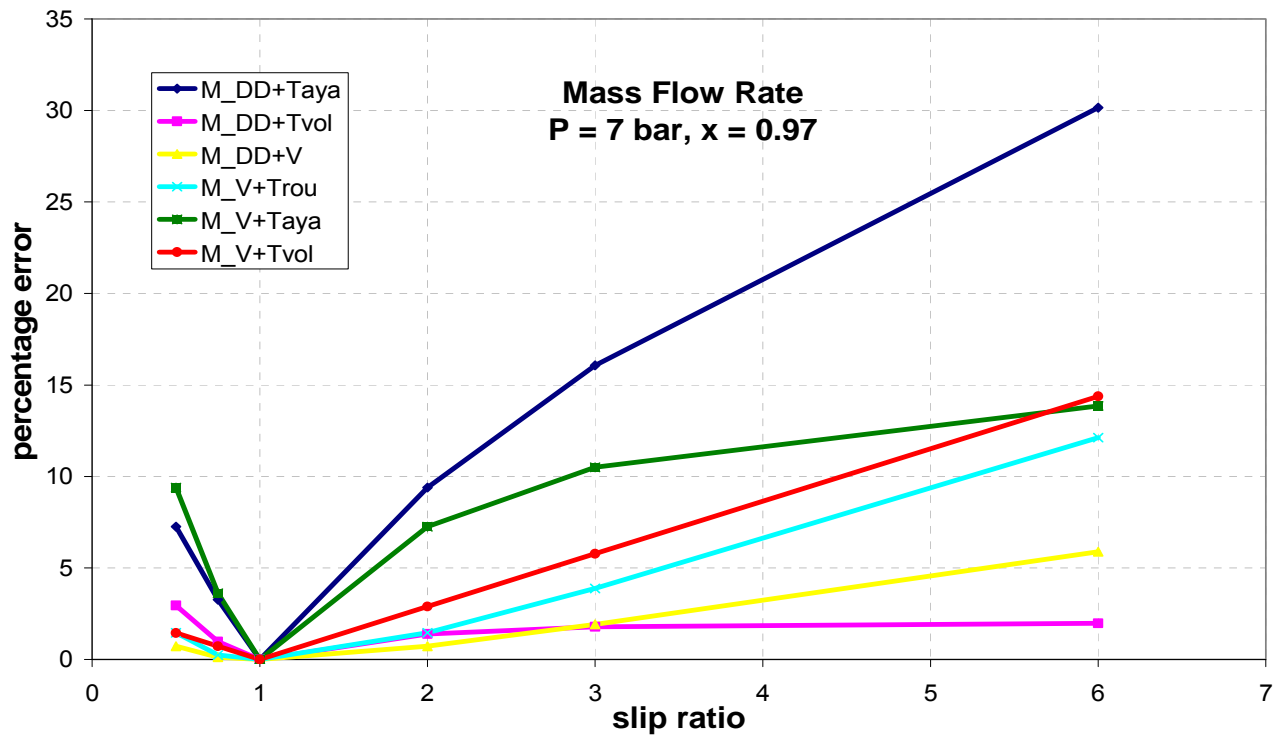


Figure 5.19: Errors per cent function of the slip ratio at 7 bars with quality set to 0.97

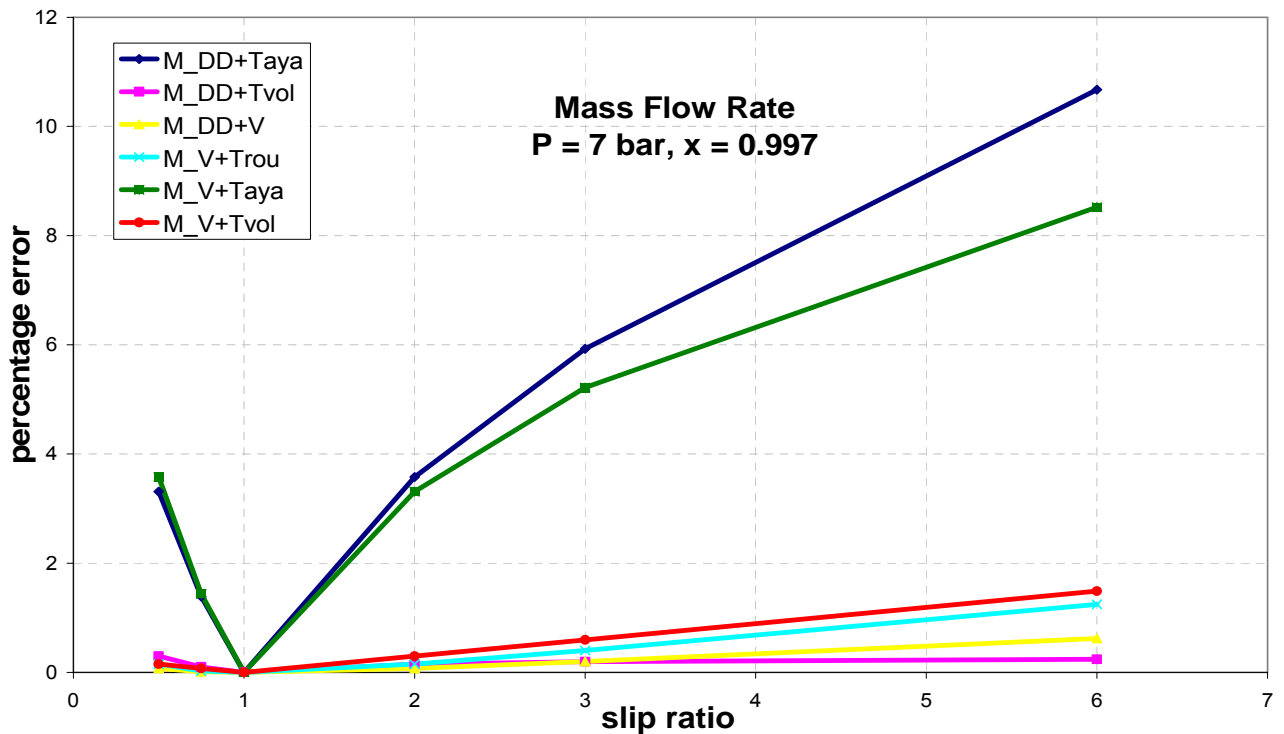


Figure 5.20: Errors per cent function of the slip ratio at 7 bars with quality set to 0.997

Table 5.4: Best and worst couplings with different slip ratios and qualities

	Quality	0.7	0.97	0.997
S < 1	BEST	DD+T_aya DD+Void	DD+Void	DD+Void
	WORST	DD+T_vol	V+T_aya	V+T_aya
S > 1	BEST	V+T_aya	DD+T_vol	DD+T_vol
	WORST	V_T_rou	DD+T_aya	DD+T_aya

5.5 Synthesis on the analytical models

The previous study demonstrates that in general two instruments are not enough to have an accurate evaluation of the mass flow rate.

Despite the dimensional analysis states that any coupling of the three instruments, the Drag Disk, the Turbine Flowmeter and the Void Fraction Detector, gives the mass flow rate value, actually the two-instrument-output value needs to be trimmed by a non-dimensional factor. The value of each non-dimensional factor, related to a certain coupling, is a function of two thermal-hydraulic variables: quality and slip ratio.

In order to calculate these factors, called K_S , K_{M1} , K_{M2} , K_{M3} , and K_{M4} , a third instrument is necessary otherwise an error in the determination of the mass flow rate cannot be avoided.

The mixture velocity measured by the Turbine Flowmeter is described by different models, Rouhani, Aya and Volumetric one. The analytical investigation revealed that, when the turbine velocity is based on the Rouhani model, the mass flow rate can be obtained using just the Turbine Flowmeter and the Drag Disk.

Considering the other two models, or the other couplings, a spool piece made of three instruments is necessary.

In addition, the use of two devices does not allow the determination of other thermal-hydraulic parameters (quality and slip ratio) besides the mass flow rate, while the configuration of three instruments gives all the information.

6 MASS FLOW RATE DATA REDUCTION FOR SPECIFIED TRANSIENTS

This chapter reports the comparison between the mass flow obtained by the RELAP5 transient data and the corresponding mass flow calculated using two and three instrument combinations, according to the equations of sections {4} and {5}.

6.1 *Determination of the mass flow rate with two instruments*

In case of two instrument combination for the mass flow measurement, the comparison between RELAP5 and spool piece results has been performed as described below.

For each Turbine model, the three possible couplings has been compared to the RELAP5 mass flow for each line. The combination of a Drag Disk and a Void Fraction Detector, which is not affected by the Turbine models, has been repeated in each part, in order to evaluate the most accurate solution.

For each line, a table summarizes the formula of the mass flow derived from the various couplings, the factors defined in section {5} and, finally, the errors per cent committed using the response of two devices versus the actual value taken from RELAP5 data [4].

6.1.1 DVI TEST

During the DVI break test, three spool pieces are involved in measuring two-phase mass flow, as stated in [5]: one located on the DVI SPLIT break line, one located on the ADS Stage-I ST and one located on the ADS Stage-I DT.

6.1.1.1 DVI SPLIT break line

Rouhani model

Table 6.1: Errors per cent between the RELAP5 mass flow and the Spool Piece mass flow - Rouhani model - DVI SPLIT line, DVI break test

Coupling	Mass Flow Rate with two devices	Thermal-hydraulic factor	Corrected	Error
DD + Void	$A \cdot [\rho_{AV} \cdot (\rho V^2)]^{1/2}$	$K_S = \left((x + (1-x)S) \cdot \left(x + \frac{(1-x)}{S} \right) \right)$	$\frac{\dot{m}_{Void+DD}}{K_S^{1/2}}$	3.33%
DD + T	$A \cdot \rho V^2 / V_T$	1	\dot{m}_{DD+T}	0.00%
T + Void	$A \cdot \rho_{AV} \cdot V_T$	$K_S = \left((x + (1-x)S) \cdot \left(x + \frac{(1-x)}{S} \right) \right)$	$\frac{\dot{m}_{Void+T-Rou}}{K_S}$	6.22%

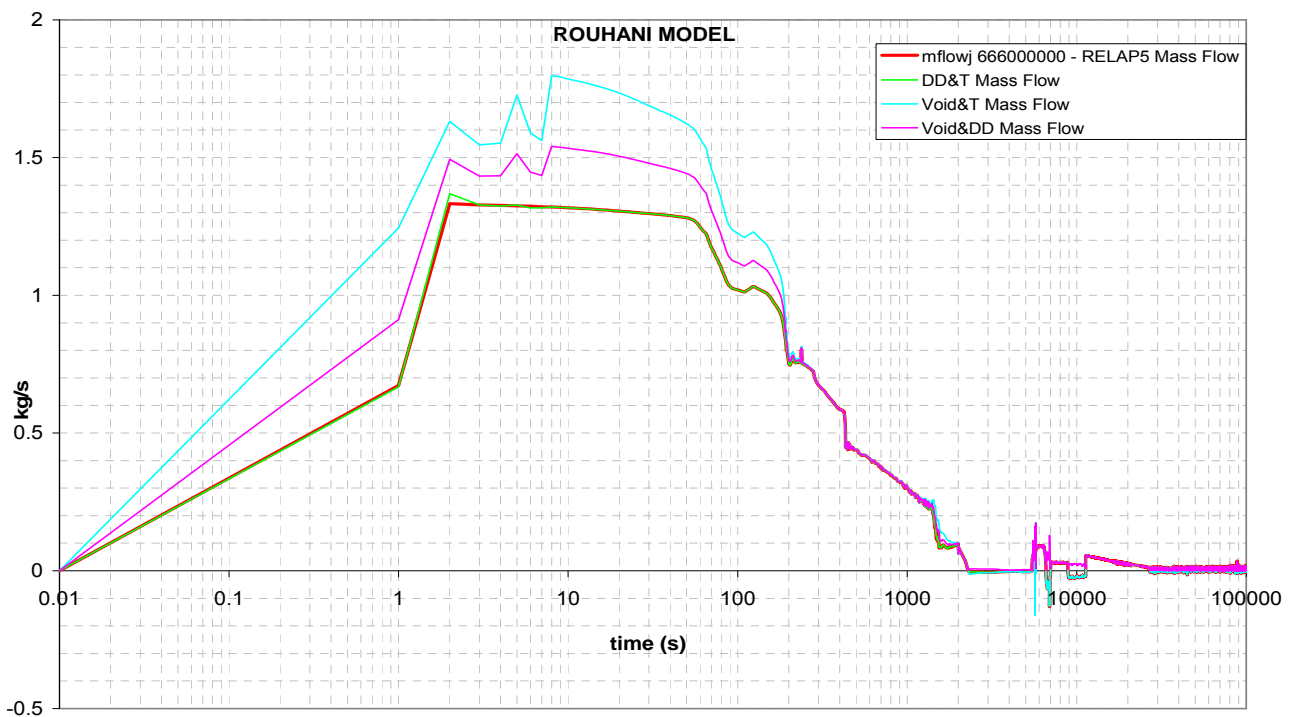


Figure 6.1: Comparison between the RELAP5 mass flow and the Spool Piece mass flow - Rouhani model - DVI SPLIT line, DVI break test

Taking into account the Rouhani model for the Turbine velocity and applying the analytical equations, the coupling of a Drag Disk and a Turbine Flowmeter returns the correct mass flow rate, as shown in Figure 6.1.

The coupling of the Void Fraction Detector with the Drag Disk appears more accurate than the coupling of a Void Fraction Detector with a Turbine Flowmeter. Anyway all the solutions present the same trend of the RELAP5 mass flow rate and the errors per cent, shown in Table 6.1 are all below 7%.

Aya Model

Table 6.2: Errors per cent between the RELAP5 mass flow and the Spool Piece mass flow - Aya model - DVI SPLIT line, DVI break test

Coupling	Mass Flow Rate with two devices	Thermal-hydraulic factor	Corrected	Error
DD + Void	$A \cdot [\rho_{AV} \cdot (\rho V^2)]^{1/2}$	$K_S = \left((x + (1-x)S) \cdot \left(x + \frac{(1-x)}{S} \right) \right)$	$\frac{\dot{m}_{Void+DD}}{K_S^{1/2}}$	3.33%
DD + T	$A \cdot \rho V^2 / V_T$	$K_{M1} = \frac{1-x+xS}{\frac{\sqrt{\rho_L(1-\alpha)} + S\sqrt{\rho_G\alpha}}{\sqrt{\rho_L(1-\alpha)} + \sqrt{\rho_G\alpha}}}$	$\frac{\dot{m}_{DD+T_Aya}}{K_{M1}}$	1.70%
T + Void	$A \cdot \rho_{AV} \cdot V_T$	$K_{M3} = \left(\frac{x+S-xS}{S} \right) \cdot \left(\frac{\sqrt{\rho_L(1-\alpha)} + S\sqrt{\rho_G\alpha}}{\sqrt{\rho_L(1-\alpha)} + \sqrt{\rho_G\alpha}} \right)$	$\frac{\dot{m}_{Void+T_Aya}}{K_{M3}}$	4.70%

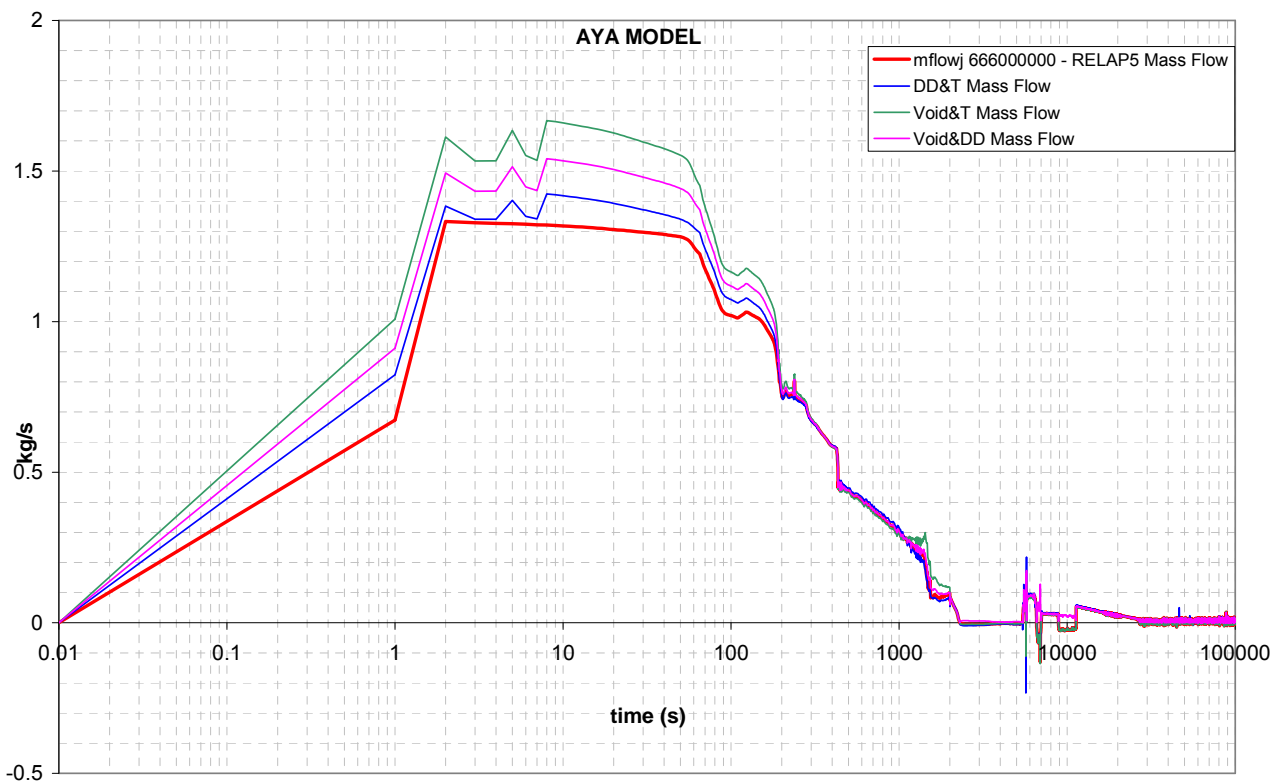


Figure 6.2: Comparison between the RELAP5 mass flow and the Spool Piece mass flow - Aya model - DVI SPLIT line, DVI break test

When the mixture velocity is modelled according to the Aya assumption, the most accurate response is given by the coupling of a Drag Disk with a Turbine Flowmeter, as indicated in Table 6.2 and in Figure 6.2.

As for the Rouhani model, the most inaccurate coupling appears to be the combination of a Void Fraction Detector and a Turbine Flowmeter.

Any response presents the same trend of the RELAP5 mass flow rate and also in this case the error per cent remains well below 5%.

Volumetric Model

Table 6.3: Errors per cent between the RELAP5 mass flow and the Spool Piece mass flow - Volumetric model - DVI SPLIT line, DVI break test

Coupling	Mass Flow Rate with two devices	Thermal-hydraulic factor	Corrected	Error
DD + Void	$A \cdot [\rho_{AV} \cdot (\rho V^2)]^{1/2}$	$K_S = \left((x + (1-x)S) \cdot \left(x + \frac{(1-x)}{S} \right) \right)$	$\frac{\dot{m}_{Void+DD}}{K_S^{1/2}}$	3.33%
DD + T	$A \cdot \rho V^2 / V_T$	$K_{M2} = \frac{(1-x+xS)}{(1-\alpha+\alpha S)}$	$\frac{\dot{m}_{DD+T_Vol}}{K_{M2}}$	13.0%
T + Void	$A \cdot \rho_{AV} \cdot V_T$	$K_{M4} = (x + S(1-x)) \cdot \left(\alpha + \frac{(1-\alpha)}{S} \right)$	$\frac{\dot{m}_{Void+T_Vol}}{K_{M4}}$	27.9%

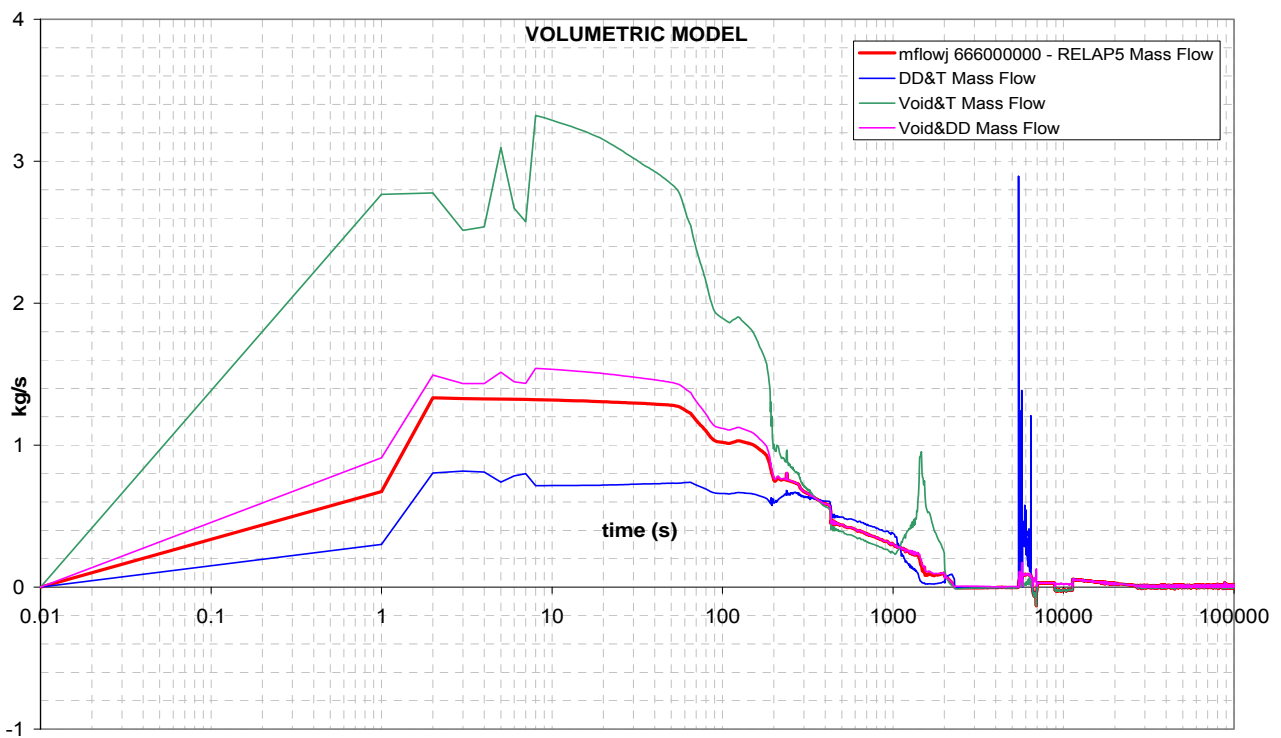


Figure 6.3: Comparison between the RELAP5 mass flow and the Spool Piece mass flow - Volumetric model - DVI SPLIT line, DVI break test

Figure 6.3 and the errors per cent shown in Table 6.3 show that the Volumetric Model applied to the Turbine Flowmeter located in the DVI SPLIT line returns the most inaccurate results. In particular, the mass flow obtained with the coupling of a Void Fraction Detector and a Turbine Flowmeter is affected by an error around 30%.

The DD+Void combination, which is not affected by the velocity model, is the most accurate.

In case of the Volumetric model, the analysis of data leads to exclude the use of a two instrument spool piece to avoid errors per cent above 10%

Despite the large errors in the different responses, the various combinations present the same trend of the RELAP5 mass flow rate.

6.1.1.2 ADS Stage-I ST

Rouhani model

Table 6.4: Errors per cent between the RELAP5 mass flow and the Spool Piece mass flow - Rouhani model - ADS Stage-I ST line, DVI break test

Coupling	Mass Flow Rate with two devices	Thermal-hydraulic factor	Corrected	Error
DD + Void	$A \cdot [\rho_{AV} \cdot (\rho V^2)]^{1/2}$	$K_S = \left((x + (1-x)S) \cdot \left(x + \frac{(1-x)}{S} \right) \right)$	$\frac{\dot{m}_{Void+DD}}{K_s^{1/2}}$	3.32%
DD + T	$A \cdot \rho V^2 / V_T$	1	\dot{m}_{DD+T}	1.77%
T + Void	$A \cdot \rho_{AV} \cdot V_T$	$K_S = \left((x + (1-x)S) \cdot \left(x + \frac{(1-x)}{S} \right) \right)$	$\frac{\dot{m}_{Void+T-Rou}}{K_s}$	4.30%

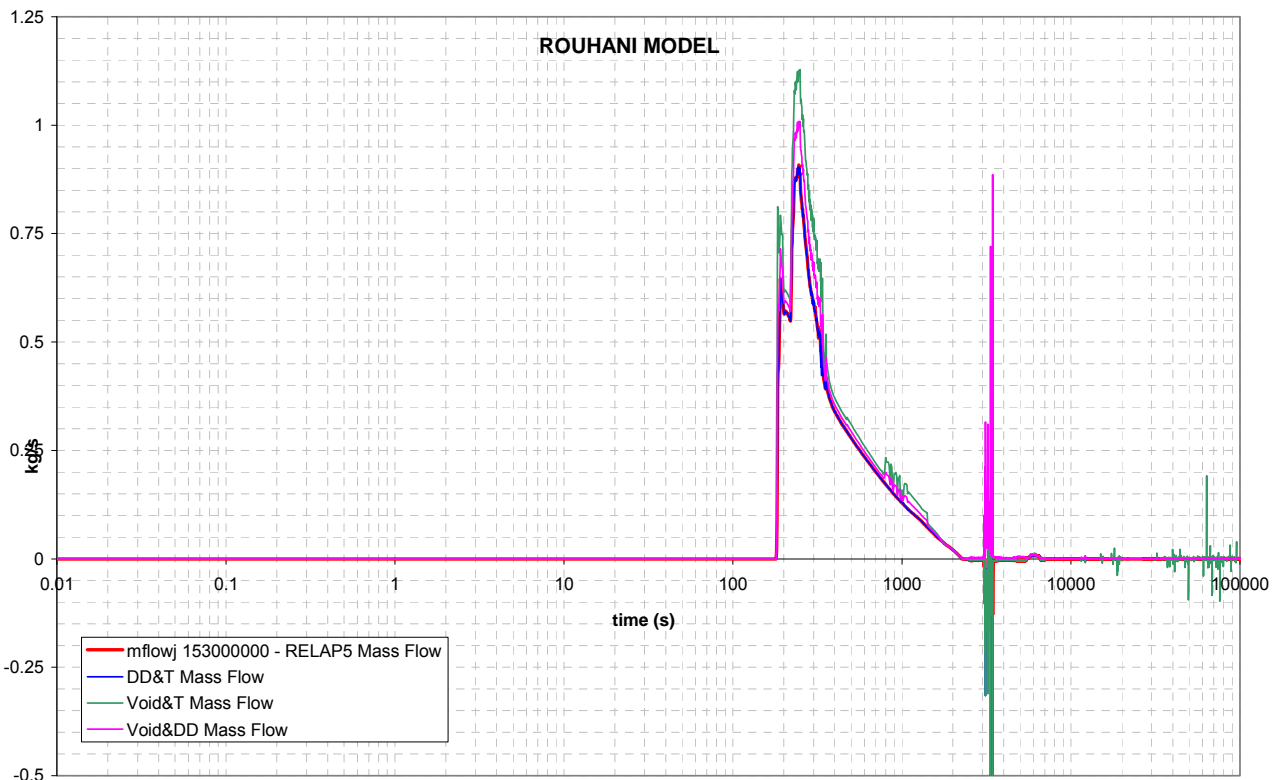


Figure 6.4: Comparison between the RELAP5 mass flow and the Spool Piece mass flow - Rouhani model - ADS Stage-I ST line, DVI break test

During the DVI break test, two-phase mass flow is foreseen in the ADS Stage-I ST line [5].

Despite the analytical analysis performed shows that the Rouhani model for the coupling of a Turbine Flowmeter with a Drag Disk gives the correct mass flow, as stated in section {5}, Table 6.4 presents a small error, probably due to the thermal-hydraulic variable uncertainty. The T_Rou+DD combination is the most accurate, while the Void+T_Rou combination is the most inaccurate. The errors are below 5%, as shown in Figure 6.4, and the trends are the same of the RELAP5 mass flow rate.

Aya Model

Table 6.5: Errors per cent between the RELAP5 mass flow and the Spool Piece mass flow - Aya model - ADS Stage-I ST line, DVI break test

Coupling	Mass Flow Rate with two devices	Thermal-hydraulic factor	Corrected	Error
DD + Void	$A \cdot [\rho_{AV} \cdot (\rho V^2)]^{1/2}$	$K_S = \left((x + (1-x)S) \cdot \left(x + \frac{(1-x)}{S} \right) \right)$	$\frac{\dot{m}_{Void+DD}}{K_S^{1/2}}$	3.32%
DD + T	$A \cdot \rho V^2 / V_T$	$K_{M1} = \frac{1-x+xS}{\frac{\sqrt{\rho_L(1-\alpha)} + S\sqrt{\rho_G\alpha}}{\sqrt{\rho_L(1-\alpha)} + \sqrt{\rho_G\alpha}}}$	$\frac{\dot{m}_{DD+T_Aya}}{K_{M1}}$	3.76%
T + Void	$A \cdot \rho_{AV} \cdot V_T$	$K_{M3} = \left(\frac{x+S-xS}{S} \right) \cdot \left(\frac{\sqrt{\rho_L(1-\alpha)} + S\sqrt{\rho_G\alpha}}{\sqrt{\rho_L(1-\alpha)} + \sqrt{\rho_G\alpha}} \right)$	$\frac{\dot{m}_{Void+T_Aya}}{K_{M3}}$	2.52%

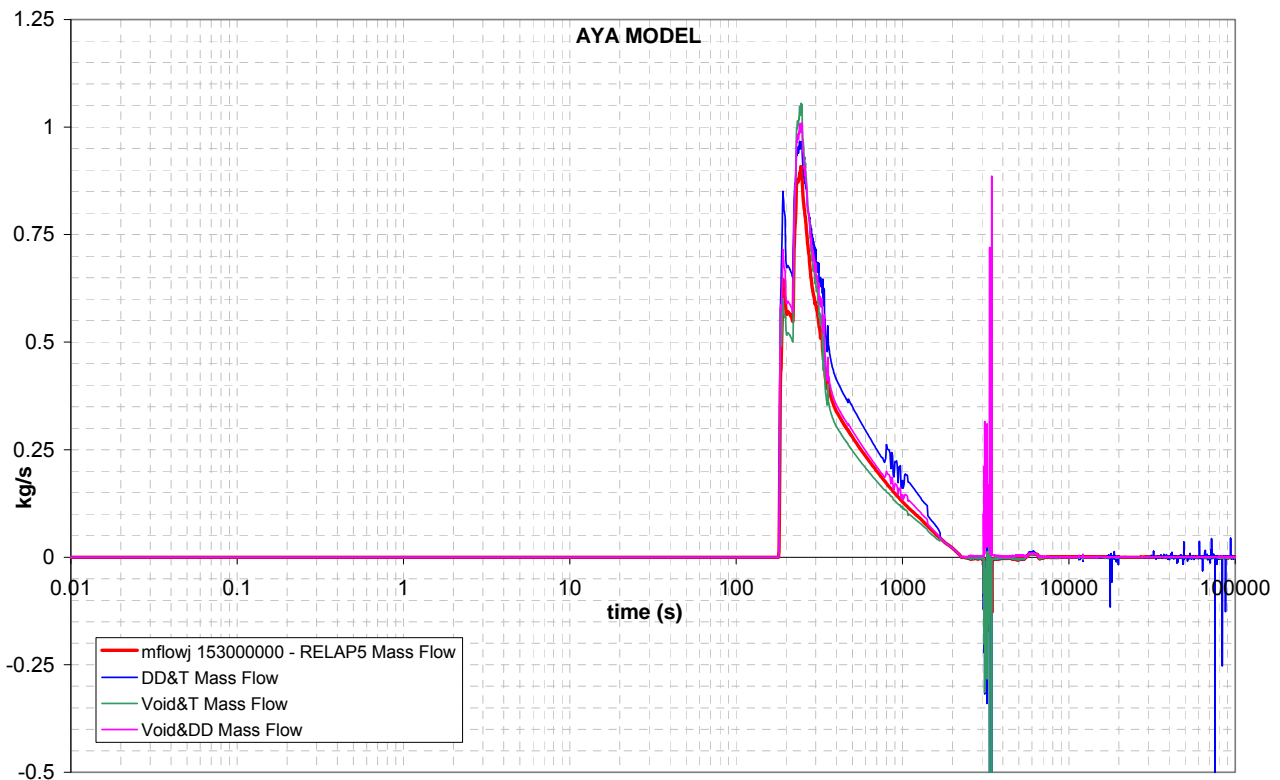


Figure 6.5: Comparison between the RELAP5 mass flow and the Spool Piece mass flow - Aya model - ADS Stage-I ST line, DVI break test

During the DVI break test, two-phase mass flow rate is foreseen in the ADS Stage-I ST line [5].

Considering the Aya model for the mixture velocity, the different couplings return errors around 3% as shown in Table 6.5. The most accurate combination is the Void Fraction Detector with a Turbine Flowmeter, as shown in Figure 6.5.

Volumetric Model

Table 6.6: Errors per cent between the RELAP5 mass flow and the Spool Piece mass flow - Volumetric model - ADS ST (stage I) line, DVI break test

Coupling	Mass Flow Rate with two devices	Thermal-hydraulic factor	Corrected	Error
DD + Void	$A \cdot [\rho_{AV} \cdot (\rho V^2)]^{1/2}$	$K_S = \left((x + (1-x)S) \cdot \left(x + \frac{(1-x)}{S} \right) \right)$	$\frac{\dot{m}_{Void+DD}}{K_S^{1/2}}$	3.32%
DD + T	$A \cdot \rho V^2 / V_T$	$K_{M2} = \frac{(1-x + xS)}{(1-\alpha + \alpha S)}$	$\frac{\dot{m}_{DD+T_Vol}}{K_{M2}}$	7.71%
T + Void	$A \cdot \rho_{AV} \cdot V_T$	$K_{M4} = (x + S(1-x)) \cdot \left(\alpha + \frac{(1-\alpha)}{S} \right)$	$\frac{\dot{m}_{Void+T_Vol}}{K_{M4}}$	10.9%

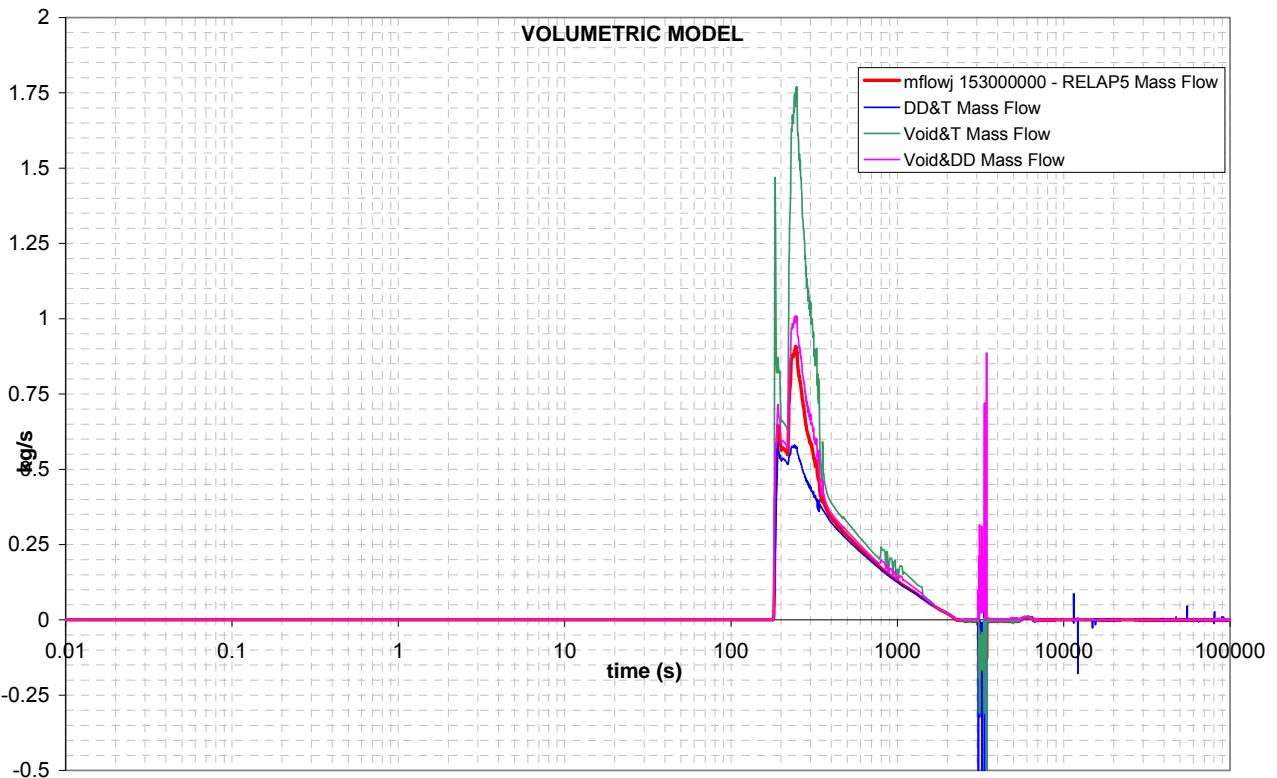


Figure 6.6: Comparison between the RELAP5 mass flow and the Spool Piece mass flow - Volumetric model - ADS Stage-I ST line, DVI break test

During the DVI break test, two-phase mass flow rate is foreseen in the ADS Stage-I ST line [5].

The volumetric model leads to significant errors, as shown in Table 6.6, around 7-11%, except for the combination of a Void Fraction Detector with a Drag Disk, for which the error is around 3.3%.

6.1.1.3 ADS Stage-I DT

Rouhani model

Table 6.7: Errors per cent between the RELAP5 mass flow and the Spool Piece mass flow - Rouhani model - ADS DT (stage I) line, DVI break test

Coupling	Mass Flow Rate with two devices	Thermal-hydraulic factor	Corrected	Error
DD + Void	$A \cdot [\rho_{AV} \cdot (\rho V^2)]^{1/2}$	$K_S = \left((x + (1-x)S) \cdot \left(x + \frac{(1-x)}{S} \right) \right)$	$\frac{\dot{m}_{Void+DD}}{K_s^{1/2}}$	8.80%
DD + T	$A \cdot \rho V^2 / V_T$	1	\dot{m}_{DD+T}	3.95%
T + Void	$A \cdot \rho_{AV} \cdot V_T$	$K_S = \left((x + (1-x)S) \cdot \left(x + \frac{(1-x)}{S} \right) \right)$	$\frac{\dot{m}_{Void+T-Rou}}{K_s}$	14.9%

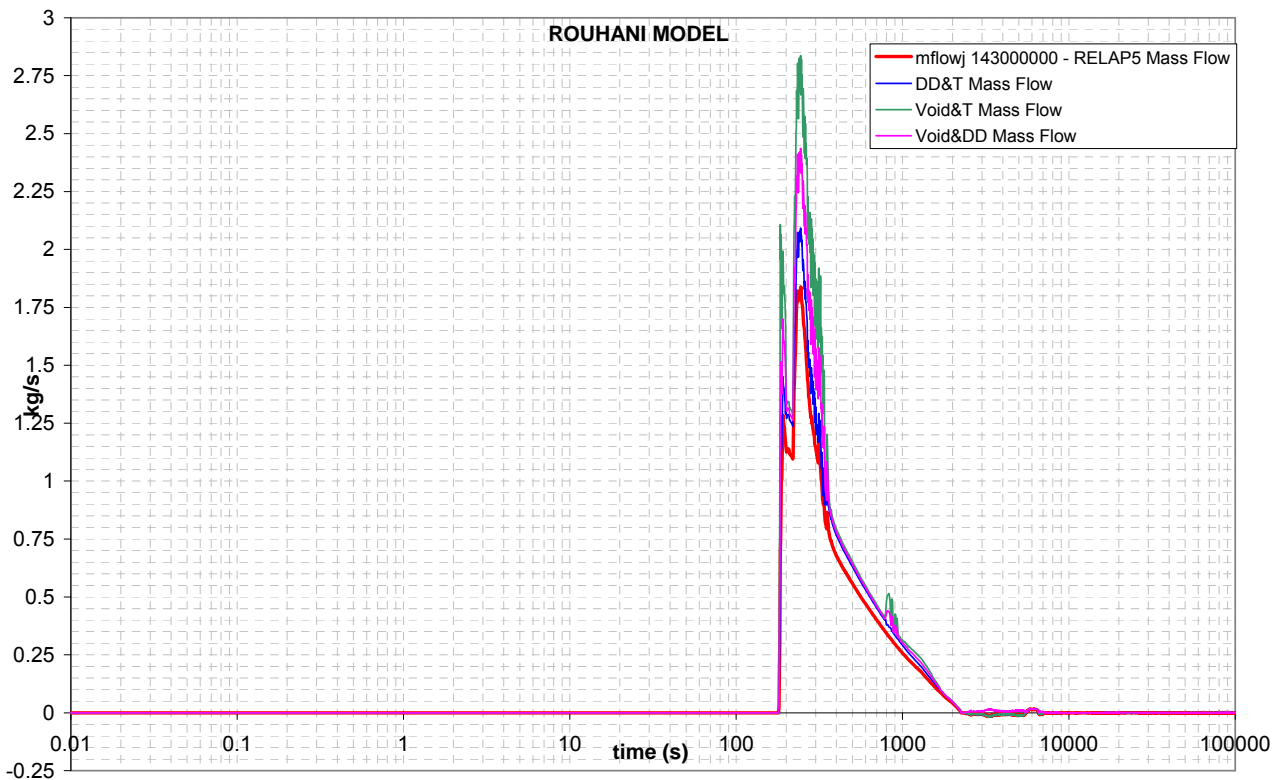


Figure 6.7: Comparison between the RELAP5 mass flow and the Spool Piece mass flow - Rouhani model - ADS Stage-I DT line, DVI break test

During the DVI break test, two-phase mass flow is foreseen in the ADS Stage-I DT line [5].

Despite the analytical analysis demonstrates that for the coupling of a Turbine Flowmeter with a Drag Disk the Rouhani model gives the correct mass flow, as pointed out in section {5}, Table 6.7 presents an error around 4%, due to the significant variation of the slip ratio. Anyway, this combination is the most accurate, while the Void+T_Rou combination involves higher error. The errors are below 15%, as shown in Figure 6.7, and the trends are the same of the RELAP5 mass flow rate.

Aya Model

Table 6.8: Errors per cent between the RELAP5 mass flow and the Spool Piece mass flow - Aya model - ADS Stage-I DT line, DVI break test

Coupling	Mass Flow Rate with two devices	Thermal-hydraulic factor	Corrected	Error
DD + Void	$A \cdot [\rho_{AV} \cdot (\rho V^2)]^{1/2}$	$K_S = \left((x + (1-x)S) \cdot \left(x + \frac{(1-x)}{S} \right) \right)$	$\frac{\dot{m}_{Void+DD}}{K_S^{1/2}}$	8.80%
DD + T	$A \cdot \rho V^2 / V_T$	$K_{M1} = \frac{1-x+xS}{\frac{\sqrt{\rho_L(1-\alpha)} + S\sqrt{\rho_G\alpha}}{\sqrt{\rho_L(1-\alpha)} + \sqrt{\rho_G\alpha}}}$	$\frac{\dot{m}_{DD+T_Aya}}{K_{M1}}$	10.9%
T + Void	$A \cdot \rho_{AV} \cdot V_T$	$K_{M3} = \left(\frac{x+S-xS}{S} \right) \cdot \left(\frac{\sqrt{\rho_L(1-\alpha)} + S\sqrt{\rho_G\alpha}}{\sqrt{\rho_L(1-\alpha)} + \sqrt{\rho_G\alpha}} \right)$	$\frac{\dot{m}_{Void+T_Aya}}{K_{M3}}$	7.92%

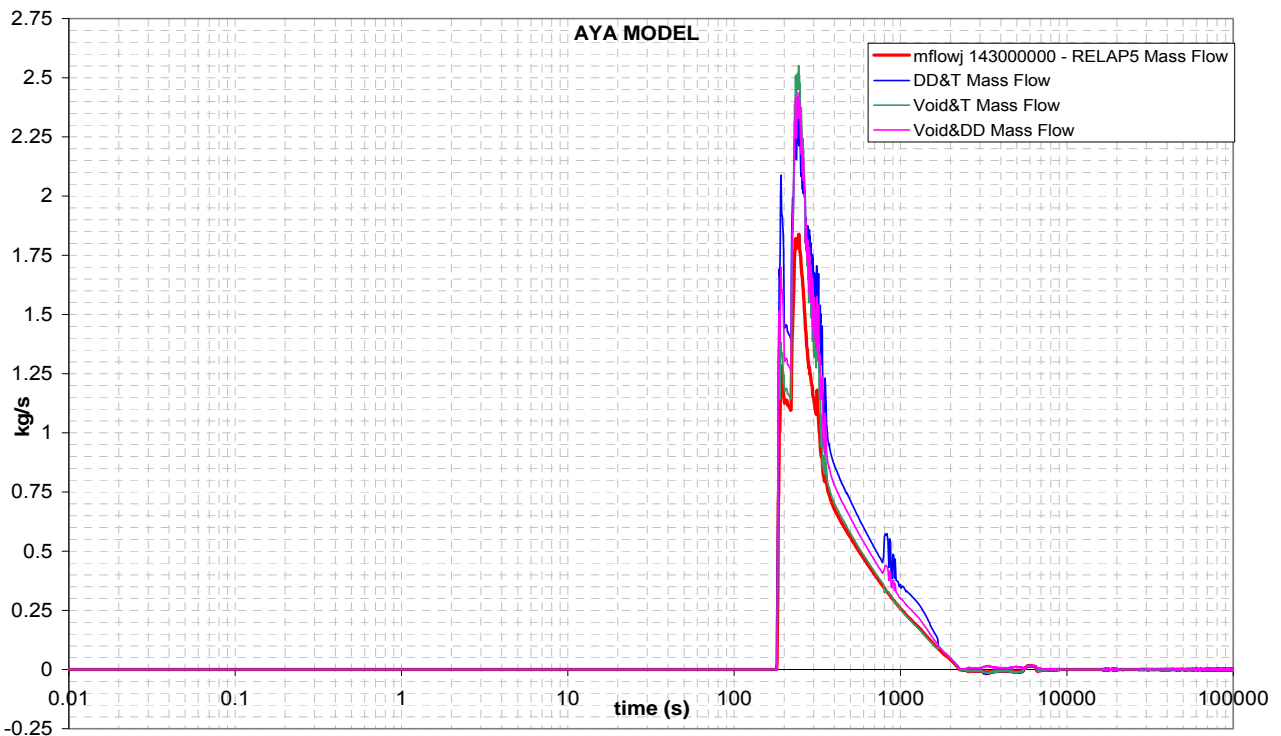


Figure 6.8: Comparison between the RELAP5 mass flow and the Spool Piece mass flow - Aya model - ADS DT (stage I) line, DVI break test

During the DVI break test, two-phase mass flow rate is foreseen in the ADS Stage-I DT line [5].

Considering the Aya model for the mixture velocity, the different couplings return errors around 8-11% as shown in Table 6.8. The most accurate combination is the Void Fraction Detector with a Turbine Flowmeter, as shown in Figure 6.8.

Volumetric Model

Table 6.9: Errors per cent between the RELAP5 mass flow and the Spool Piece mass flow - Volumetric model - ADS Stage-I DT line, DVI break test

Coupling	Mass Flow Rate with two devices	Thermal-hydraulic factor	Corrected	Error
DD + Void	$A \cdot [\rho_{AV} \cdot (\rho V^2)]^{1/2}$	$K_S = \left((x + (1-x)S) \cdot \left(x + \frac{(1-x)}{S} \right) \right)$	$\frac{\dot{m}_{Void+DD}}{K_S^{1/2}}$	8.80%
DD + T	$A \cdot \rho V^2 / V_T$	$K_{M2} = \frac{(1-x + xS)}{(1-\alpha + \alpha S)}$	$\frac{\dot{m}_{DD+T_Vol}}{K_{M2}}$	6.25%
T + Void	$A \cdot \rho_{AV} \cdot V_T$	$K_{M4} = (x + S(1-x)) \cdot \left(\alpha + \frac{(1-\alpha)}{S} \right)$	$\frac{\dot{m}_{Void+T_Vol}}{K_{M4}}$	33.5%

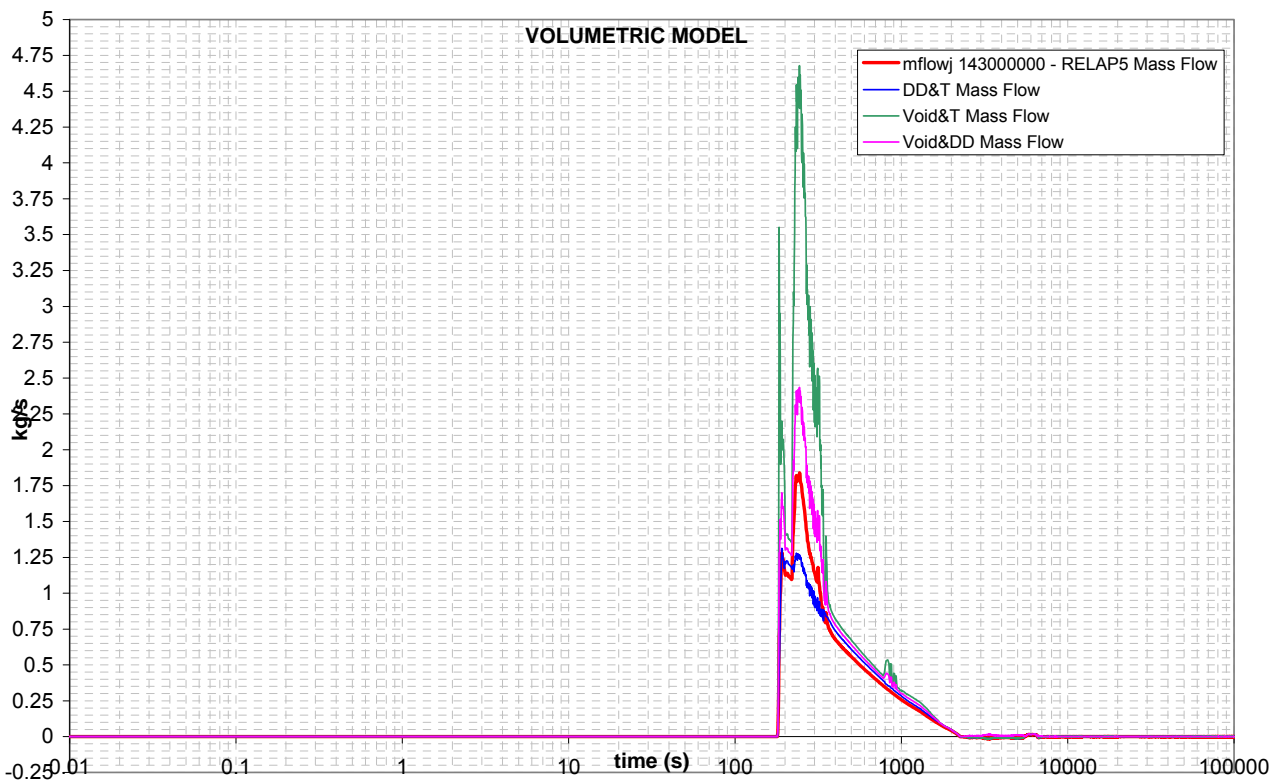


Figure 6.9: Comparison between the RELAP5 mass flow and the Spool Piece mass flow - Volumetric model - ADS Stage-I DT line, DVI break test

During the DVI break test, the Volumetric model applied to the ADS Stage-I DT gives significant errors, in particular for the coupling of a Turbine Flowmeter and a Void Fraction Detector, as shown in Figure 6.9 and Table 6.9. The other two combinations involve an error below 10%.

6.1.2 EBT TEST

During the EBT break test, three spool pieces are involved in measuring two-phase mass flow, as stated in [5]: one located on the EBT SPLIT break line, one located on the ADS Stage-I ST and one located on the ADS Stage-I DT.

6.1.2.1 EBT SPLIT break line

Rouhani model

Table 6.10: Errors per cent between the RELAP5 mass flow and the Spool Piece mass flow - Rouhani model - EBT SPLIT line, EBT break test

Coupling	Mass Flow Rate with two devices	Thermal-hydraulic factor	Corrected	Error
DD + Void	$A \cdot [\rho_{AV} \cdot (\rho V^2)]^{1/2}$	$K_S = \left((x + (1-x)S) \cdot \left(x + \frac{(1-x)}{S} \right) \right)$	$\frac{\dot{m}_{Void+DD}}{K_S^{1/2}}$	0.88%
DD + T	$A \cdot \rho V^2 / V_T$	1	\dot{m}_{DD+T}	0.00%
T + Void	$A \cdot \rho_{AV} \cdot V_T$	$K_S = \left((x + (1-x)S) \cdot \left(x + \frac{(1-x)}{S} \right) \right)$	$\frac{\dot{m}_{Void+T_Rou}}{K_S}$	1.22%

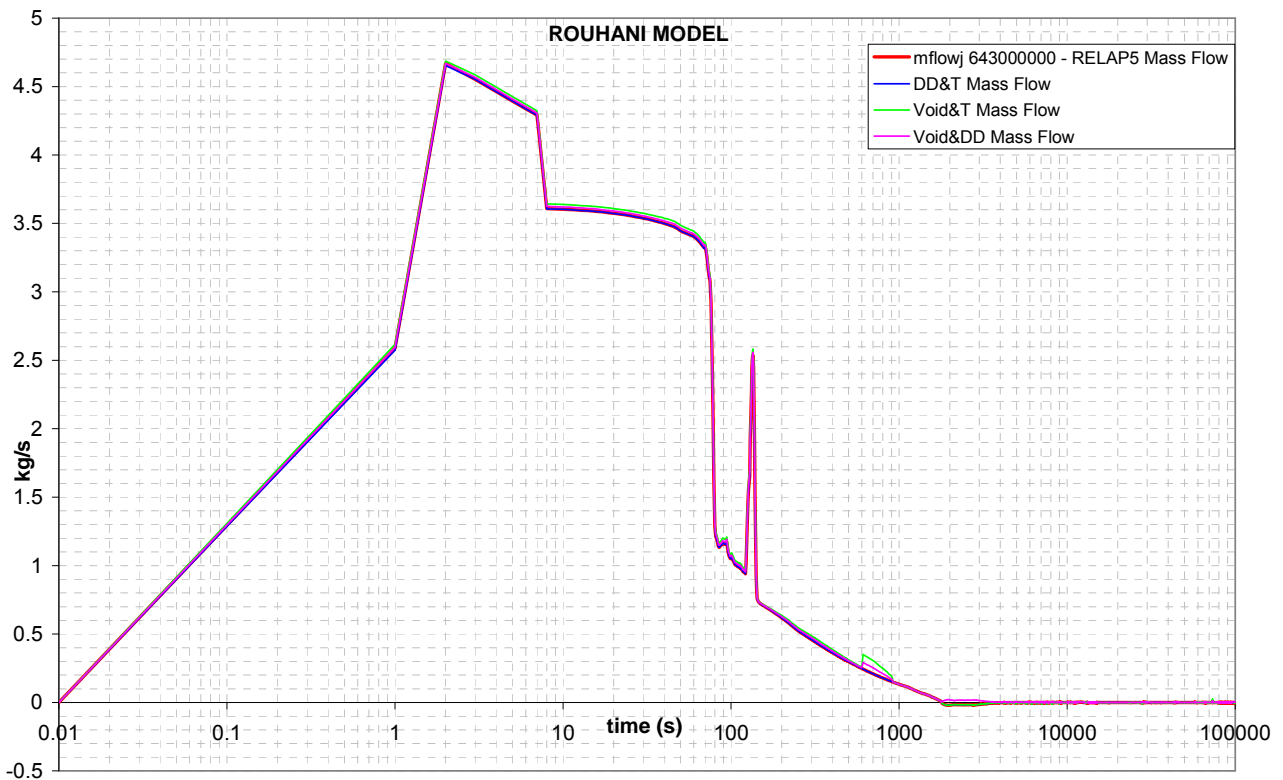


Figure 6.10: Comparison between the RELAP5 mass flow and the Spool Piece mass flow - Rouhani model - EBT SPLIT line, EBT break test

The considerations are the same of section {6.1.1.1 – Rouhani model}, but the errors, as shown in Table 6.10, are lower. Figure 6.10 shows that any coupling is suitable to determine the mass flow. The agreement between the various solutions is due to the limited range of the slip ratio; in fact, as shown in [5], the liquid and gas velocities in the EBT SPLIT line during the EBT break test are very similar and the slip ratio is around $1.1 \div 1.2$, therefore the flow may be considered almost homogeneous.

The section 8 of this document shows that when the slip ratio is close the unity value the velocity model is unique.

A Spool Piece arranged by two instruments appears to be enough for this position.

Aya Model

Table 6.11: Errors per cent between the RELAP5 mass flow and the Spool Piece mass flow - Aya model - EBT SPLIT line, EBT break test

Coupling	Mass Flow Rate with two devices	Thermal-hydraulic factor	Corrected	Error
DD + Void	$A \cdot [\rho_{AV} \cdot (\rho V^2)]^{1/2}$	$K_S = \left((x + (1-x)S) \cdot \left(x + \frac{(1-x)}{S} \right) \right)$	$\frac{\dot{m}_{Void+DD}}{K_s^{1/2}}$	0.88%
DD + T	$A \cdot \rho V^2 / V_T$	$K_{M1} = \frac{1-x+xS}{\frac{\sqrt{\rho_L(1-\alpha)} + S\sqrt{\rho_G\alpha}}{\sqrt{\rho_L(1-\alpha)} + \sqrt{\rho_G\alpha}}}$	$\frac{\dot{m}_{DD+T_Aya}}{K_{M1}}$	2.55%
T + Void	$A \cdot \rho_{AV} \cdot V_T$	$K_{M3} = \left(\frac{x+S-xS}{S} \right) \cdot \left(\frac{\sqrt{\rho_L(1-\alpha)} + S\sqrt{\rho_G\alpha}}{\sqrt{\rho_L(1-\alpha)} + \sqrt{\rho_G\alpha}} \right)$	$\frac{\dot{m}_{Void+T_Aya}}{K_{M3}}$	1.91%

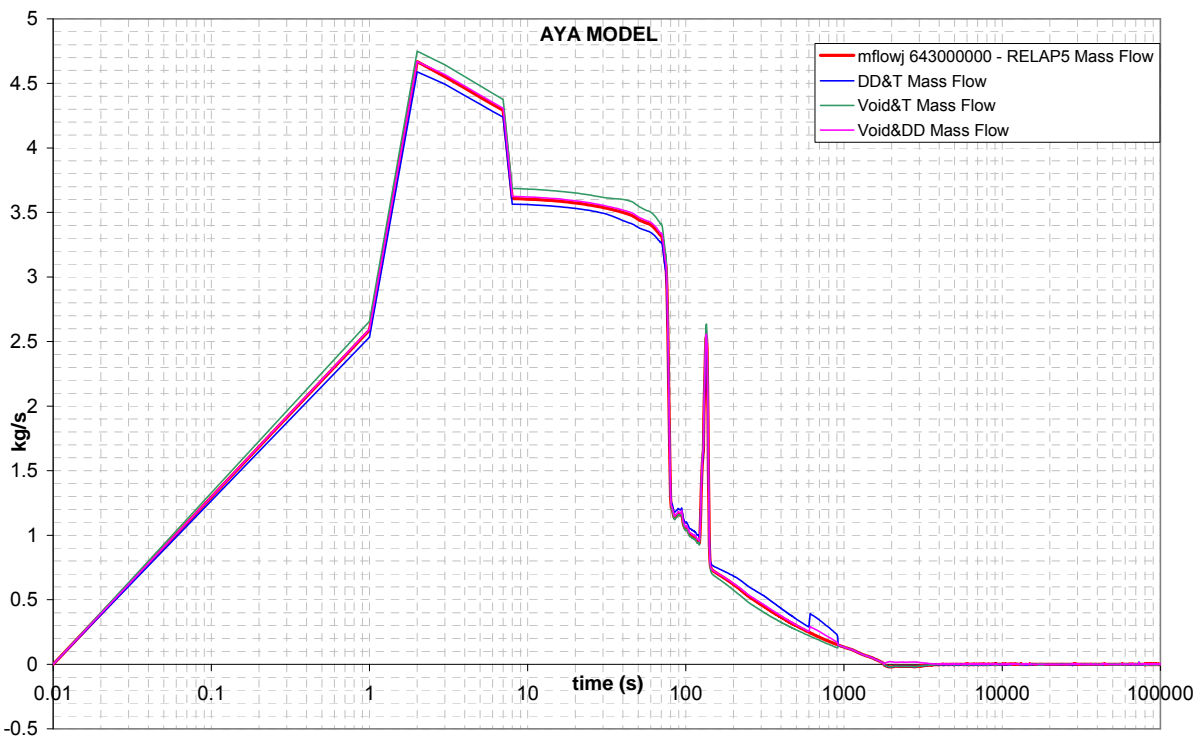


Figure 6.11: Comparison between the RELAP5 mass flow and the Spool Piece mass flow - Aya model - EBT SPLIT line, EBT break test

The considerations are the same of the previous section {6.1.2.1 – Rouhani model}. The most accurate coupling is the combination of a Void Fraction Detector with a Drag Disk, but each solution may be adopted, as indicated in Table 6.11.

Volumetric Model

Table 6.12: Errors per cent between the RELAP5 mass flow and the Spool Piece mass flow - Volumetric model - EBT SPLIT line, EBT break test

Coupling	Mass Flow Rate with two devices	Thermal-hydraulic factor	Corrected	Error
DD + Void	$A \cdot [\rho_{AV} \cdot (\rho V^2)]^{1/2}$	$K_S = \left((x + (1-x)S) \cdot \left(x + \frac{(1-x)}{S} \right) \right)$	$\frac{\dot{m}_{Void+DD}}{K_S^{1/2}}$	0.88%
DD + T	$A \cdot \rho V^2 / V_T$	$K_{M2} = \frac{(1-x + xS)}{(1-\alpha + \alpha S)}$	$\frac{\dot{m}_{DD+T_Vol}}{K_{M2}}$	7.42%
T + Void	$A \cdot \rho_{AV} \cdot V_T$	$K_{M4} = (x + S(1-x)) \cdot \left(\alpha + \frac{(1-\alpha)}{S} \right)$	$\frac{\dot{m}_{Void+T_Vol}}{K_{M4}}$	9.48%

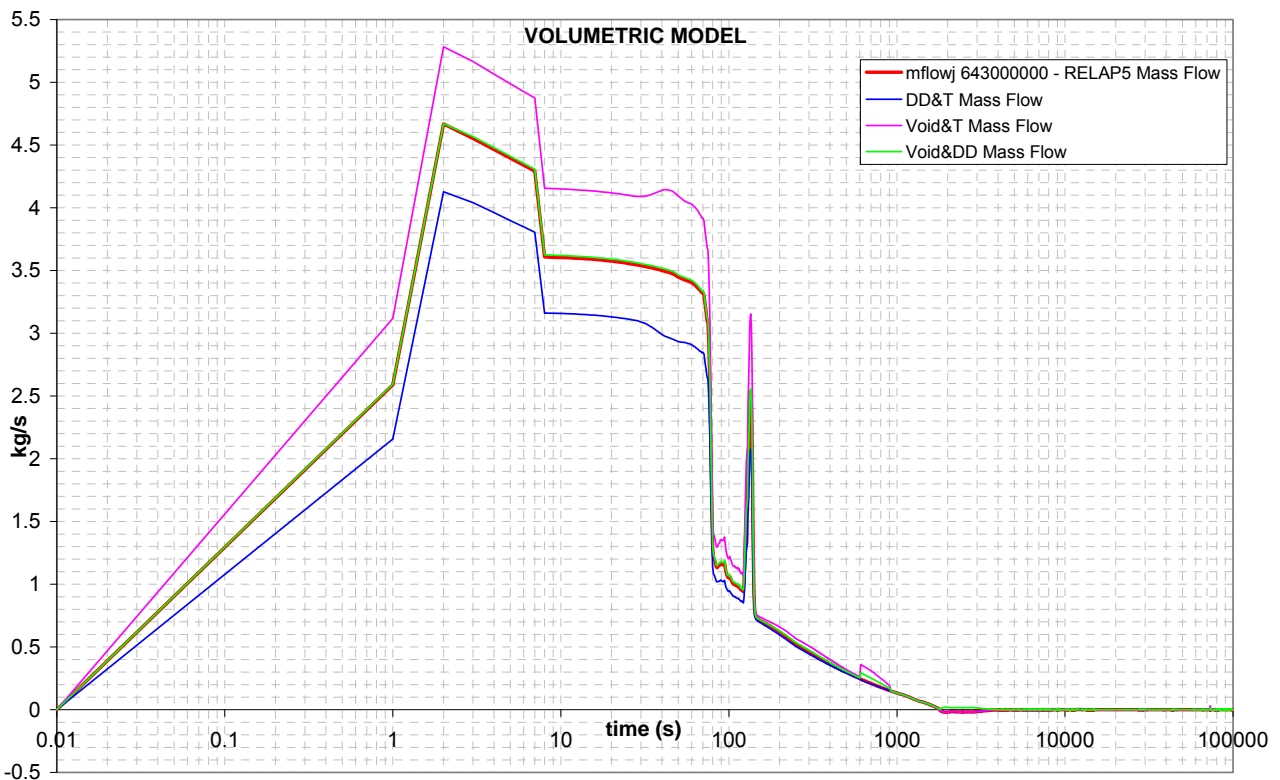


Figure 6.12: Comparison between the RELAP5 mass flow and the Spool Piece mass flow - Volumetric model - EBT SPLIT line, EBT break test

The volumetric model shows important errors for the coupling of a Turbine Flowmeter with the Void Fraction Detector or with a Drag Disk. The best coupling is represented by a Drag Disk and a Void Fraction Detector, as shown in Figure 6.12 and in Table 6.12, but also in the other cases, the error is below 10%.

6.1.2.2 ADS Stage-I ST

Rouhani model

Table 6.13: Errors per cent between the RELAP5 mass flow and the Spool Piece mass flow - Rouhani model - ADS Stage-I ST line, EBT break test

Coupling	Mass Flow Rate with two devices	Thermal-hydraulic factor	Corrected	Error
DD + Void	$A \cdot [\rho_{AV} \cdot (\rho V^2)]^{1/2}$	$K_S = \left((x + (1-x)S) \cdot \left(x + \frac{(1-x)}{S} \right) \right)$	$\frac{\dot{m}_{Void+DD}}{K_S^{1/2}}$	2.08%
DD + T	$A \cdot \rho V^2 / V_T$	1	\dot{m}_{DD+T}	0.00%
T + Void	$A \cdot \rho_{AV} \cdot V_T$	$K_S = \left((x + (1-x)S) \cdot \left(x + \frac{(1-x)}{S} \right) \right)$	$\frac{\dot{m}_{Void+T-Rou}}{K_S}$	4.53%

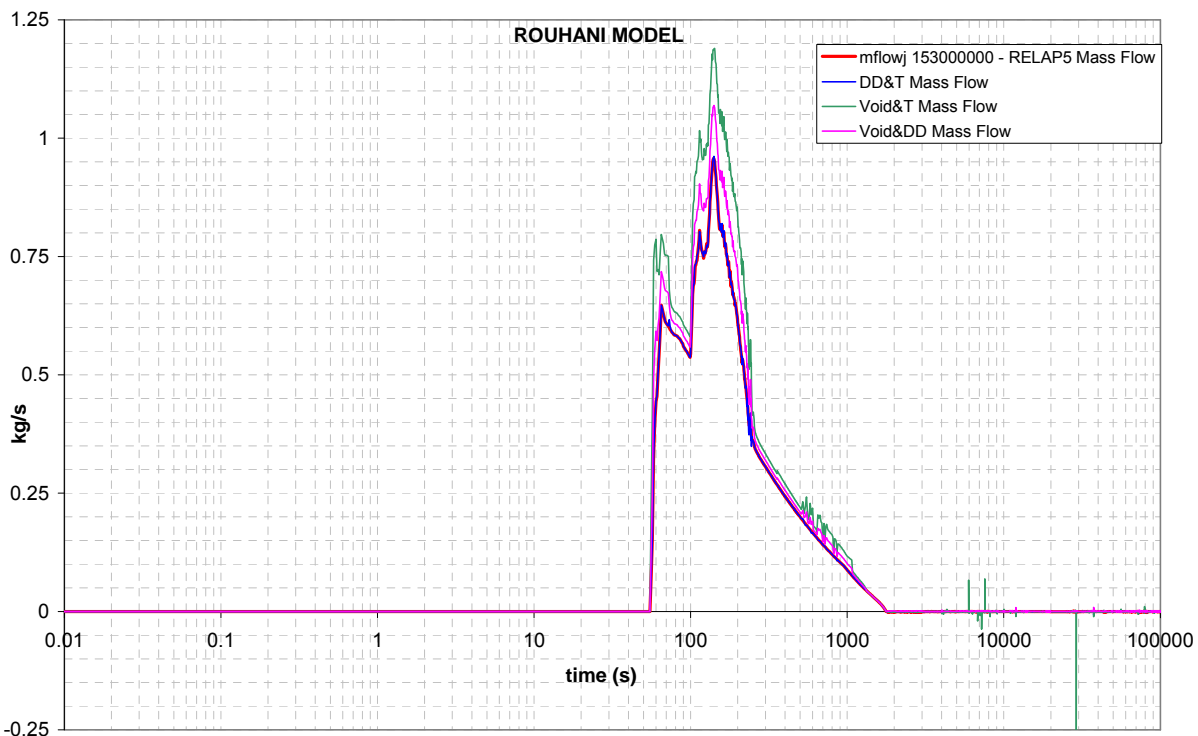


Figure 6.13: Comparison between the RELAP5 mass flow and the Spool Piece mass flow - Rouhani model - ADS Stage-I ST line, EBT break test

During the EBT break test, two-phase mass flow is foreseen in the ADS Stage-I ST line [5]. The most accurate solution is the coupling of a Drag Disk with a Turbine Flowmeter, which returns the exact value. The combination of a Void Fraction Detector with a Turbine Flowmeter gives the worst results, but in general the errors are below 10% as indicated in Table 6.13.

Aya Model

Table 6.14: Errors per cent between the RELAP5 mass flow and the Spool Piece mass flow - Aya model – ADS Stage-I ST line, EBT break test

Coupling	Mass Flow Rate with two devices	Thermal-hydraulic factor	Corrected	Error
DD + Void	$A \cdot [\rho_{AV} \cdot (\rho V^2)]^{1/2}$	$K_S = \left((x + (1-x)S) \cdot \left(x + \frac{(1-x)}{S} \right) \right)$	$\frac{\dot{m}_{Void+DD}}{K_S^{1/2}}$	2.08%
DD + T	$A \cdot \rho V^2 / V_T$	$K_{M1} = \frac{1-x+xS}{\sqrt{\rho_L(1-\alpha)} + S\sqrt{\rho_G\alpha}}$ $\frac{\sqrt{\rho_L(1-\alpha)} + S\sqrt{\rho_G\alpha}}{\sqrt{\rho_L(1-\alpha)} + \sqrt{\rho_G\alpha}}$	$\frac{\dot{m}_{DD+T_Aya}}{K_{M1}}$	3.08%
T + Void	$A \cdot \rho_{AV} \cdot V_T$	$K_{M3} = \left(\frac{x+S-xS}{S} \right) \cdot \left(\frac{\sqrt{\rho_L(1-\alpha)} + S\sqrt{\rho_G\alpha}}{\sqrt{\rho_L(1-\alpha)} + \sqrt{\rho_G\alpha}} \right)$	$\frac{\dot{m}_{Void+T_Aya}}{K_{M3}}$	2.61%

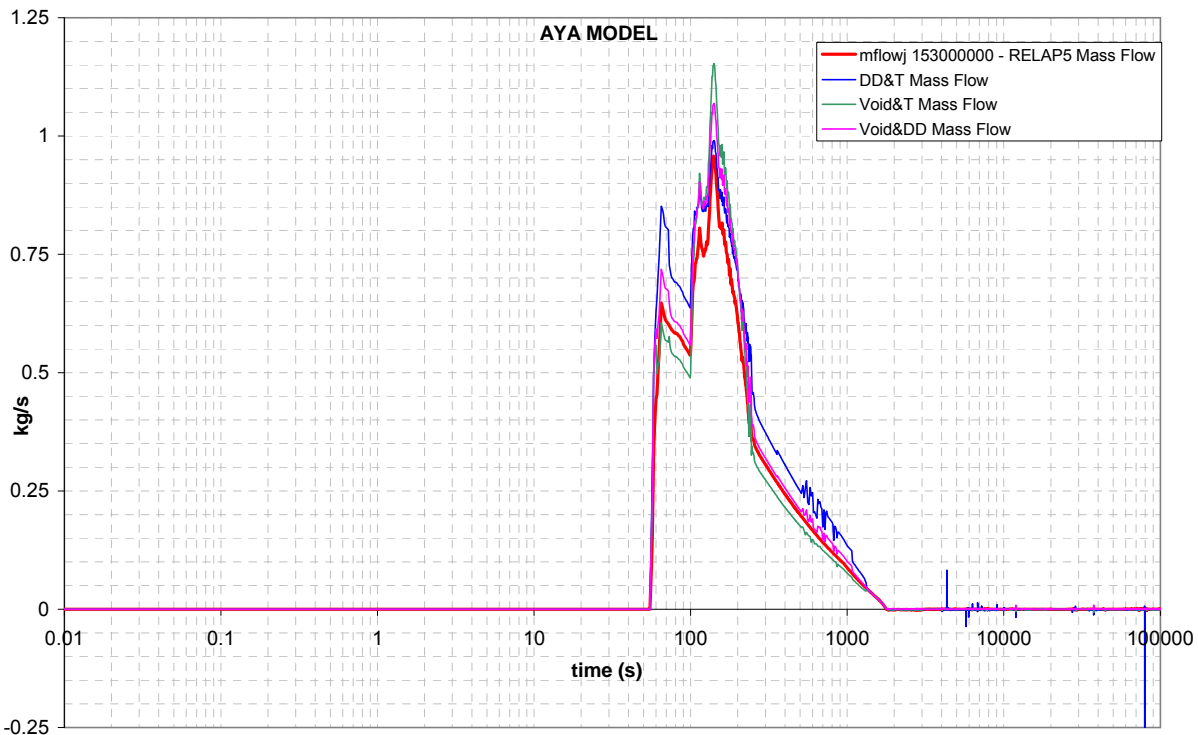


Figure 6.14: Comparison between the RELAP5 mass flow and the Spool Piece mass flow - Aya model – ADS Stage-I ST line, EBT break test

During the EBT break test, two-phase mass flow rate is foreseen in the ADS Stage-I ST line [5]. The errors concerning the various couplings according to the Aya models are around 3%. This leads to the consideration that all the solutions can be adopted, with an advantage for the Drag Disk and Void Fraction Detector combination, which difference is 2%, as indicated in Table 6.14.

Volumetric Model

Table 6.15: Errors per cent between the RELAP5 mass flow and the Spool Piece mass flow - Volumetric model - ADS ST (stage I) line, EBT break test

Coupling	Mass Flow Rate with two devices	Thermal-hydraulic factor	Corrected	Error
DD + Void	$A \cdot [\rho_{AV} \cdot (\rho V^2)]^{1/2}$	$K_S = \left((x + (1-x)S) \cdot \left(x + \frac{(1-x)}{S} \right) \right)$	$\frac{\dot{m}_{Void+DD}}{K_S^{1/2}}$	2.08%
DD + T	$A \cdot \rho V^2 / V_T$	$K_{M2} = \frac{(1-x+xS)}{(1-\alpha+\alpha S)}$	$\frac{\dot{m}_{DD+T_Vol}}{K_{M2}}$	6.99%
T + Void	$A \cdot \rho_{AV} \cdot V_T$	$K_{M4} = (x + S(1-x)) \cdot \left(\alpha + \frac{(1-\alpha)}{S} \right)$	$\frac{\dot{m}_{Void+T_Vol}}{K_{M4}}$	14.2%

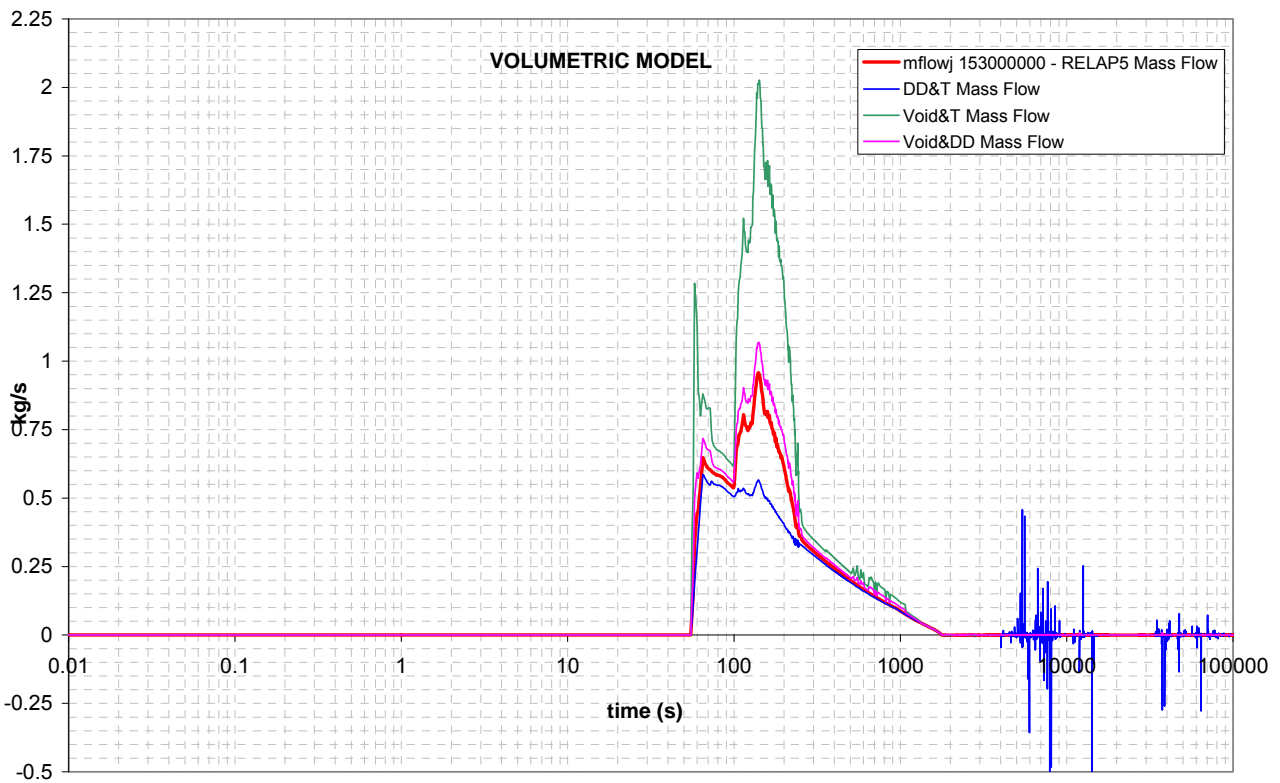


Figure 6.15: Comparison between the RELAP5 mass flow and the Spool Piece mass flow - Volumetric model - ADS Stage-I ST line, EBT break test

During the EBT break test, two-phase mass flow rate is foreseen in the ADS Stage-I ST line [5].

The Volumetric model applied to the ADS Stage-I ST during the EBT test gives an error around 14% for the coupling of a Turbine Flowmeter with a Void Fraction Detector, while the other cases have an error below 7% with a minimum for a Void Fraction Detector with a Drag Disk.

6.1.2.3 ADS Stage-I DT

Rouhani model

Table 6.16: Errors per cent between the RELAP5 mass flow and the Spool Piece mass flow - Rouhani model - ADS Stage-I DT line, EBT break test

Coupling	Mass Flow Rate with two devices	Thermal-hydraulic factor	Corrected	Error
DD + Void	$A \cdot [\rho_{AV} \cdot (\rho V^2)]^{1/2}$	$K_s = \left((x + (1-x)S) \cdot \left(x + \frac{(1-x)}{S} \right) \right)$	$\frac{\dot{m}_{Void+DD}}{K_s^{1/2}}$	5.27%
DD + T	$A \cdot \rho V^2 / V_T$	1	\dot{m}_{DD+T}	0.00%
T + Void	$A \cdot \rho_{AV} \cdot V_T$	$K_s = \left((x + (1-x)S) \cdot \left(x + \frac{(1-x)}{S} \right) \right)$	$\frac{\dot{m}_{Void+T_Rou}}{K_s}$	11.6%

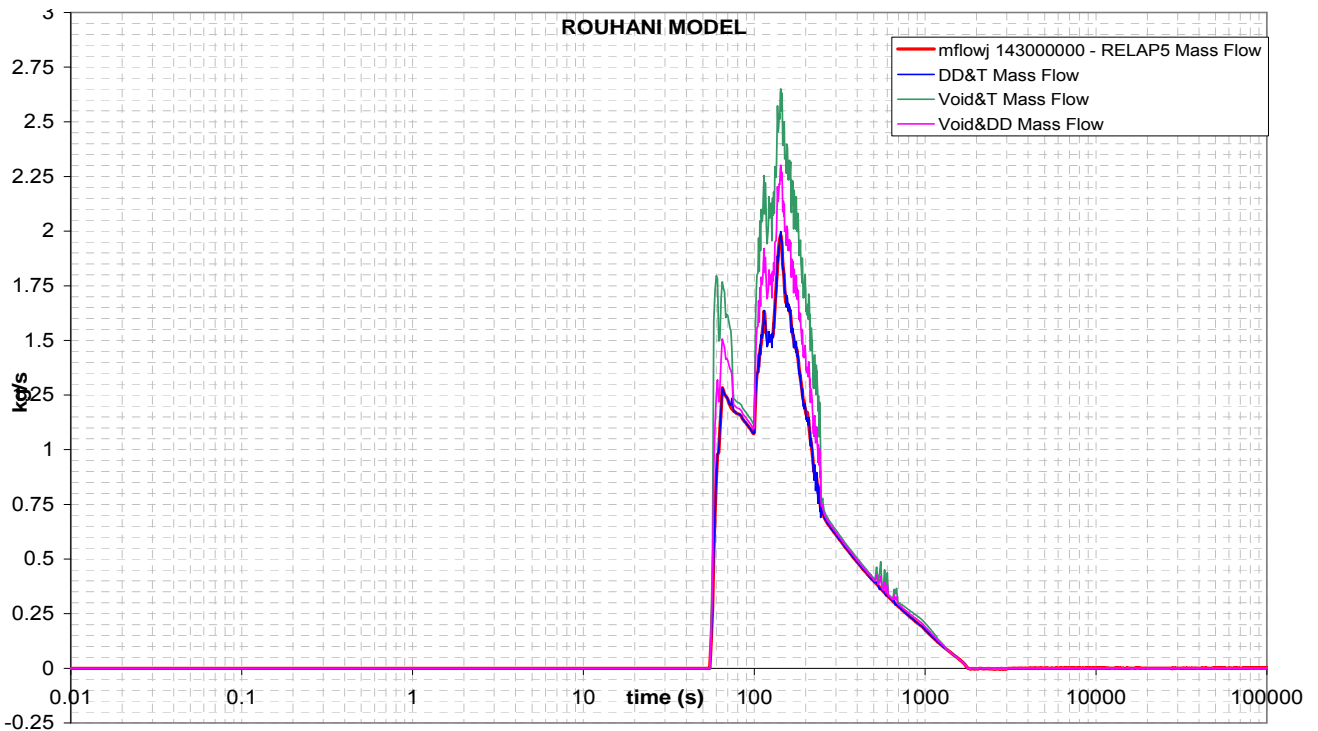


Figure 6.16: Comparison between the RELAP5 mass flow and the Spool Piece mass flow - Rouhani model - ADS Stage-I DT line, EBT break test

During the EBT break test, two-phase mass flow is foreseen in the ADS Stage-I DT line [5]. The considerations are similar to those in section {6.1.2.2- Rouhani model}. The T_Rou+DD combination is the most accurate, while the Void+T_Rou combination returns an error around 12%. The trends are the same of the RELAP5 mass flow rate.

Aya Model

Table 6.17: Errors per cent between the RELAP5 mass flow and the Spool Piece mass flow - Aya model – ADS Stage-I DT line, EBT break test

Coupling	Mass Flow Rate with two devices	Thermal-hydraulic factor	Corrected	Error
DD + Void	$A \cdot [\rho_{AV} \cdot (\rho V^2)]^{1/2}$	$K_S = \left((x + (1-x)S) \cdot \left(x + \frac{(1-x)}{S} \right) \right)$	$\frac{\dot{m}_{Void+DD}}{K_S^{1/2}}$	5.27%
DD + T	$A \cdot \rho V^2 / V_T$	$K_{M1} = \frac{1-x+xS}{\frac{\sqrt{\rho_L(1-\alpha)} + S\sqrt{\rho_G\alpha}}{\sqrt{\rho_L(1-\alpha)} + \sqrt{\rho_G\alpha}}}$	$\frac{\dot{m}_{DD+T_Aya}}{K_{M1}}$	6.41%
T + Void	$A \cdot \rho_{AV} \cdot V_T$	$K_{M3} = \left(\frac{x+S-xS}{S} \right) \cdot \left(\frac{\sqrt{\rho_L(1-\alpha)} + S\sqrt{\rho_G\alpha}}{\sqrt{\rho_L(1-\alpha)} + \sqrt{\rho_G\alpha}} \right)$	$\frac{\dot{m}_{Void+T_Aya}}{K_{M3}}$	6.11%

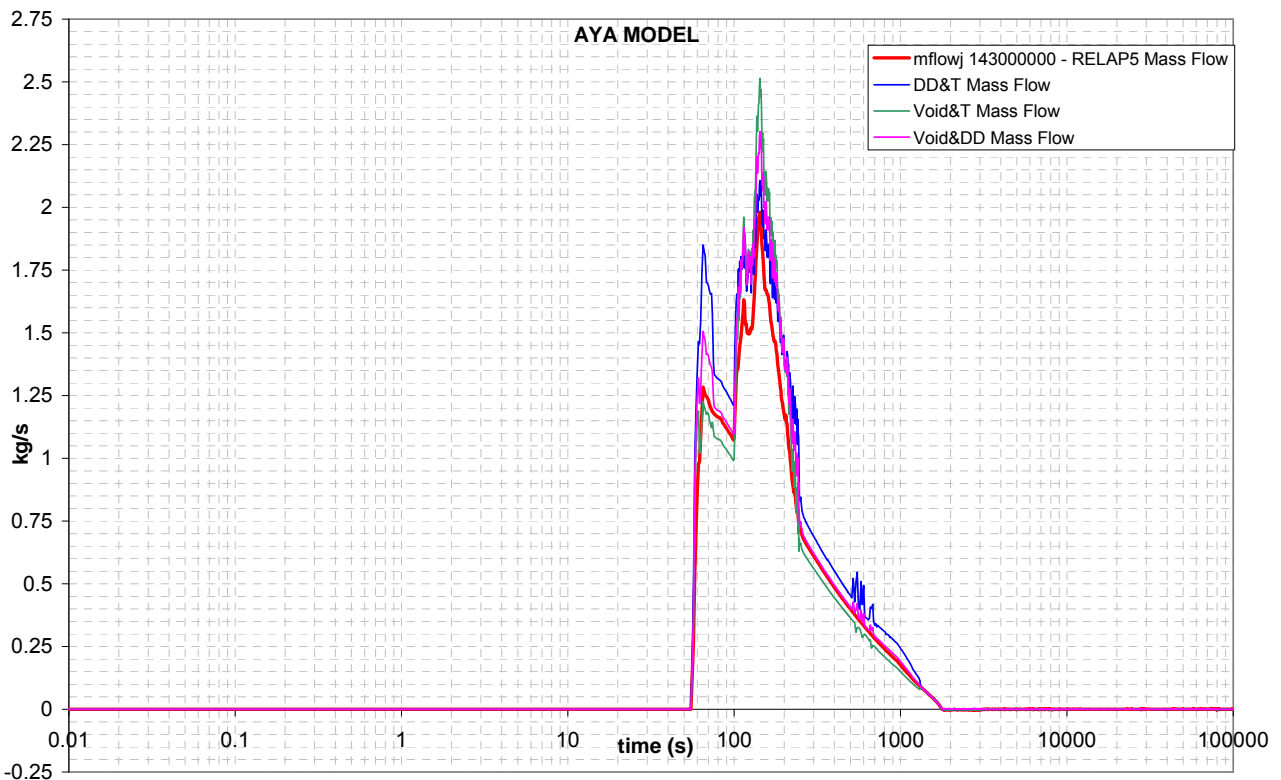


Figure 6.17: Comparison between the RELAP5 mass flow and the Spool Piece mass flow - Aya model – ADS Stage-I DT line, EBT break test

Considering the Aya model for the mixture velocity, the different couplings return errors around 6%; therefore every combination can be used to estimate the mass flow rate.

Volumetric Model

Table 6.18: Errors per cent between the RELAP5 mass flow and the Spool Piece mass flow - Volumetric model - ADS Stage-I DT line, EBT break test

Coupling	Mass Flow Rate with two devices	Thermal-hydraulic factor	Corrected	Error
DD + Void	$A \cdot [\rho_{AV} \cdot (\rho V^2)]^{1/2}$	$K_S = \left((x + (1-x)S) \cdot \left(x + \frac{(1-x)}{S} \right) \right)$	$\frac{\dot{m}_{Void+DD}}{K_S^{1/2}}$	5.27%
DD + T	$A \cdot \rho V^2 / V_T$	$K_{M2} = \frac{(1-x + xS)}{(1-\alpha + \alpha S)}$	$\frac{\dot{m}_{DD+T_Vol}}{K_{M2}}$	10.4%
T + Void	$A \cdot \rho_{AV} \cdot V_T$	$K_{M4} = (x + S(1-x)) \cdot \left(\alpha + \frac{(1-\alpha)}{S} \right)$	$\frac{\dot{m}_{Void+T_Vol}}{K_{M4}}$	34.6%

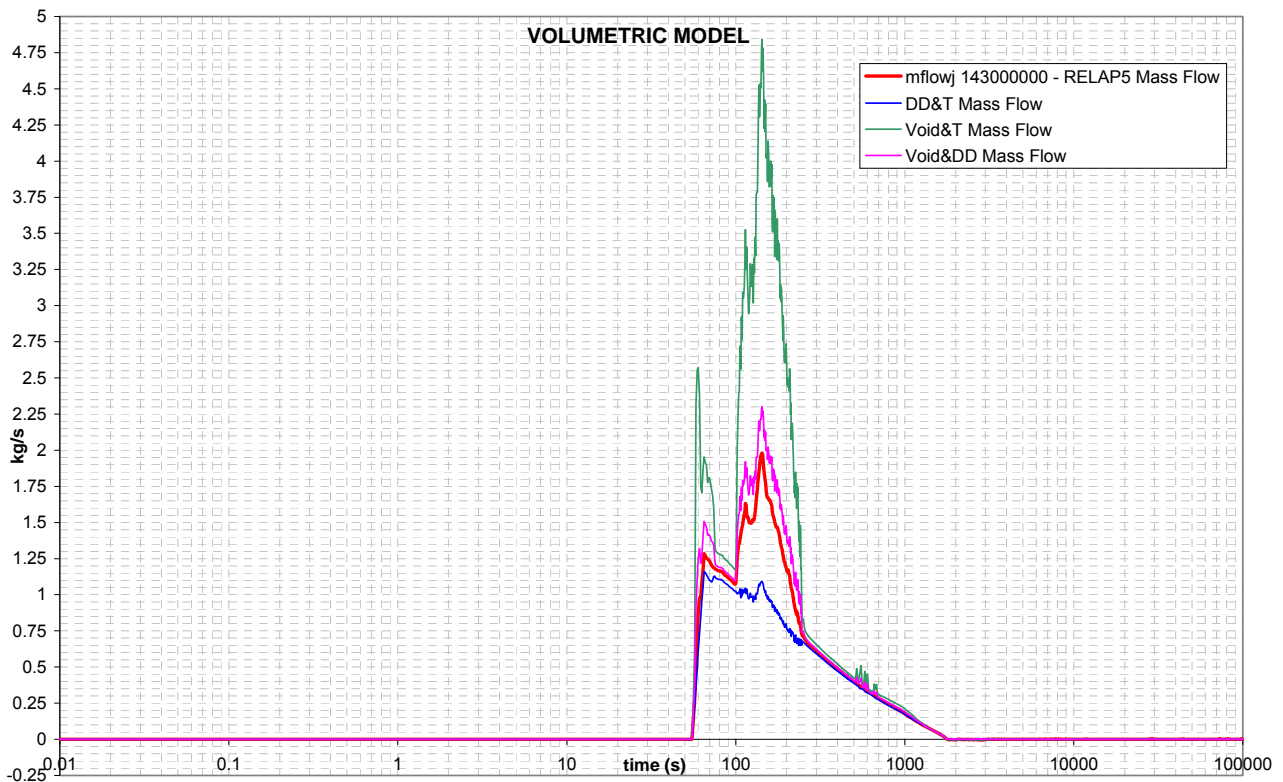


Figure 6.18: Comparison between the RELAP5 mass flow and the Spool Piece mass flow - Volumetric model – ADS Stage-I DT line, EBT break test

The volumetric model leads to significant errors except for the combination of the Void Fraction Detector with the Drag Disk, for which the error is below 6%. The use of a Turbine Flowmeter and a Void Fraction Detector seems unattainable.

6.1.3 ADS TEST

During the ADS break test, two spool pieces are involved in measuring two-phase mass flow, as reported in [5]: one on the ADS SPLIT break line and one on the ADS Stage-I DT.

6.1.3.1 ADS SPLIT break line

Rouhani model

Table 6.19: Errors per cent between the RELAP5 mass flow and the Spool Piece mass flow - Rouhani model - ADS SPLIT line, ADS break test

Coupling	Mass Flow Rate with two devices	Thermal-hydraulic factor	Corrected	Error
DD + Void	$A \cdot [\rho_{AV} \cdot (\rho V^2)]^{1/2}$	$K_S = \left((x + (1-x)S) \cdot \left(x + \frac{(1-x)}{S} \right) \right)$	$\frac{\dot{m}_{Void+DD}}{K_s^{1/2}}$	8.03%
DD + T	$A \cdot \rho V^2 / V_T$	1	\dot{m}_{DD+T}	0.14%
T + Void	$A \cdot \rho_{AV} \cdot V_T$	$K_S = \left((x + (1-x)S) \cdot \left(x + \frac{(1-x)}{S} \right) \right)$	$\frac{\dot{m}_{Void+T-Rou}}{K_s}$	18.0%

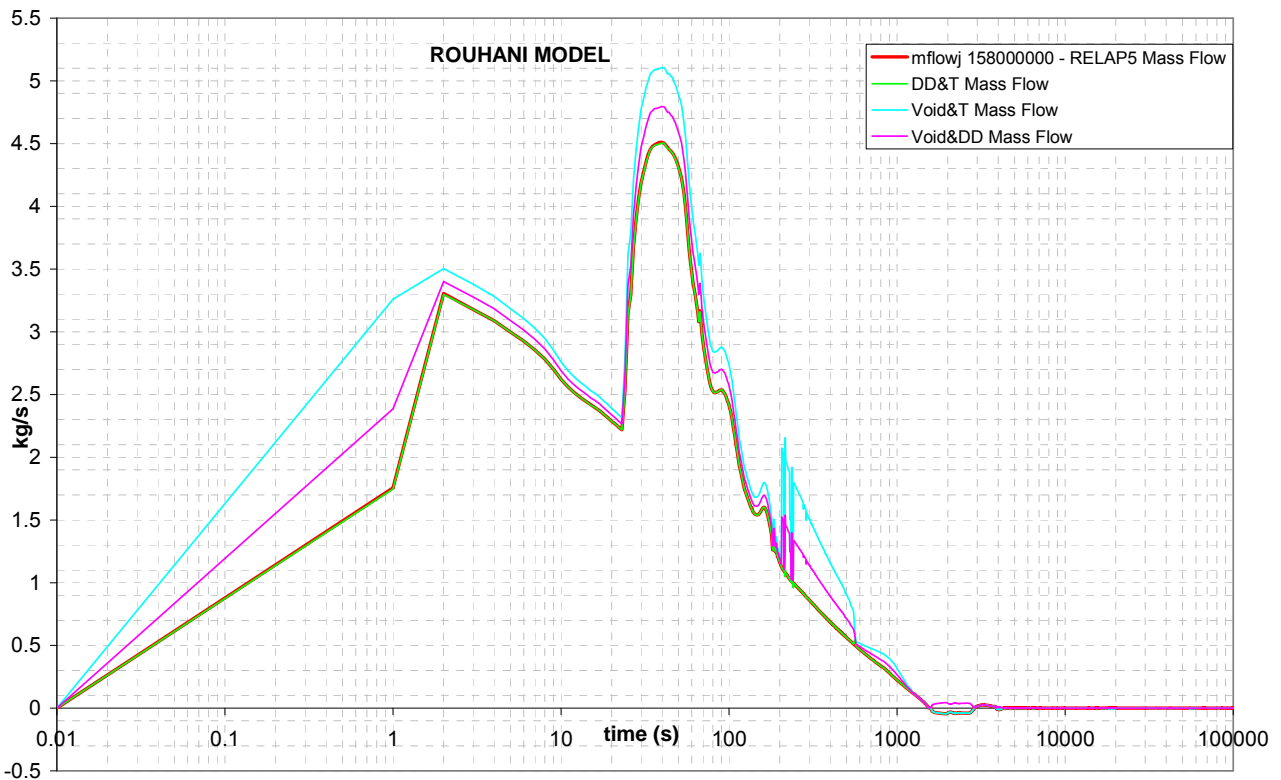


Figure 6.19: Comparison between the RELAP5 mass flow and the Spool Piece mass flow - Rouhani model - ADS SPLIT line, ADS break test

Applying the Rouhani model to the Turbine Flowmeter, the coupling of a Drag Disk with a Turbine Flowmeter returns the correct mass flow rate as shown in Figure 6.19.

The coupling of a Void Fraction Detector with a Drag Disk appears more accurate than the coupling of a Void Fraction Detector with a Turbine Flowmeter. The combination of a Drag Disk with a Void Fraction Detector involves an error below 8%, while the Turbine Flowmeter and the Void Fraction Detector takes to a significant error, around 18%, as shown in Table 6.19.

Aya Model

Table 6.20: Errors per cent between the RELAP5 mass flow and the Spool Piece mass flow - Aya model - ADS SPLIT line, ADS break test

Coupling	Mass Flow Rate with two devices	Thermal-hydraulic factor	Corrected	Error
DD + Void	$A \cdot [\rho_{AV} \cdot (\rho V^2)]^{1/2}$	$K_S = \left((x + (1-x)S) \cdot \left(x + \frac{(1-x)}{S} \right) \right)$	$\frac{\dot{m}_{Void+DD}}{K_S^{1/2}}$	8.03%
DD + T	$A \cdot \rho V^2 / V_T$	$K_{M1} = \frac{1-x+xS}{\frac{\sqrt{\rho_L(1-\alpha)} + S\sqrt{\rho_G\alpha}}{\sqrt{\rho_L(1-\alpha)} + \sqrt{\rho_G\alpha}}}$	$\frac{\dot{m}_{DD+T_Aya}}{K_{M1}}$	17.6%
T + Void	$A \cdot \rho_{AV} \cdot V_T$	$K_{M3} = \left(\frac{x+S-xS}{S} \right) \cdot \left(\frac{\sqrt{\rho_L(1-\alpha)} + S\sqrt{\rho_G\alpha}}{\sqrt{\rho_L(1-\alpha)} + \sqrt{\rho_G\alpha}} \right)$	$\frac{\dot{m}_{Void+T_Aya}}{K_{M3}}$	4.11%

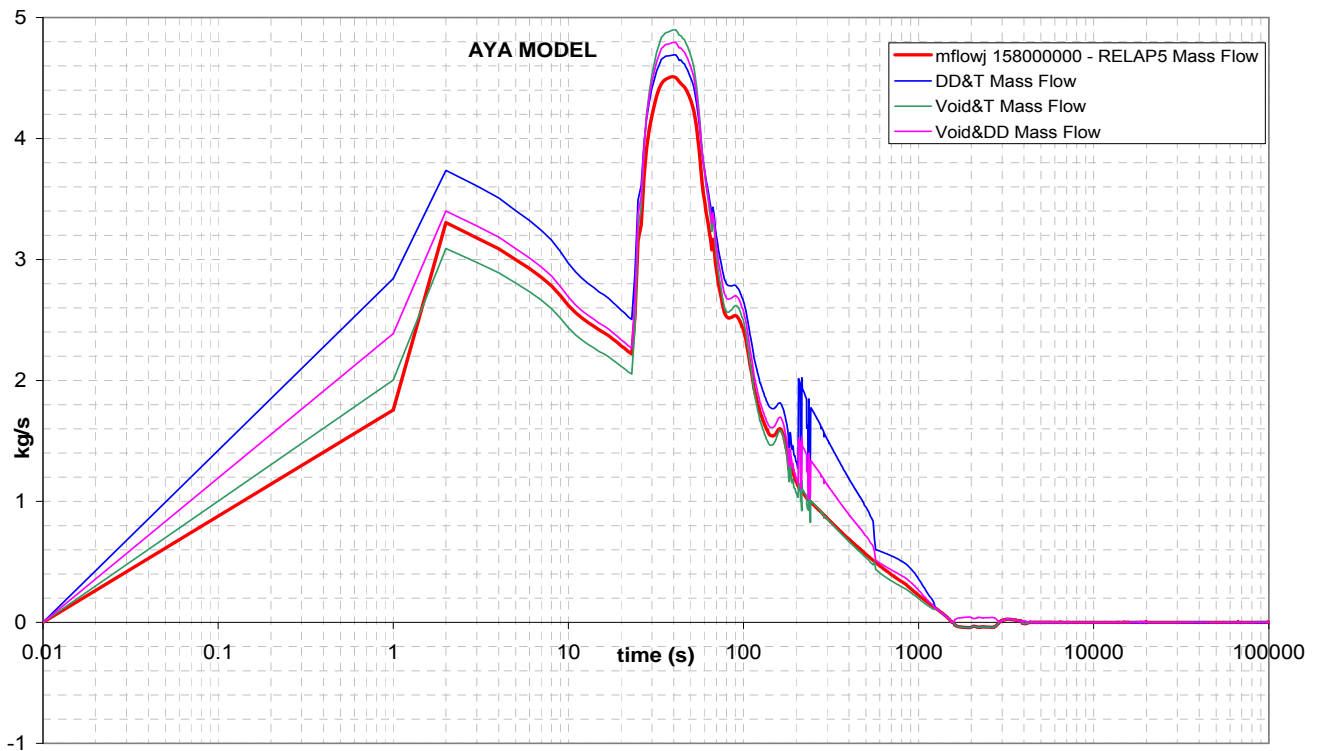


Figure 6.20: Comparison between the RELAP5 mass flow and the Spool Piece mass flow - Aya model - ADS SPLIT line, ADS break test

When the mixture velocity is described by the Aya model, the ADS SPLIT mass flow rate is better simulated by the coupling of a Void Fraction Detector and a Turbine Flowmeter, as shown in Table 6.20. The other two combinations return larger errors, around 8% for the DD+Void coupling and around 17.6% for the DD+T coupling.

Volumetric Model

Table 6.21: Errors per cent between the RELAP5 mass flow and the Spool Piece mass flow - Volumetric model - ADS SPLIT line, ADS break test

Coupling	Mass Flow Rate with two devices	Thermal-hydraulic factor	Corrected	Error
DD + Void	$A \cdot [\rho_{AV} \cdot (\rho V^2)]^{1/2}$	$K_S = \left((x + (1-x)S) \cdot \left(x + \frac{(1-x)}{S} \right) \right)$	$\frac{\dot{m}_{Void+DD}}{K_S^{1/2}}$	8.03%
DD + T	$A \cdot \rho V^2 / V_T$	$K_{M2} = \frac{(1-x+xS)}{(1-\alpha+\alpha S)}$	$\frac{\dot{m}_{DD+T_Vol}}{K_{M2}}$	13.8%
T + Void	$A \cdot \rho_{AV} \cdot V_T$	$K_{M4} = (x + S(1-x)) \cdot \left(\alpha + \frac{(1-\alpha)}{S} \right)$	$\frac{\dot{m}_{Void+T_Vol}}{K_{M4}}$	33.9%

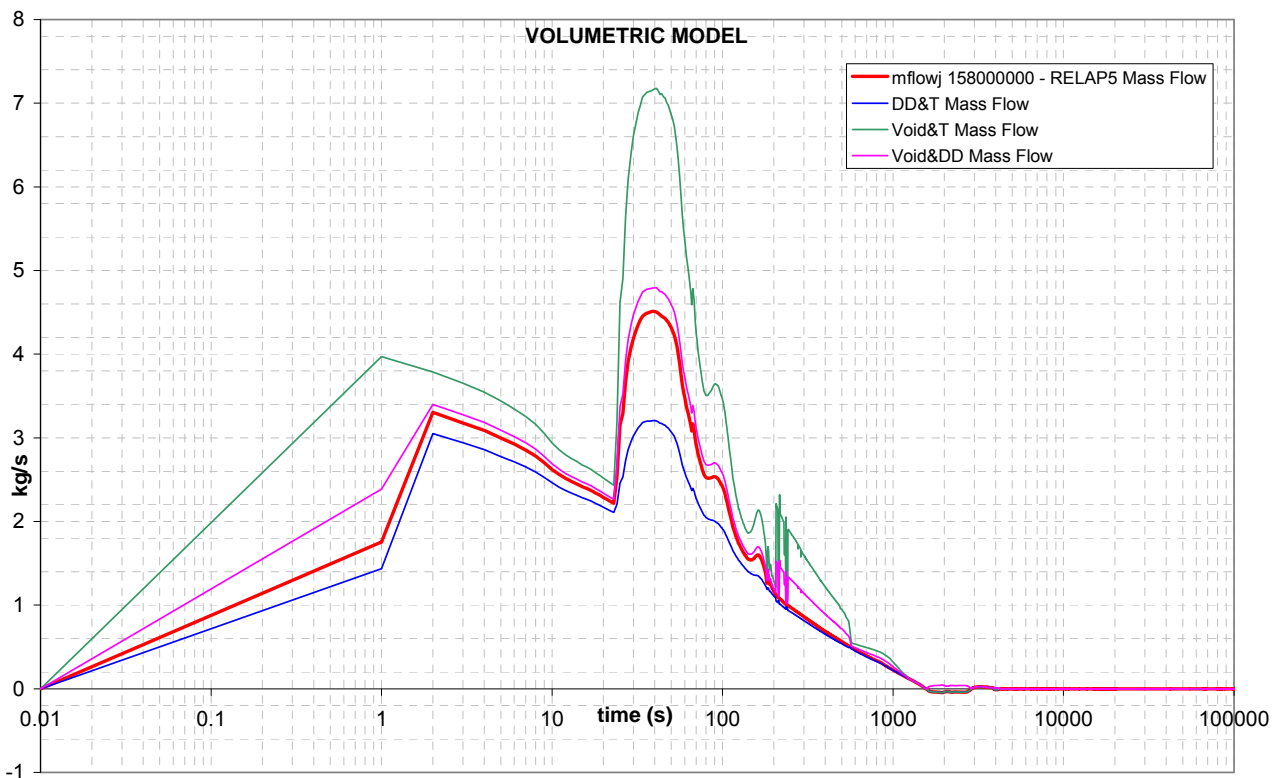


Figure 6.21: Comparison between the RELAP5 mass flow and the Spool Piece mass flow - Volumetric model - ADS SPLIT line, ADS break test

When the mixture velocity is described by the Volumetric model, the ADS SPLIT mass flow rate is better simulated by the coupling of a Void Fraction Detector and a Drag Disk, as shown in Table 6.21 with an error below 10%. The other two solutions presents not acceptable errors, around 14% for the DD+T combination, and 34% for the T+Void combination.

6.1.3.2 ADS Stage-I DT

Rouhani model

Table 6.22: Errors per cent between the RELAP5 mass flow and the Spool Piece mass flow - Rouhani model - ADS Stage-I DT line, ADS break test

Coupling	Mass Flow Rate with two devices	Thermal-hydraulic factor	Corrected	Error
DD + Void	$A \cdot [\rho_{AV} \cdot (\rho V^2)]^{1/2}$	$K_S = \left((x + (1-x)S) \cdot \left(x + \frac{(1-x)}{S} \right) \right)$	$\frac{\dot{m}_{Void+DD}}{K_s^{1/2}}$	4.50%
DD + T	$A \cdot \rho V^2 / V_T$	1	\dot{m}_{DD+T}	0.33%
T + Void	$A \cdot \rho_{AV} \cdot V_T$	$K_S = \left((x + (1-x)S) \cdot \left(x + \frac{(1-x)}{S} \right) \right)$	$\frac{\dot{m}_{Void+T_Rou}}{K_s}$	10.7%

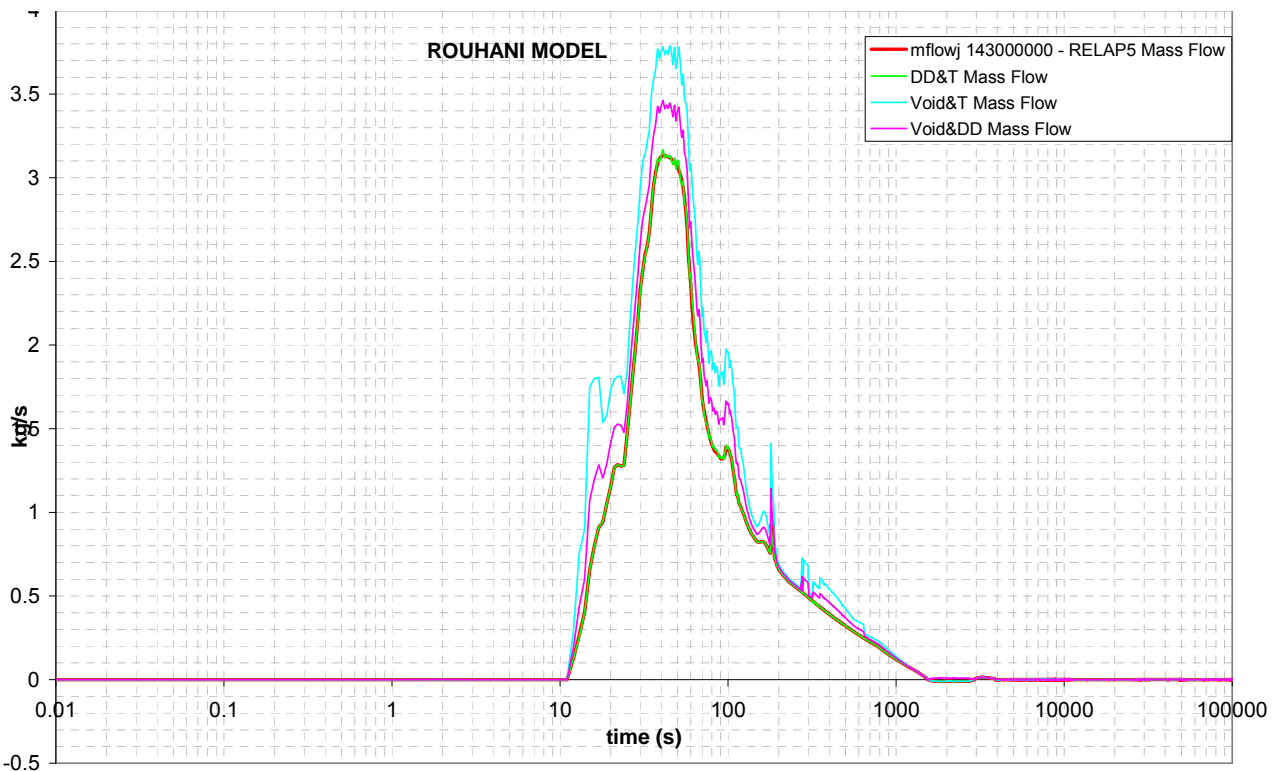


Figure 6.22: Comparison between the RELAP5 mass flow and the Spool Piece mass flow - Rouhani model - ADS Stage-I ST line, ADS break test

During the ADS break test, the ADS Stage-I DT experiments two-phase mass flow rate. According to the Rouhani model, the minimum error of about 0.4% is achieved by the combination of a Drag

Disk and a Turbine Flowmeter. The coupling of a Void Fraction Detector and a Turbine Flowmeter returns the less accurate results, with an error around 11%, while a Void Fraction Detector and a Drag Disk output gives an error below 5%, as shown in Table 6.22.

Aya Model

Table 6.23: Errors per cent between the RELAP5 mass flow and the Spool Piece mass flow - Aya model - ADS Stage-I DT line, ADS break test

Coupling	Mass Flow Rate with two devices	Thermal-hydraulic factor	Corrected	Error
DD + Void	$A \cdot [\rho_{AV} \cdot (\rho V^2)]^{1/2}$	$K_S = \left((x + (1-x)S) \cdot \left(x + \frac{(1-x)}{S} \right) \right)$	$\frac{\dot{m}_{Void+DD}}{K_S^{1/2}}$	4.50%
DD + T	$A \cdot \rho V^2 / V_T$	$K_{M1} = \frac{1-x+xS}{\frac{\sqrt{\rho_L(1-\alpha)} + S\sqrt{\rho_G\alpha}}{\sqrt{\rho_L(1-\alpha)} + \sqrt{\rho_G\alpha}}}$	$\frac{\dot{m}_{DD+T_Aya}}{K_{M1}}$	7.75%
T + Void	$A \cdot \rho_{AV} \cdot V_T$	$K_{M3} = \left(\frac{x+S-xS}{S} \right) \cdot \left(\frac{\sqrt{\rho_L(1-\alpha)} + S\sqrt{\rho_G\alpha}}{\sqrt{\rho_L(1-\alpha)} + \sqrt{\rho_G\alpha}} \right)$	$\frac{\dot{m}_{Void+T_Aya}}{K_{M3}}$	6.09%

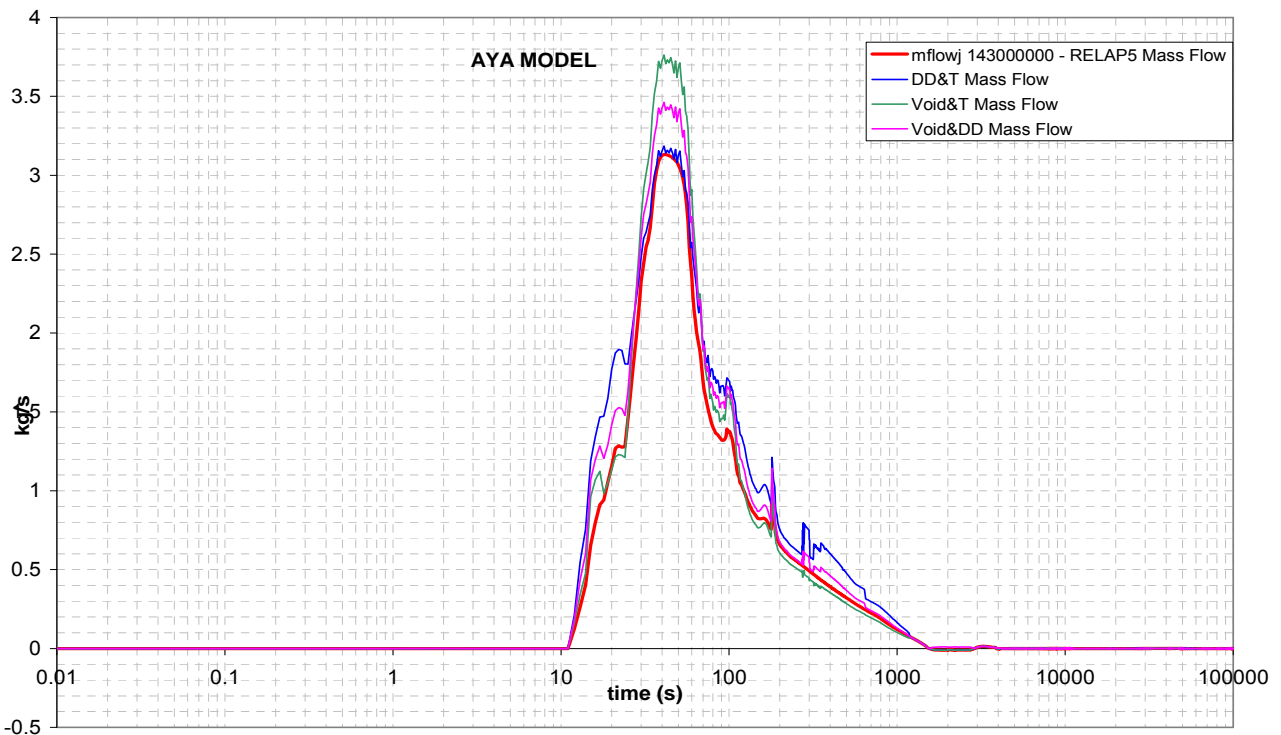


Figure 6.23: Comparison between the RELAP5 mass flow and the Spool Piece mass flow - Aya model - ADS Stage-I DT line, ADS break test

During the ADS break test, the ADS Stage-I DT experiments two-phase mass flow rate. According to the Aya model, the various couplings return an error below 8%. The best combination is the coupling of a Drag Disk and a Void Fraction Detector.

Volumetric Model

Table 6.24: Errors per cent between the RELAP5 mass flow and the Spool Piece mass flow - Volumetric model - ADS Stage-I DT line, ADS break test

Coupling	Mass Flow Rate with two devices	Thermal-hydraulic factor	Corrected	Error
DD + Void	$A \cdot [\rho_{AV} \cdot (\rho V^2)]^{1/2}$	$K_S = \left((x + (1-x)S) \cdot \left(x + \frac{(1-x)}{S} \right) \right)$	$\frac{\dot{m}_{Void+DD}}{K_S^{1/2}}$	4.50%
DD + T	$A \cdot \rho V^2 / V_T$	$K_{M2} = \frac{(1-x + xS)}{(1-\alpha + \alpha S)}$	$\frac{\dot{m}_{DD+T_Vol}}{K_{M2}}$	12.4%
T + Void	$A \cdot \rho_{AV} \cdot V_T$	$K_{M4} = (x + S(1-x)) \cdot \left(\alpha + \frac{(1-\alpha)}{S} \right)$	$\frac{\dot{m}_{Void+T_Vol}}{K_{M4}}$	34.8%

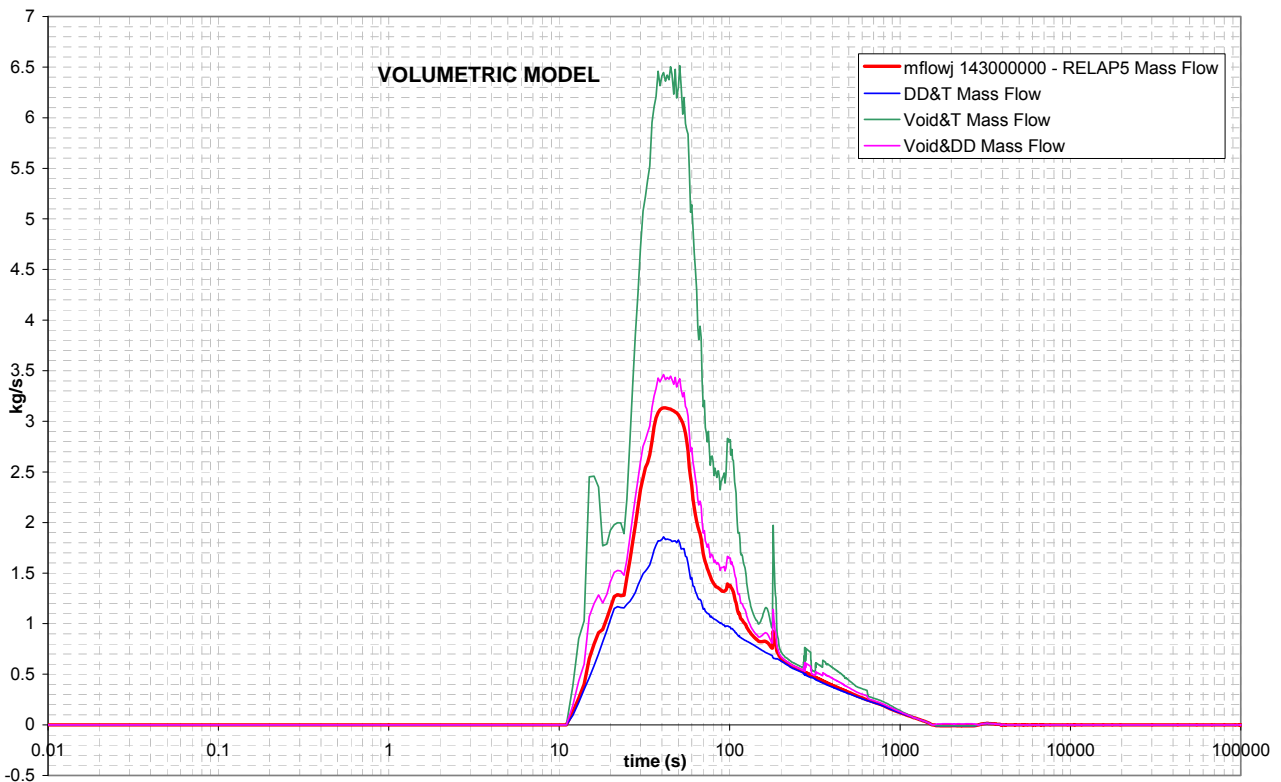


Figure 6.24: Comparison between the RELAP5 mass flow and the Spool Piece mass flow - Volumetric model - ADS Stage-I DT line, ADS break test

During the ADS break test, the ADS Stage-I DT experiments two-phase mass flow rate. According to the Volumetric model, the Spool Piece arranged with a Void Fraction Detector and a Drag Disk returns an error around 4.5%. The combination of a Void Fraction Detector with a Turbine Flowmeter returns an error greater than 30%, as indicated in Table 6.24.

6.1.4 Synthesis on two instrument spool piece

The analytical analysis on the use of a two-instrument-Spool Piece to determine the two-phase mass flow rate has led to the following conclusions:

- As reported in the tables of section {6.1}, in general, the combination of two devices does not give the exact mass flow rate;
- Each coupling returns a signal that follows the trend of the RELAP5 mass flow rate;
- Theoretically, the unique combination that provides the exact mass flow rate is the Drag Disk and Turbine Flowmeter coupling, according to the Rouhani model for the mixture velocity;
- The Volumetric Model appears to be the most inaccurate for each line;
- The error derived by the use of two instruments is affected by the slip ratio; during the EBT transient test the liquid and gas velocities in the EBT SPLIT break line are very similar and the slip ratio is around 1.1, as reported in [5]. Figures of section {6.1.2} demonstrate that any combination may be suitable to measure the mass flow rate with minimum error. For all the other lines the involved errors are high, because two-phase velocities are very different.
- Preliminary experiments are required to find out which velocity model better adapts to the Turbine Flowmeter in the various thermal-hydraulic conditions occurring in the different lines during the transients. It is also possible that different models may be applied to several thermal-hydraulic conditions, like low or high mass flow, quality, velocities or flow regimes. Anyway, some considerations can be done on each model: if the mixture velocity is described by the Rouhani model, the most accurate coupling in every line for each transient is the Drag Disk with the Turbine Flowmeter; while, if the Volumetric model simulates better the Turbine behaviour, the best combination is represented by the Void Fraction Detector and the Drag Disk, therefore without the Turbine Flowmeter; finally, according to the Aya model, the DD+T spool piece is not suggested.
- In conclusion, considering the use of all the velocity models, for the five involved lines, the use of spool pieces arranged by two instruments leads to the lowest errors if the following solution is adopted:
 - DVI SPLIT break line: Drag Disk + Turbine Flowmeter
 - EBT SPLIT break line: Drag Disk + Void Fraction Detector
 - ADS SPLIT break line: Drag Disk + Void Fraction Detector
 - ADS ST (stage I) line Drag Disk + Void Fraction Detector
 - ADS ST (stage I) line Drag Disk + Void Fraction Detector

In fact, if the turbine velocity is described by the Rouhani model, the error is minimum, but, when the other two models – Aya and Volumetric – are taken into consideration, the errors are definitely higher, thus the average error of the DD+T spool piece is larger than the DD+Void spool piece.

Anyway, the errors committed in each position using the coupling of a Drag Disk and a Turbine Flowmeter is slight higher than the use of a Drag Disk and a Void Fraction Detector, in particular for the EBT SPLIT break line and this could largely simplify the spool piece set-up.

6.2 Determination of the mass flow rate with three instruments

The determination of the mass flow using three devices theoretically does not involve errors. The output combination of a Drag Disk, a Turbine Flowmeter and a Void Fraction Detector returns also the quality and the slip ratio, as indicated in section {5.2}.

An appropriate numerical program has been developed in order to demonstrate the feasibility to obtain the mass flow, the liquid and gas velocities and the quality from the theoretical responses of the three instruments, coupled to the absolute pressure. In this section the calculation procedure is presented for each velocity model.

The use of three instruments make the choice of the models to reduce the Turbine velocities to be the only element that brings uncertainty.

6.2.1 Rouhani model

The Turbine Flowmeter response, modelled according to the Rouhani assumption, make the use of three instruments redundant for the determination of the mass flow. In section {6.1} it is shown that the coupling of a Turbine Flowmeter and a Drag Disk returns the correct results. The necessity to determine also the quality, the liquid and gas velocities requires the use of the third device, the Void Fraction Detector.

The pressure and temperature values are also necessary to calculate the density values.

$$\rho_{AV} = \alpha\rho_G + (1 - \alpha)\rho_L \quad (6.1)$$

$$V_T = V_L \frac{\alpha\rho_G S^2 + (1 - \alpha)\rho_L}{\alpha\rho_G S + (1 - \alpha)\rho_L} \quad (6.2)$$

$$(\rho V^2) = V_L^2 (\alpha\rho_G S^2 + (1 - \alpha)\rho_L) \quad (6.3)$$

From equation (6.1) it is possible to determine the void fraction. Instead the equations (6.2) and (6.3) present two unknown terms: the slip ratio S and the liquid velocity V_L . To get both the values, a mathematical system has to be solved with the use of an appropriate numeric program. In this software program the equations (6.2) and (6.3), rearranged as follows:

$$S = \sqrt{\frac{\left(\frac{\rho V^2}{V_L^2}\right) - (1-\alpha)\rho_L}{\alpha\rho_G}} \quad (6.4)$$

$$V_L = V_T \frac{\alpha\rho_G S + (1-\alpha)\rho_L}{\alpha\rho_G S^2 + (1-\alpha)\rho_L} \quad (6.5)$$

are written in a iterative routine in which initially, the liquid velocity is set to a guess value. The slip ratio and the liquid velocity are calculated according to (6.4) and (6.5). The difference between the two values of the liquid velocity is derived and stored in a vector. Then, the guess liquid velocity is increased and the calculation process is repeated. After an appropriate number of cycles, the vector which contains all the differences is analysed and the absolute minimum point is identified. The liquid velocity and the slip ratio are taken in that position. Finally the quality and the gas velocity are calculated using:

$$x = \frac{1}{1 + \frac{1-\alpha}{\alpha} \frac{\rho_L}{\rho_G} \frac{1}{S}} \quad (6.6)$$

$$V_G = S \cdot V_L \quad (6.7)$$

Once available the quality, the slip ratio, the liquid velocity and the void fraction, the mass flow value is derived using the expressions in section {5}, using the explicit responses of two instruments and the quantities derived by the third instrument:

$$\dot{m}_{DD+T} = A \cdot \rho V^2 \Big/ V_T \quad (6.8)$$

The use of the Drag Disk and the Turbine Flowmeter outputs does not require the knowledge of other quantities.

$$\dot{m} = \frac{\dot{m}_{Void+T}}{K_s} = A \cdot \frac{\left(\frac{\rho V^2}{V_T}\right)}{K_s} = A \cdot \frac{\left(\frac{\rho V^2}{V_T}\right)}{\left[\left(x + (1-x)S\right) \cdot \left(x + \frac{(1-x)}{S}\right)\right]} \quad (6.9)$$

$$\dot{m} = \frac{\dot{m}_{Void+DD}}{K_s^{1/2}} = A \cdot \left[\frac{\rho_{AV} (\rho V^2)}{K_s} \right]^{1/2} = A \cdot \left[\frac{\rho_{AV} (\rho V^2)}{\left[\left(x + (1-x)S\right) \cdot \left(x + \frac{(1-x)}{S}\right)\right]} \right]^{1/2} \quad (6.10)$$

The use of Turbine Flowmeter and Void Fraction Detector outputs (6.9) or Drag Disk and Void Fraction Detector outputs (6.10) require the knowledge of the quality and the slip ratio, in order to calculate the factor K_s : therefore three instruments are necessary to get the mass flow.

The formulas (6.8), (6.9) and (6.10) return exactly the same results.

6.2.2 Aya Model

The considerations are the same of section {6.2.1}. Applying the Aya model, there is a different formula for the turbine velocity, as follows:

$$V_T = V_L \frac{\sqrt{\rho_L(1-\alpha)} + S\sqrt{\rho_G\alpha}}{\sqrt{\rho_L(1-\alpha)} + \sqrt{\rho_G\alpha}} \quad (6.11)$$

while the void fraction value and the momentum value are derived by means of the equations (6.1) and (6.3).

An appropriate numeric program addresses the mathematical system in order to get the slip ratio and the liquid velocity. The converging procedure is exactly the same described for the Rouhani model, but the equations are slightly different, as follows:

$$S = \frac{\left(\frac{V_T}{V_L} \cdot (\sqrt{\rho_L(1-\alpha)} + \sqrt{\rho_G\alpha}) - \sqrt{\rho_L(1-\alpha)} \right)}{\sqrt{\rho_G\alpha}} \quad (6.12)$$

$$V_L = \sqrt{\frac{(\rho V^2)}{(\alpha\rho_G S^2 + (1-\alpha)\rho_L)}} \quad (6.13)$$

The quality and the gas velocity are determined according to equation (6.6) and (6.7).

Different to the Rouhani model, any couple of two instruments does not give the exact mass flow rate and the mass flow rate has to be corrected by a thermal-hydraulic factor, K_s , K_{M1} , K_{M3} :

$$\dot{m} = \frac{\dot{m}_{DD+T}}{K_{M1}} = A \cdot \frac{(\rho V^2) / V_T}{K_{M1}} = A \cdot \frac{(\rho V^2) / V_T}{1 - x + xS} \frac{\sqrt{\rho_L(1-\alpha)} + S\sqrt{\rho_G\alpha}}{\sqrt{\rho_L(1-\alpha)} + \sqrt{\rho_G\alpha}} \quad (6.14)$$

$$\dot{m} = \frac{\dot{m}_{Void+T}}{K_s} = A \cdot \frac{(\rho V^2) / V_T}{K_s} = A \cdot \frac{(\rho V^2) / V_T}{\left((x + (1-x)S) \cdot \left(x + \frac{(1-x)}{S} \right) \right)} \quad (6.15)$$

$$\dot{m} = \frac{\dot{m}_{Void+T}}{K_{M3}} = A \cdot \frac{(\rho V^2) / V_T}{K_{M3}} = A \cdot \frac{(\rho V^2) / V_T}{\left(\frac{x + S - xS}{S} \right) \cdot \left(\frac{\sqrt{\rho_L(1-\alpha)} + S\sqrt{\rho_G\alpha}}{\sqrt{\rho_L(1-\alpha)} + \sqrt{\rho_G\alpha}} \right)} \quad (6.16)$$

The formulas (6.14), (6.15) and (6.16) return exactly the same results.

6.2.3 Volumetric model

The considerations are the same of section {6.2.1}. Applying the Volumetric model there is a different expression for the turbine velocity, as follows:

$$V_T = V_L (S\alpha + (1-\alpha)) \quad (6.17)$$

while the void fraction value and the momentum value are derived by means of the equations (6.1) and (6.3).

An appropriate numeric program addresses the mathematical system in order to get the slip ratio and the liquid velocity. The converging procedure is exactly the same described for the Rouhani model, but the equations are slightly different, as follows:

$$S = \frac{\frac{V_T}{V_L} - (1-\alpha)}{\alpha} \quad (6.18)$$

$$V_L = \sqrt{\frac{(\rho V^2)}{(\alpha\rho_G S^2 + (1-\alpha)\rho_L)}} \quad (6.19)$$

The quality and the gas velocity are determined according to equation (6.6) and (6.7).

Different to the Rouhani model, there is no coupling of two instruments that gives the exact mass flow rate, because it shall be corrected by a thermal-hydraulic factor K_s , K_{M2} , K_{M4} :

$$\dot{m} = \frac{\dot{m}_{DD+T}}{K_{M2}} = A \cdot \frac{(\rho V^2) / V_T}{K_{M2}} = A \cdot \frac{(\rho V^2) / V_T}{\frac{(1-x+xS)}{(1-\alpha+\alpha S)}} \quad (6.20)$$

$$\dot{m} = \frac{\dot{m}_{Void+T}}{K_s} = A \cdot \frac{(\rho V^2) / V_T}{K_s} = A \cdot \frac{(\rho V^2) / V_T}{\left((x+(1-x)S) \cdot \left(x + \frac{(1-x)}{S} \right) \right)} \quad (6.21)$$

$$\dot{m} = \frac{\dot{m}_{Void+T}}{K_{M4}} = A \cdot \frac{(\rho V^2) / V_T}{K_{M4}} = A \cdot \frac{(\rho V^2) / V_T}{(x+S(1-x)) \cdot \left(\alpha + \frac{(1-\alpha)}{S} \right)} \quad (6.22)$$

The expressions (6.20), (6.21) and (6.22) return exactly the same results.

6.2.4 Synthesis on three instrument spool piece

Both the theoretical outputs of the different instruments and the pressure values obtained substituting the RELAP5 thermal-hydraulic variables during the transients have been used to test the numerical program and to evaluate the considerations about the use of a complete spool piece, arranged with three instruments. The comparison of the obtained results with the RELAP data shows a full agreement.

Analytically, there is no uncertainty in the assessment of mass flow, quality, slip ratio and velocities by using a Drag Disk, a Turbine Flowmeter and a Void Fraction Detector.

The numerical program presents some problems when the quality is close to zero or negative and when the gas and liquid velocities are opposite. In general, the Aya model gives the most inaccurate results, due to the presence of square roots in the formulas.

The calculation of the thermal-hydraulic factors, K_s , K_{M1} , K_{M2} , K_{M3} , K_{M4} and the numeric procedure shown in the previous section would allow the calculation of the mass flow and quality during the SPES3 break tests, using a complete spool piece.

7 HOMOGENEOUS MODEL

Homogenous two-phase flow is defined a flow in which the two phases are uniformly distributed at any cross section in the pipe with no slip between phases.

$$V_G = V_L \quad (S = 1) \quad (7.1)$$

This hypothesis is not applicable in the SPES3 transients, as indicated in [5], because the slip ratio is extremely far from the unity for each test at any instant.

The instrument outputs have not been simulated with homogenous model, because the analytical results of the devices would be incorrect.

The coupling of two instruments returns theoretically the value of the two-phase mass flow, but the determination of quality, slip ratio, liquid and gas velocity appears to be impossible.

The application of the homogeneous model only gives an approximate view about the other thermal-hydraulic variables, also considering the related error values acceptable.

According to the homogenous model, the Void Fraction Detector formula does not change, because it is not affected by the slip ratio, and it is described by (4.12). The variation of the momentum flux obtained by a Drag Disk and the mixture velocity achieved by a Turbine Flowmeter is pointed out in the formulas as follows:

$$(\rho V^2) = \alpha \rho_G V_G^2 + (1 - \alpha) \rho_L V_L^2 = V_L^2 (\alpha \rho_G + (1 - \alpha) \rho_L) \quad (7.2)$$

$$V_T = \frac{\alpha \rho_G V_G^2 + (1 - \alpha) \rho_L V_L^2}{\alpha \rho_G V_G + (1 - \alpha) \rho_L V_L} = V_L \quad \text{Rouhani model} \quad (7.3)$$

$$V_T = \frac{V_L \sqrt{\rho_L (1 - \alpha)} + V_G \sqrt{\rho_G \alpha}}{\sqrt{\rho_L (1 - \alpha)} + \sqrt{\rho_G \alpha}} = V_L \quad \text{Aya model} \quad (7.4)$$

$$V_T = \alpha V_G + (1 - \alpha) V_L = V_L \quad \text{Volumetric model} \quad (7.5)$$

The three models for the turbine flowmeter collapse into one, in which the turbine velocity is equal to the liquid velocity that is equal to the gas velocity.

The couplings of two instruments to determine the mass flow according to the homogeneous model leads to the following formulas:

Void Fraction Detector + Drag Disk

$$\begin{aligned} \dot{m}_{Void+DD} &= A \cdot [\rho_{AV} \cdot (\rho V^2)]^{1/2} = A \cdot [(\alpha \rho_G + (1-\alpha) \rho_L) \cdot V_L^2 (\alpha \rho_G + (1-\alpha) \rho_L)]^{1/2} = \\ &= A \cdot V_L (\alpha \rho_G + (1-\alpha) \rho_L) \end{aligned} \quad (7.6)$$

Turbine Flowmeter + Drag Disk

$$\dot{m}_{T+DD} = A \cdot \left[\frac{(\rho V^2)}{V_T} \right] = A \cdot \left[\frac{V_L^2 (\alpha \rho_G + (1-\alpha) \rho_L)}{V_L} \right] = A \cdot V_L (\alpha \rho_G + (1-\alpha) \rho_L) \quad (7.7)$$

Void Fraction Detector + Turbine Flowmeter

$$\dot{m}_{Void+T} = A \cdot V_T \cdot \rho_{AV} = A \cdot V_L \cdot (\alpha \rho_G + (1-\alpha) \rho_L) \quad (7.8)$$

The equations (7.6), (7.7) and (7.8) show that there is no difference between the different couplings.

Considering the combination of a Drag Disk and a Turbine Flowmeter, the effective outputs of the instruments can be reproduced by the homogenous expressions in order to get the void fraction:

$$(\rho V^2)_{REAL} = V_L^2 (\alpha \rho_G + (1-\alpha) \rho_L) \quad (7.9)$$

where

- $(\rho V^2)_{REAL}$ is the real output of the Turbine Flowmeter
- α is the void fraction, unknown
- V_L is the liquid velocity, that, according to the homogeneous model, is equal to the gas and turbine velocity
- ρ_G, ρ_L are the liquid and gas density, depending on the pressure, that is known.

and

$$V_T = V_L \quad (7.10)$$

Combining the previous expressions, it is possible to determine the void fraction:

$$(\rho V^2)_{REAL} = V_T^2 (\alpha \rho_G + (1-\alpha) \rho_L) \Rightarrow \alpha = \frac{\rho_L - (\rho V^2)_{REAL} / V_T^2}{(\rho_L - \rho_G)} \quad (7.11)$$

Finally the quality can be calculated, setting $S = 1$ in the equation (6.6), as

$$x = \frac{1}{1 + \frac{1 - \alpha}{\alpha} \frac{\rho_L}{\rho_G}} \quad (7.12)$$

To demonstrate the feasibility of the derivation of the void fraction and quality by the homogenous models, the DVI SPLIT break line, the EBT SPLIT break line and the ADS Stage-I ST line during the DVI test have been considered. The void fraction at any time step and the quality have been calculated using the formulas (7.11) and (7.12) and compared to quality and void fraction extracted by the RELAP5 simulations described in [4] and [5].

7.1 DVI break test

7.1.1 DVI SPLIT break line

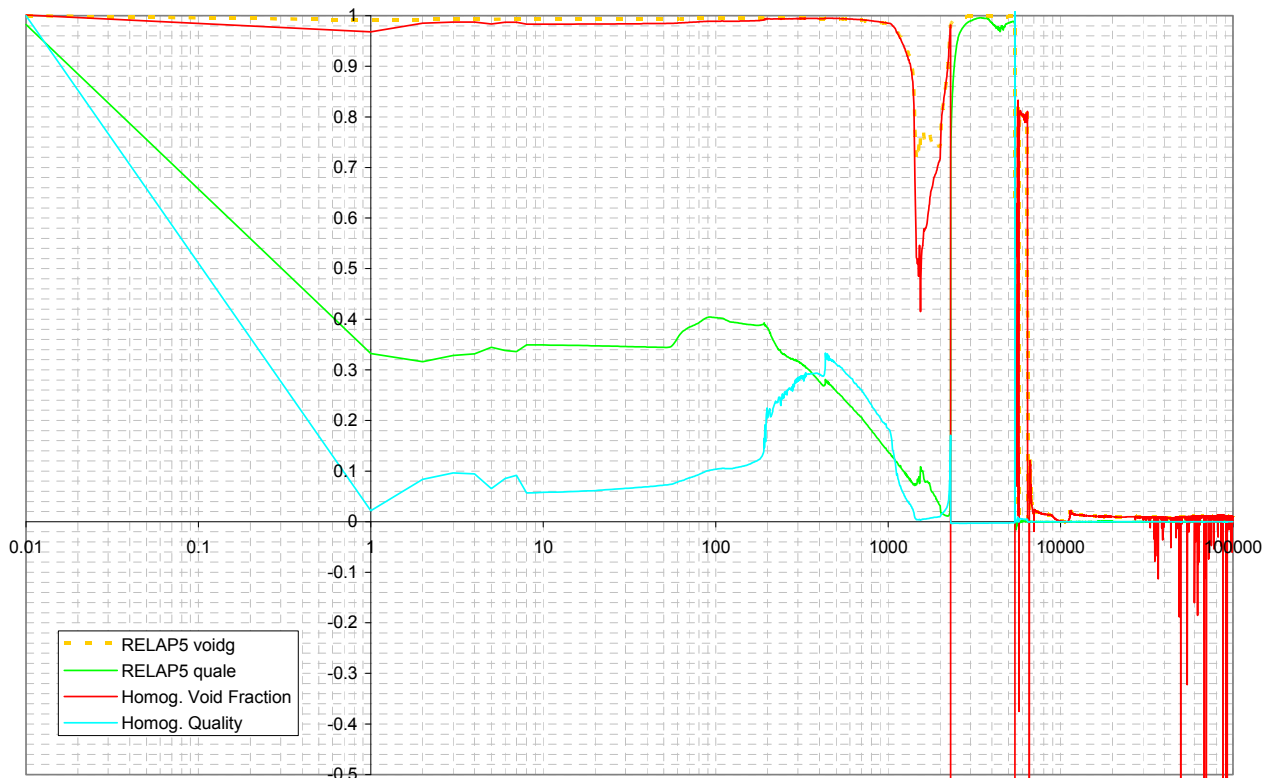


Figure 7.1: Comparison between the RELAP5 quality and void fraction in volume 667030000 versus the quality and void fraction obtained by the homogenous model, DVI SPLIT break line, DVI break test.

The Figure 7.1 shows the difference between the RELAP5 void fraction and quality values and the same quantities derived by the homogenous model. About the void fraction, the two curves are very similar up to 2300 seconds, whereas the quality curves show the same trend but they are quite different. After 2300 seconds, there is no relationship between the two quantities. In particular, the void fraction derived by the homogenous model presents negative results, which are impossible.

7.1.2 ADS Stage-I ST line

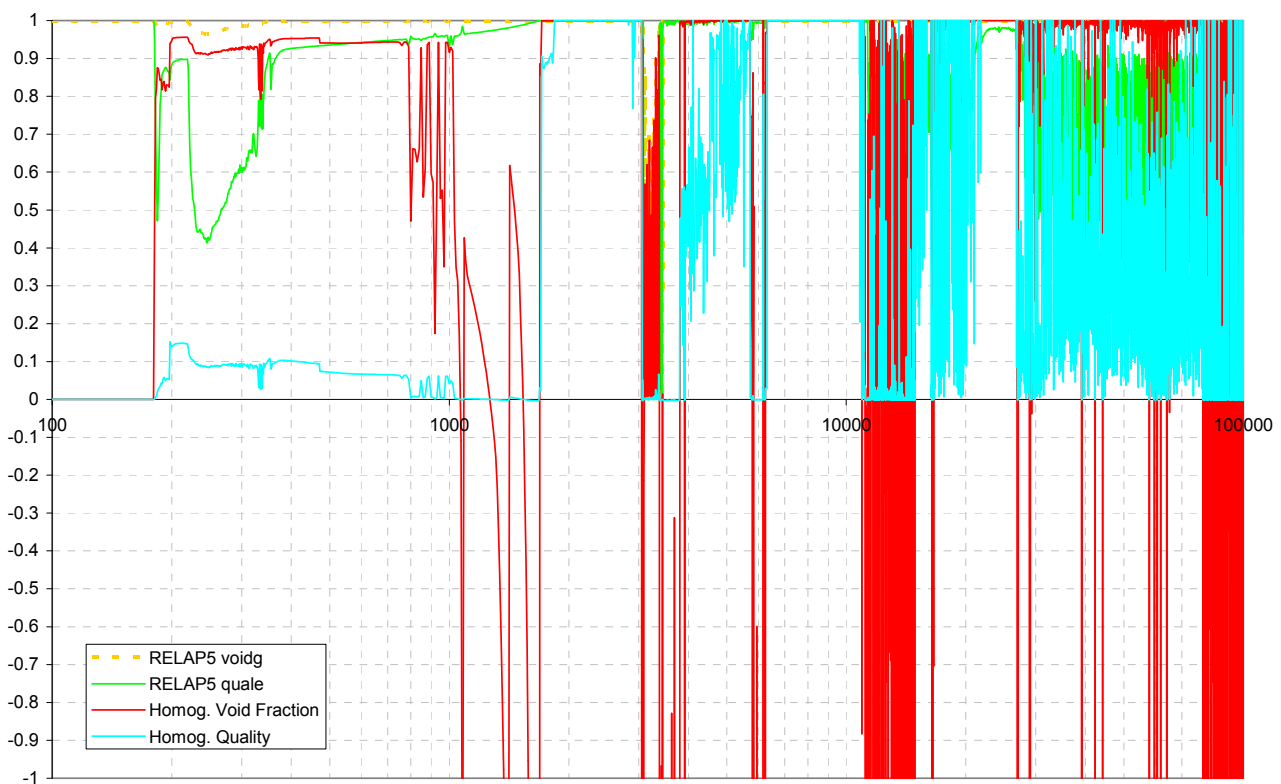


Figure 7.2: Comparison between the RELAP5 quality and void fraction in volume 134010000 versus the quality and void fraction obtained by the homogenous model, ADS Stage-I ST line, DVI break test.

The situation described by Figure 7.2 is very similar to the DVI SPLIT break line. The first 180 seconds are not shown because the ADS Stage-I does not work. Until 1000 seconds there is an acceptable agreement between the void fraction trends, whereas the quality curves are always different. After 1000 seconds there is no relationship between the two quantities.

7.2 EBT break test

7.2.1 EBT SPLIT break line

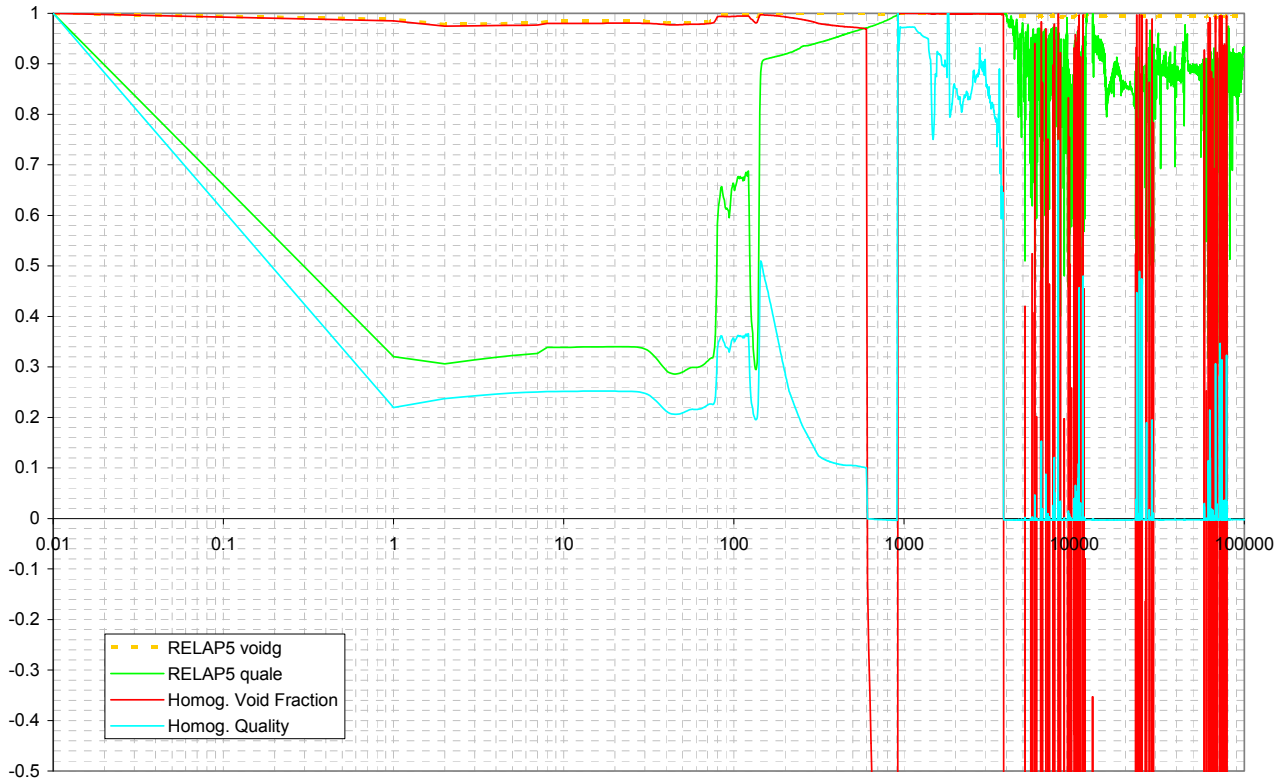


Figure 7.3: Comparison between the RELAP5 quality and void fraction in volume 644030000 versus the quality and void fraction obtained by the homogenous model, EBT SPLIT break line, EBT break test.

As indicated by Figure 7.3, for the EBT SPLIT break line during the EBT break test, the void fraction derived by RELAP5 data and the void fraction calculated using the homogenous model are identical until 600 seconds and the qualities are slightly different, but they follows the same trend. After 1000 seconds there is no relationship and the void fractions assume impossible values.

7.3 Synthesis on the homogeneous model

The Figure 7.1, Figure 7.2 and Figure 7.3 show that the application of the homogeneous model in the determination of void fraction and quality is not possible. In particular, the difference between the RELAP5 quality and the homogenous quality is unacceptable. The other results are not presented because they describe the same situation.

The homogeneous model is not suitable in data reduction application where there are high slip ratios and the fast transient response. Moreover, these conditions do not allow the use of void fraction correlations that link the quality, the pressure and the void fraction without the knowledge of the slip.

8 TWIN VENTURI METER

This section reports the investigation analyses and the results about the possibility to obtain information on void fraction, quality and mixture density upstream and downstream of the break using a coupling of two Venturi meters located upstream and downstream of the break. For generic industrial applications, the Venturi meters are used to determine the single-phase mass flow rate, gas or liquid, returning a pressure signal, as follows

$$\dot{m} = \gamma \cdot A \sqrt{\rho \cdot \Delta P} \quad (8.1)$$

Where

- \dot{m} is the mass flow rate in kg/s
- γ is a coefficient based on the structural parameters and flow regimes
- A is the cross-sectional area of the pipe in m²
- ρ is the density of the fluid in kg/m³
- ΔP is the pressure drop measured by the instrument in Pa

The instrument returns the pressure drop. The absolute pressure and temperature measurements lead to the determination of the density, which permits to have the mass flow.

Table 8.1: List of variables derived by [4] upstream and downstream of the break

Break valve	Upstream	Downstream
Mass flow rate	Void Fraction	Void Fraction
	Quality	Quality
	Liquid Velocity	Liquid Velocity
	Gas Velocity	Gas Velocity
	Pressure	Pressure
	Liquid Density	Liquid Density
	Gas Density	Gas Density
	Flow Regimes	Flow Regimes

This procedure is achievable in single-phase flow, but usually this method cannot be used in two-phase flow, because of the different acceleration of the two phases in the nozzle, the possibility of various flow regimes and the thermal-hydraulic unbalance due to the slip ratio limit the application.

The Venturi meter signal is considered without errors, not affected by flow conditions or problems in calibration, repeatability and accuracy.

The analytical analysis is based on the information derived by the RELAP5 data taken upstream and downstream the break for each line for each transient [4]. The variables necessary for the study are shown in Table 8.1.

The analysis is based on the consideration that the signals of the two Venturi meters can be coupled to develop a relationship between the mixture densities upstream and downstream of the break. It is important to underline that the thermal-hydraulic conditions before the break, at any instant, are different from the conditions after the break, due to the difference of pressure (which is in general higher upstream of the valve).

As the mixture density in two-phase conditions cannot be simply derived by pressure and temperature, , an attempt to obtain such quantity by the outputs of two coupled Venturi meters is done in order to avoid the use of a Void Fraction Detector, based on the following quantities:

- Void Fraction upstream
- Quality upstream
- Mixture density upstream
- Void Fraction downstream
- Quality downstream
- Mixture density downstream

Because the mass flow does not change upstream and downstream the break, the two Venturi meter signals can be combined as follows:

$$\dot{m} = \gamma_{up} \cdot A_{up} \sqrt{\rho_{up} \cdot \Delta P_{up}} \quad \text{Upstream Venturi meter} \quad (8.2)$$

$$\dot{m} = \gamma_{down} \cdot A_{down} \sqrt{\rho_{down} \cdot \Delta P_{down}} \quad \text{Downstream Venturi meter} \quad (8.3)$$

$$\gamma_{up} \cdot A_{up} \sqrt{\rho_{up} \cdot \Delta P_{up}} = \gamma_{down} \cdot A_{down} \sqrt{\rho_{down} \cdot \Delta P_{down}} \quad (8.4)$$

Considering that the instruments return the differential pressure signal indicated as Y_{up} and Y_{down} for the upstream and downstream devices, respectively, they can be expressed as:

$$Y_{up} = \Delta P_{up} = \frac{\dot{m}^2}{(\gamma_{up} \cdot A_{up})^2} \cdot \frac{1}{\rho_{up}} \quad (8.5)$$

$$Y_{down} = \Delta P_{down} = \frac{\dot{m}^2}{(\gamma_{down} \cdot A_{down})^2} \cdot \frac{1}{\rho_{down}} \quad (8.6)$$

The ratio between the upstream and downstream densities can be expressed as:

$$\frac{\rho_{down}}{\rho_{up}} = \frac{Y_{up}}{Y_{down}} \frac{(\gamma_{up} \cdot A_{up})^2}{(\gamma_{down} \cdot A_{down})^2} \quad (8.7)$$

The right hand side of equation (8.7) is theoretically known and the numeric value depends on the geometrical characteristics of the pipes (diameters) and the instrument outputs, so it is possible to determine the ratio between the two densities.

On the basis of the assumption that the thermal-hydraulic variables upstream of the break are related to the downstream ones, a proper numerical program has been developed to derive the downstream void fraction starting from upstream values of pressure, void fraction and slip ratio.

The calculation process is the following: stated a certain value of upstream pressure, set the slip ratio equal to 1, chosen a value for the void fraction, the program allows to obtain quality and enthalpy upstream of the break. Considering an isenthalpic expansion, it is possible to obtain pressure downstream and still assuming $S = 1$, to get quality and void fraction downstream.

The objective is to search for a theoretical correlation between upstream and downstream Venturi DP (values measured during the tests) to get back the mixture density.

The details of the process are described in the followings.

The slip ratio term has been initially set to the unitary value ($S=1$) and later changed by using the actual values derived by RELAP5 data (the assumption to have the liquid velocity equal to the gas velocity is unfeasible in the investigated situations). The upstream pressure (p_{UP}) and the downstream pressure (p_{DOWN}) are chosen on the basis of possible test conditions, then, the liquid and gas densities are calculated. A dummy array for the void fraction is taken:

$$\alpha_{UP} = [0, 0.05, 0.1, \dots, 0.95, 1] \quad (8.8)$$

For each point of the vector, the quality and the mixture density upstream of the break are obtained using the expressions:

$$x_{UP} = \frac{1}{1 + \frac{1 - \alpha_{UP}}{\alpha_{UP}} \frac{\rho_L^{UP}}{\rho_G^{UP}}} \quad (8.9)$$

$$\rho_{UP} = (1 - \alpha_{UP}) \rho_L^{UP} + \alpha_{UP} \cdot \rho_G^{UP} \quad (8.10)$$

Using the quality vector upstream of the break, the enthalpy vector is identified:

$$h_{UP} = h_L^{UP} + x_{UP} \cdot (h_G^{UP} - h_L^{UP}) \quad (8.11)$$

Where

h_{UP} is the enthalpy of the mixture upstream of the break in J/kg

h_L^{UP} is the enthalpy of the liquid phase at upstream pressure p_{UP} in J/kg

h_G^{UP} is the enthalpy of the gas phase at upstream pressure p_{UP} in J/kg

Since the expansion through the valve is isenthalpic, as stated by the RELAP5 data [4], the upstream enthalpy and the downstream enthalpies are equal:

$$h_{UP} = h_{DOWN} \quad (8.12)$$

The downstream enthalpy vector allows the calculation of the quality vector after the break, as

$$x_{DOWN} = \frac{h_{DOWN} - h_L^{DOWN}}{h_G^{DOWN} - h_L^{DOWN}} \quad (8.13)$$

Where

h_{DOWN} is the enthalpy of the mixture downstream of the break in J/kg

h_L^{DOWN} is the enthalpy of the liquid phase at downstream pressure p_{DOWN} in J/kg

h_G^{DOWN} is the enthalpy of the gas phase at downstream pressure p_{DOWN} in J/kg

For each value of the quality vector, the void fraction values can be estimated, as follows

$$\alpha_{DOWN} = \frac{1}{1 + \frac{1 - x_{DOWN}}{x_{DOWN}} \frac{\rho_G^{DOWN}}{\rho_L^{DOWN}}} \quad (8.14)$$

Finally, the mixture density vector downstream of the break is derived by

$$\rho_{DOWN} = (1 - \alpha_{DOWN}) \rho_L^{DOWN} + \alpha_{DOWN} \cdot \rho_G^{DOWN} \quad (8.15)$$

Because the unique signal that can be obtained by the coupling of the two Venturi meters is the ratio of the mixture densities, Eq. (8.7), each vector have been plotted as a function of the ratio between the upstream and downstream density for two different situations, described in

Table 8.2, in order to identify the relationship between the quantities.

Table 8.2: Different case analysed for the determination of the relationships between the density ratio and the other thermal-hydraulic variables

		Pressure [bar]	Liq. Density [kg/m ³]	Gas Density [kg/m ³]	Liq. Enthalpy [J/kg]	Gas. Enthalpy [J/kg]
CASE 1	Upstream	140	617.5284	88.7605	1578593.5	2633025.1
	Downstream	5	914.7753	2.7004	642516.0	2749358.3
CASE 2	Upstream	15	865.8601	7.6849	847897.6	2792665.7
	Downstream	7	901.9661	3.7103	699701.4	2764162.8

Figure 8.1, Figure 8.2, Figure 8.3, Figure 8.4, Figure 8.5 and Figure 8.6 show the upstream and downstream void fraction, quality and mixture density as function of the ratio between the mixture densities, when the pressure before the break is *considerably higher* than the pressure after the break. Instead Figure 8.7, Figure 8.8, Figure 8.9, Figure 8.10, Figure 8.11 and Figure 8.12 show the upstream and downstream void fraction, quality and mixture density as a function of the ratio between the densities, when the pressure before the break is *slightly higher* than the pressure after the break.

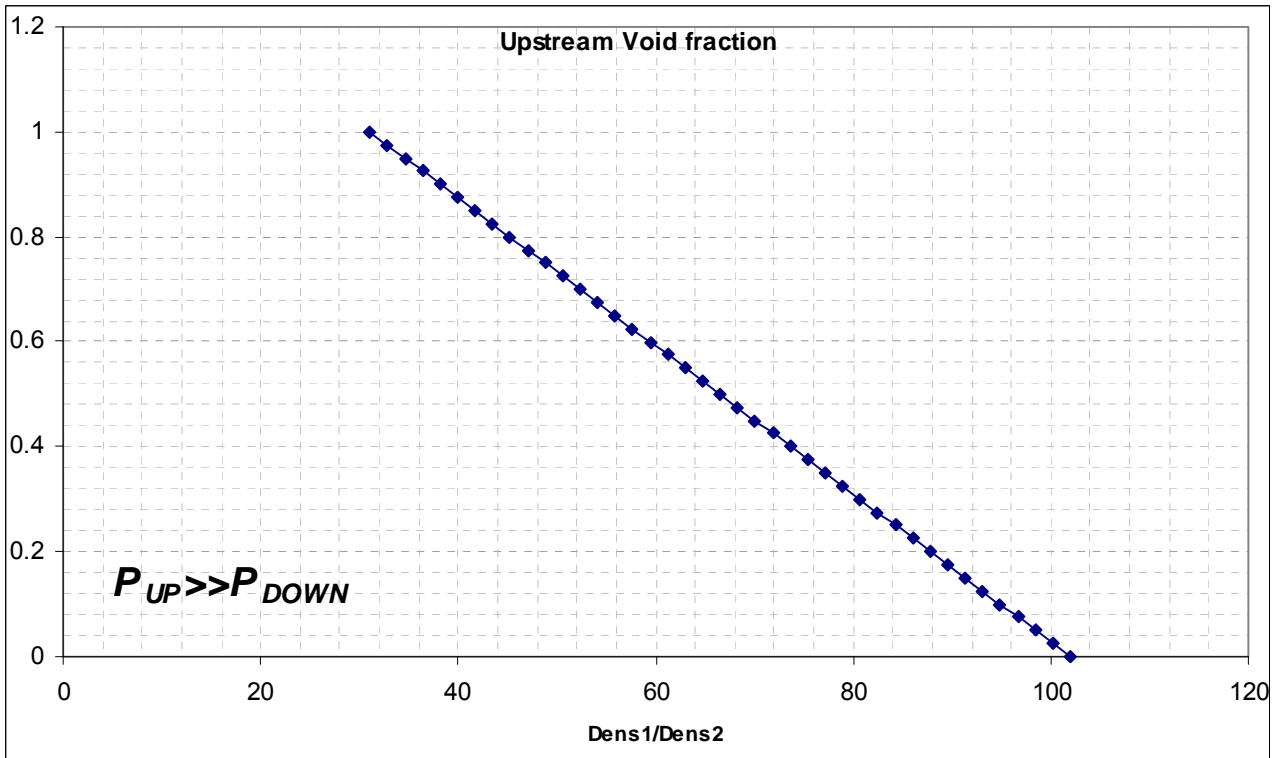


Figure 8.1: Upstream void fraction versus the ratio between the upstream and downstream mixture density in CASE 1.

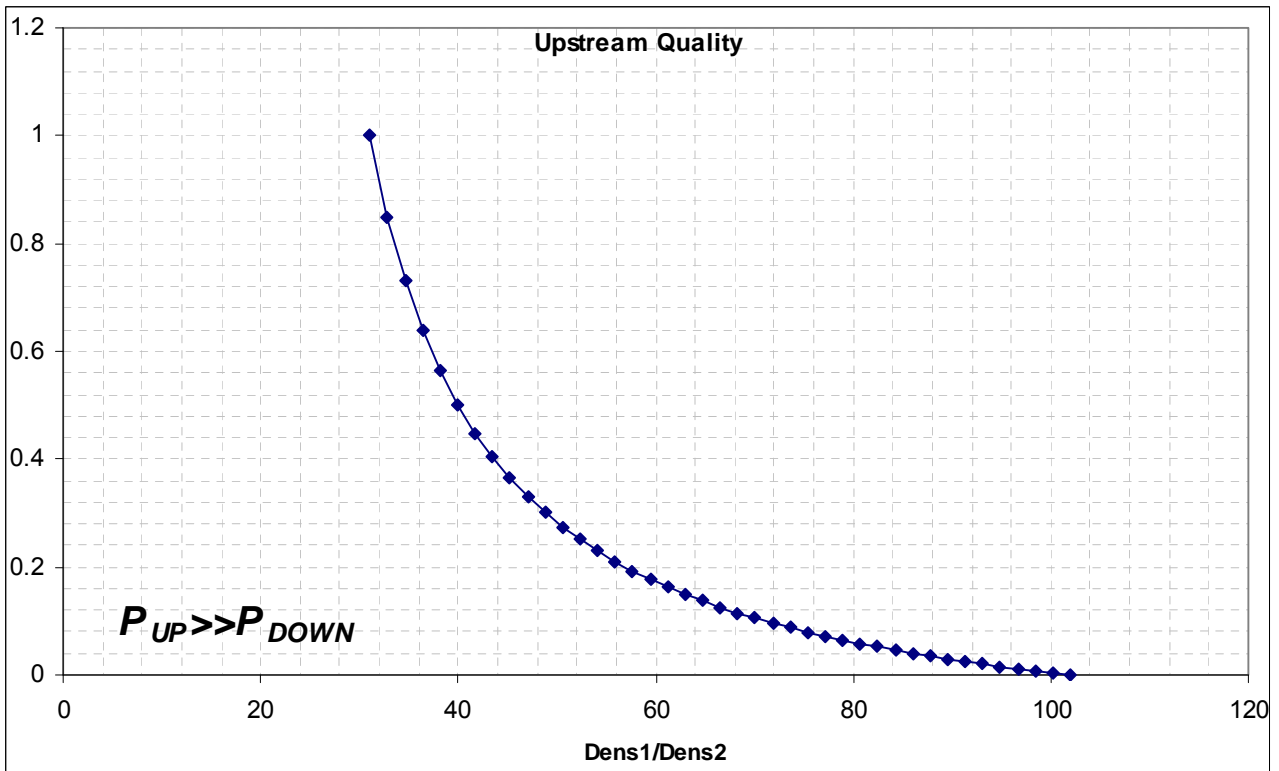


Figure 8.2: Upstream quality versus the ratio between the upstream and downstream mixture density in CASE 1.

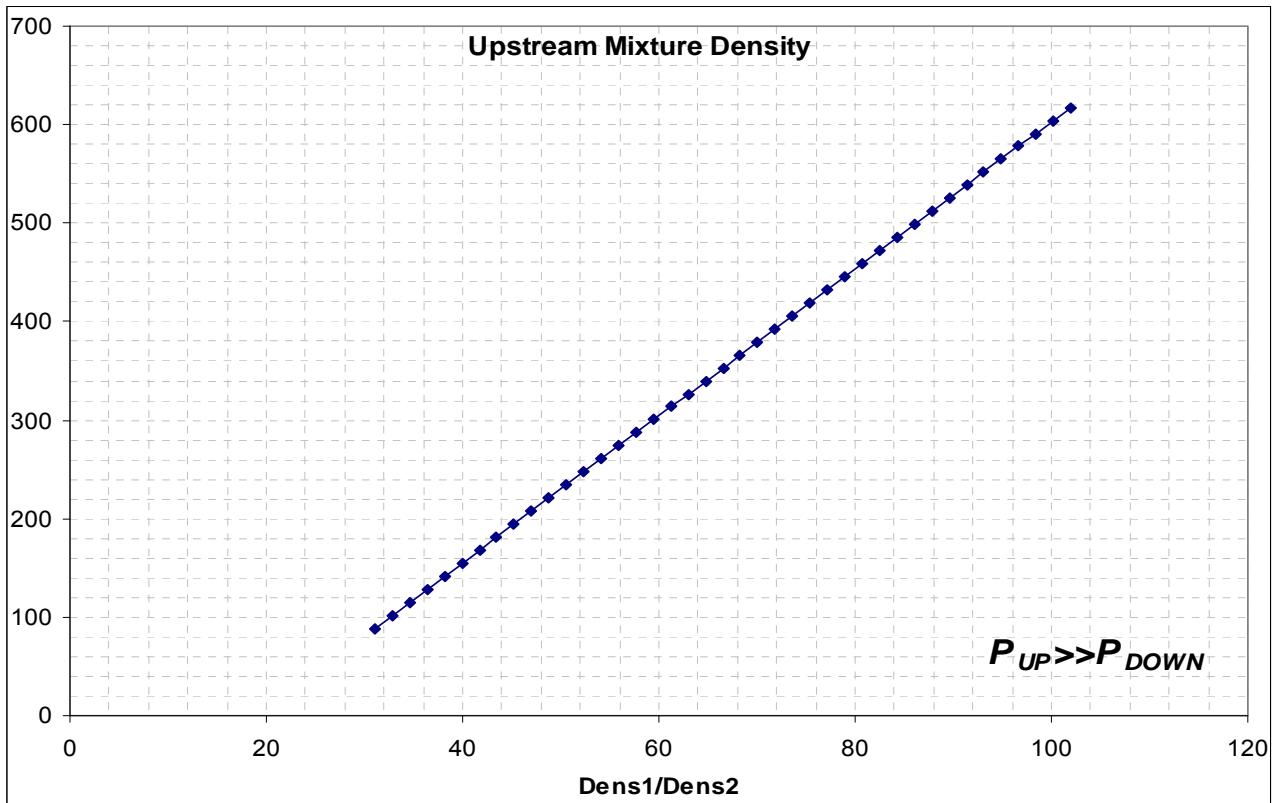


Figure 8.3: Upstream mixture density versus the ratio between the upstream and downstream mixture density in CASE 1.

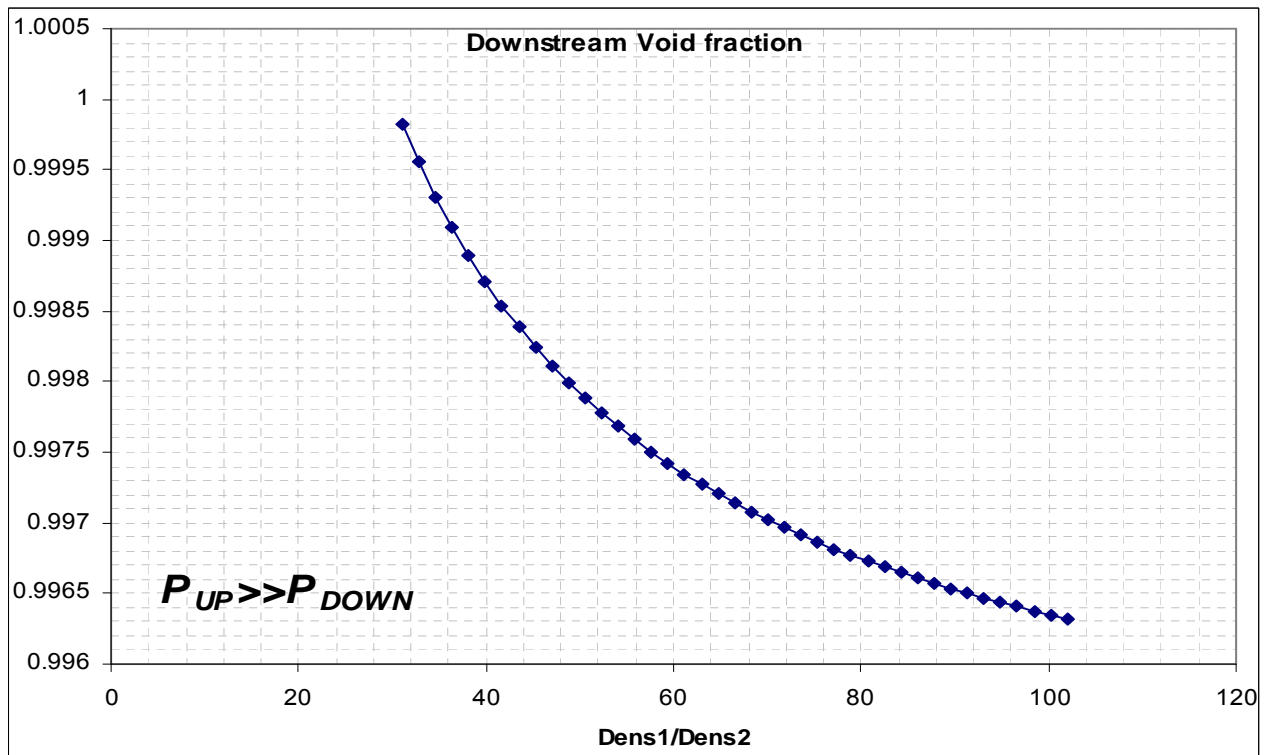


Figure 8.4: Downstream void fraction versus the ratio between the upstream and downstream mixture density in CASE 1.

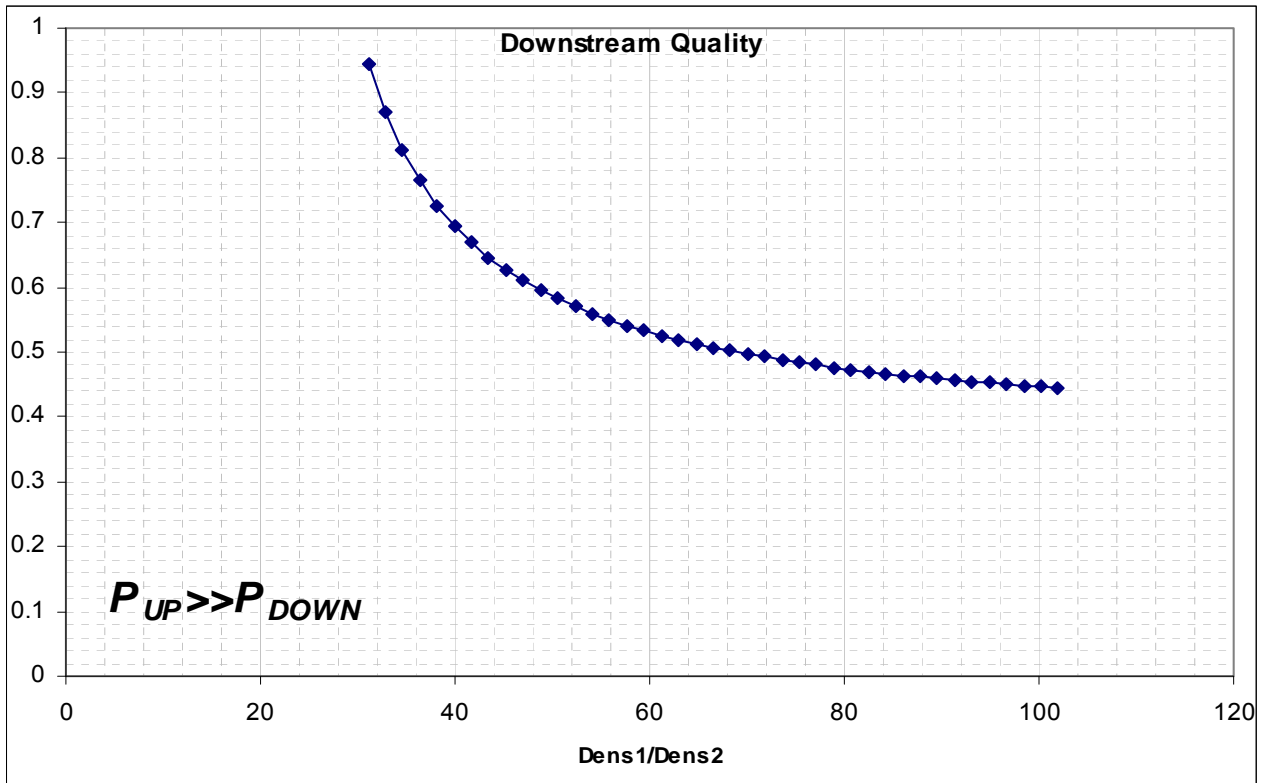


Figure 8.5: Downstream quality versus the ratio between the upstream and downstream mixture density in CASE 1.

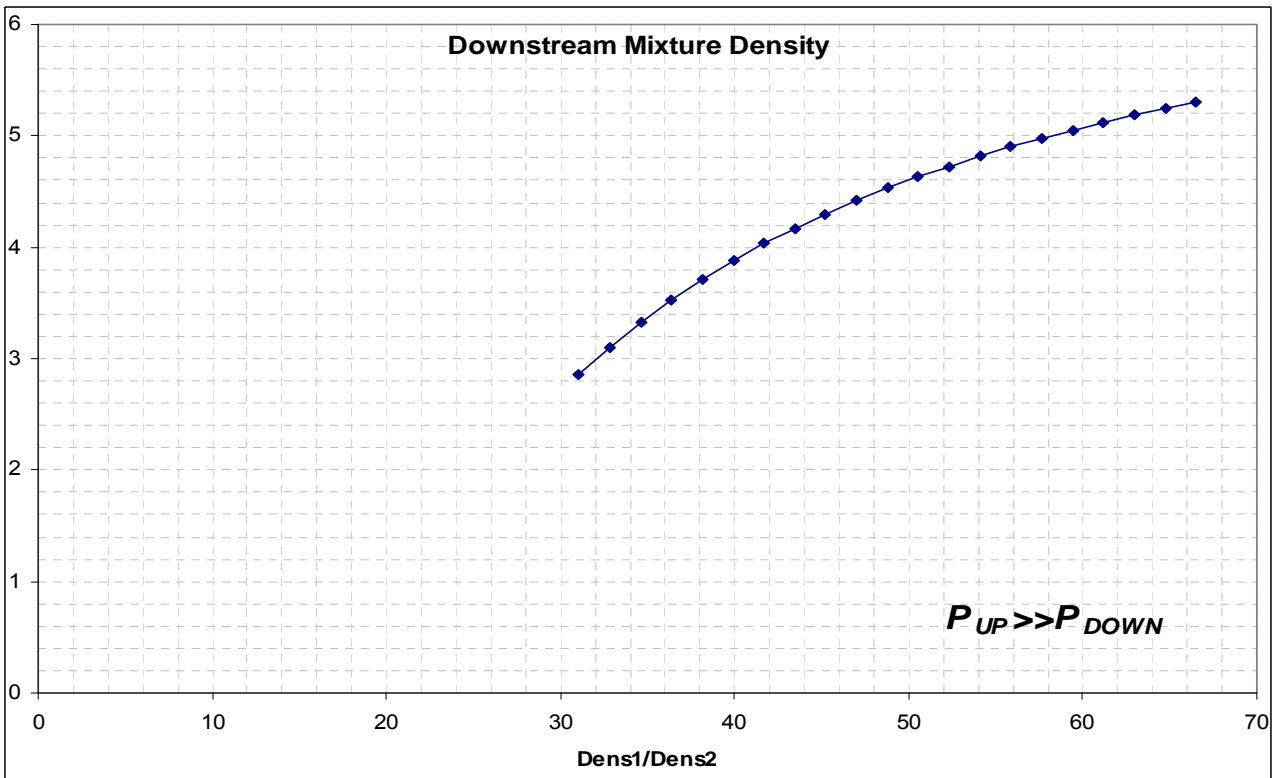


Figure 8.6: Downstream mixture density versus the ratio between the upstream and downstream mixture density in CASE 1.

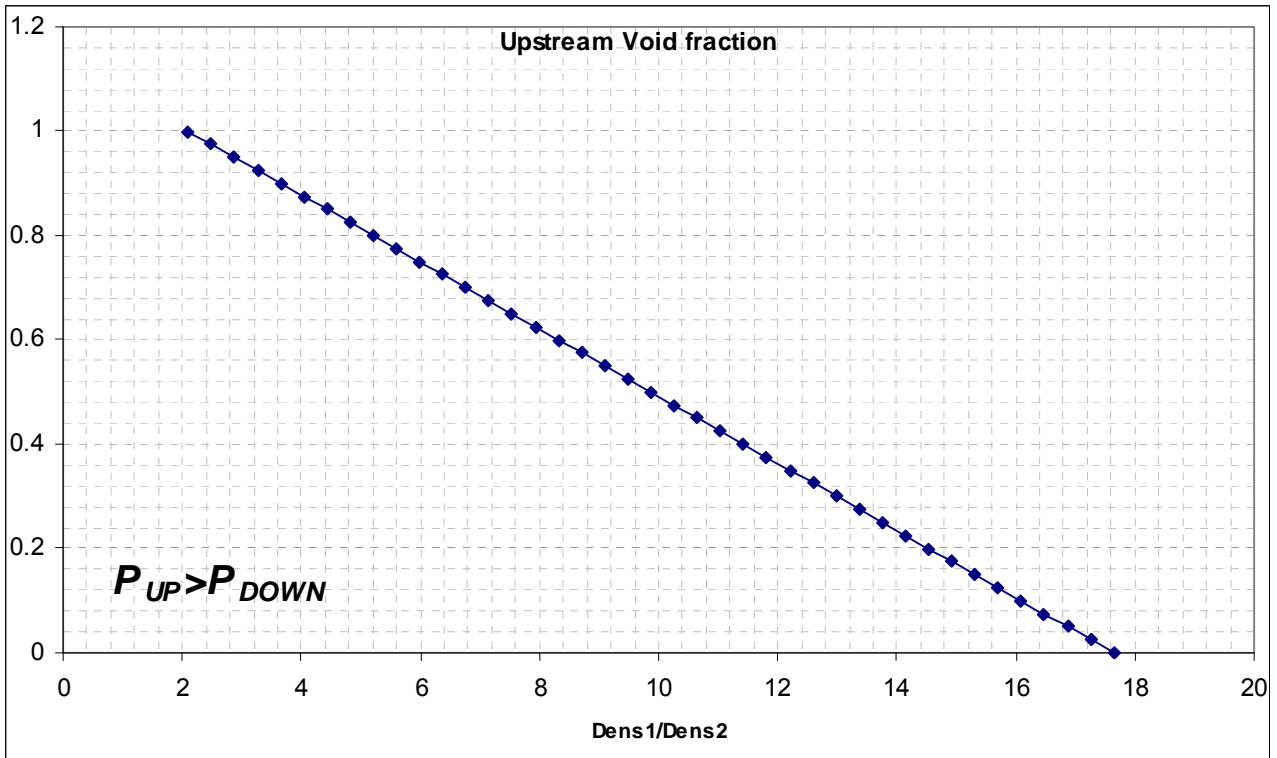


Figure 8.7: Upstream Void Fraction versus the ratio between the upstream and downstream mixture density in CASE 2.

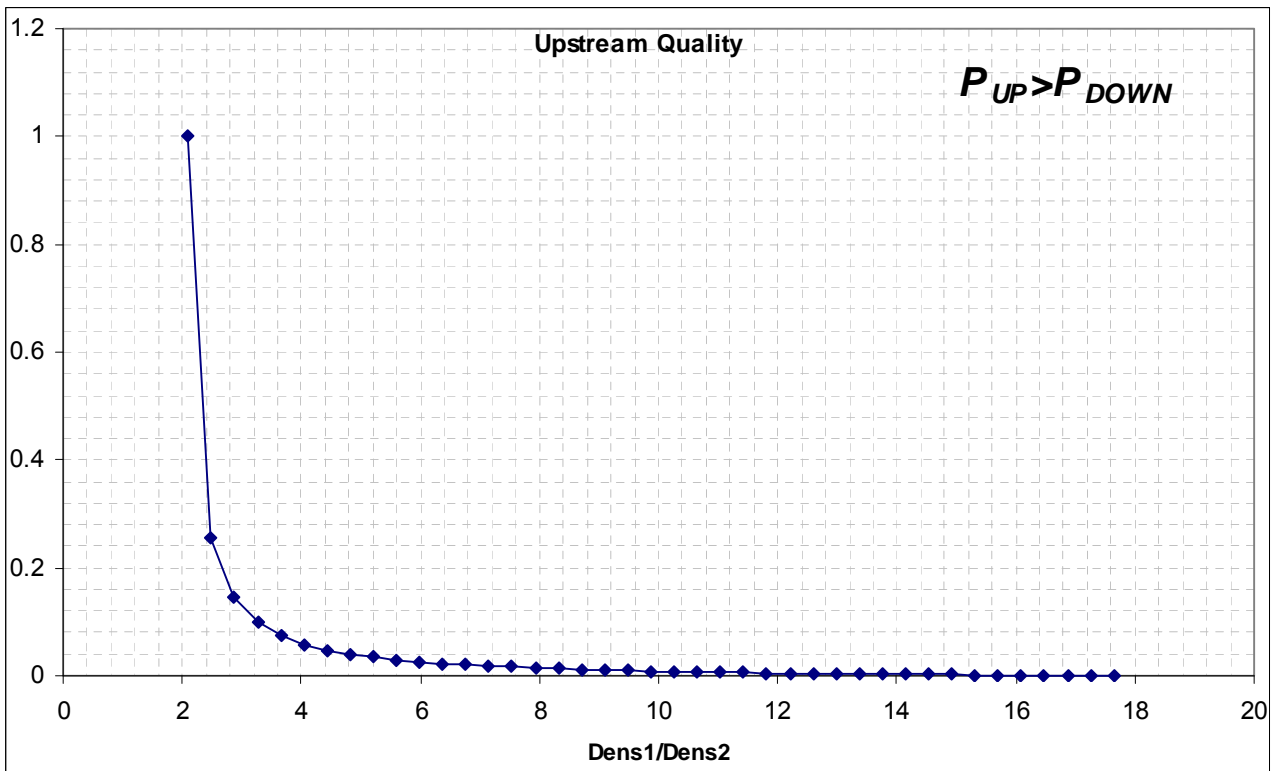


Figure 8.8: Upstream Quality versus the ratio between the upstream and downstream mixture density in CASE 2.

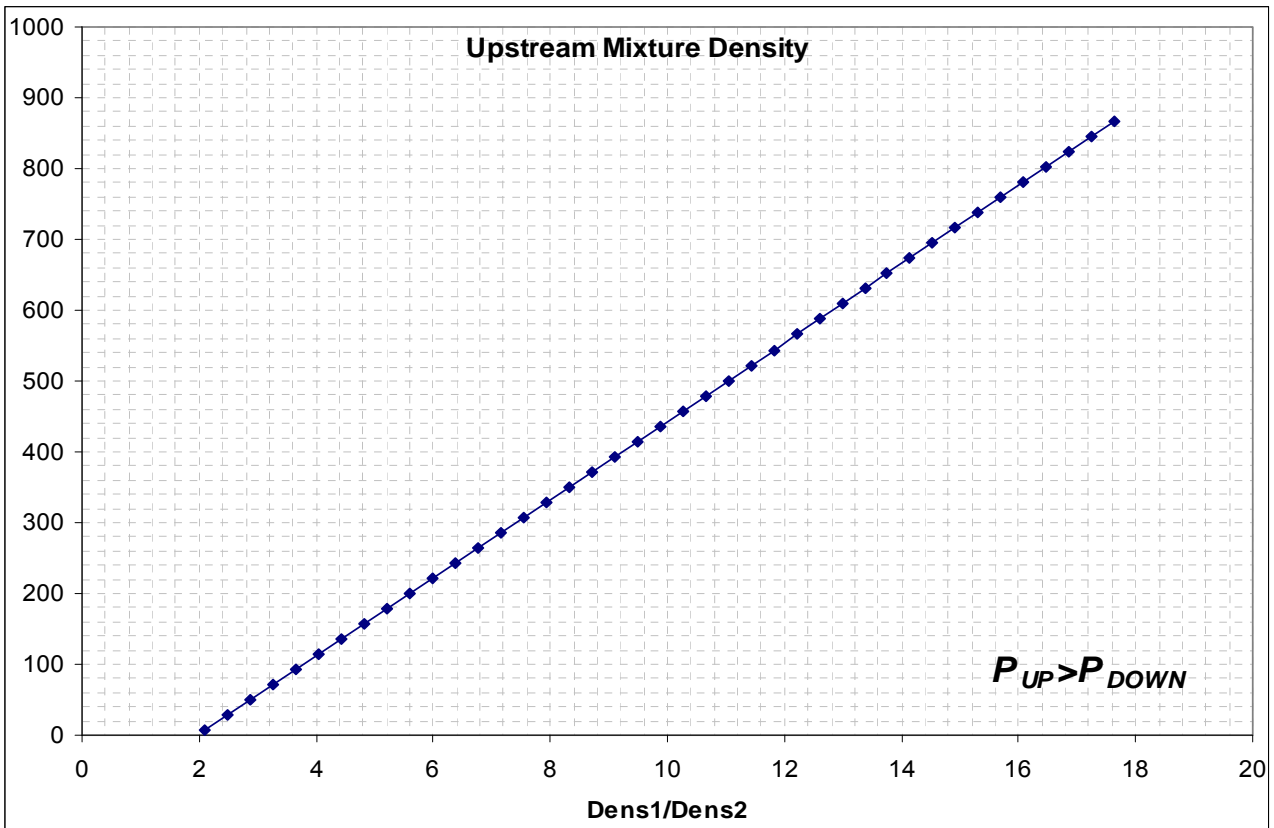


Figure 8.9: Upstream Mixture Density versus the ratio between the upstream and downstream mixture density in CASE 2.

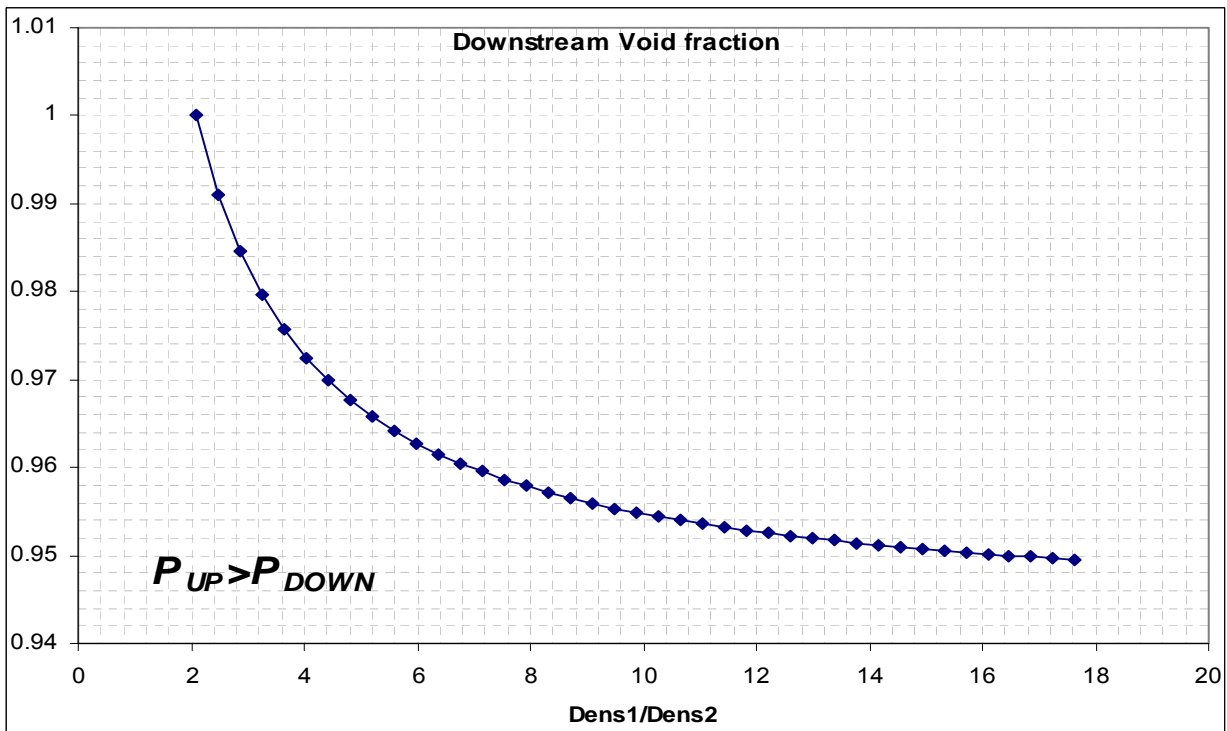


Figure 8.10: Downstream Void Fraction versus the ratio between the upstream and downstream mixture density in CASE 2.

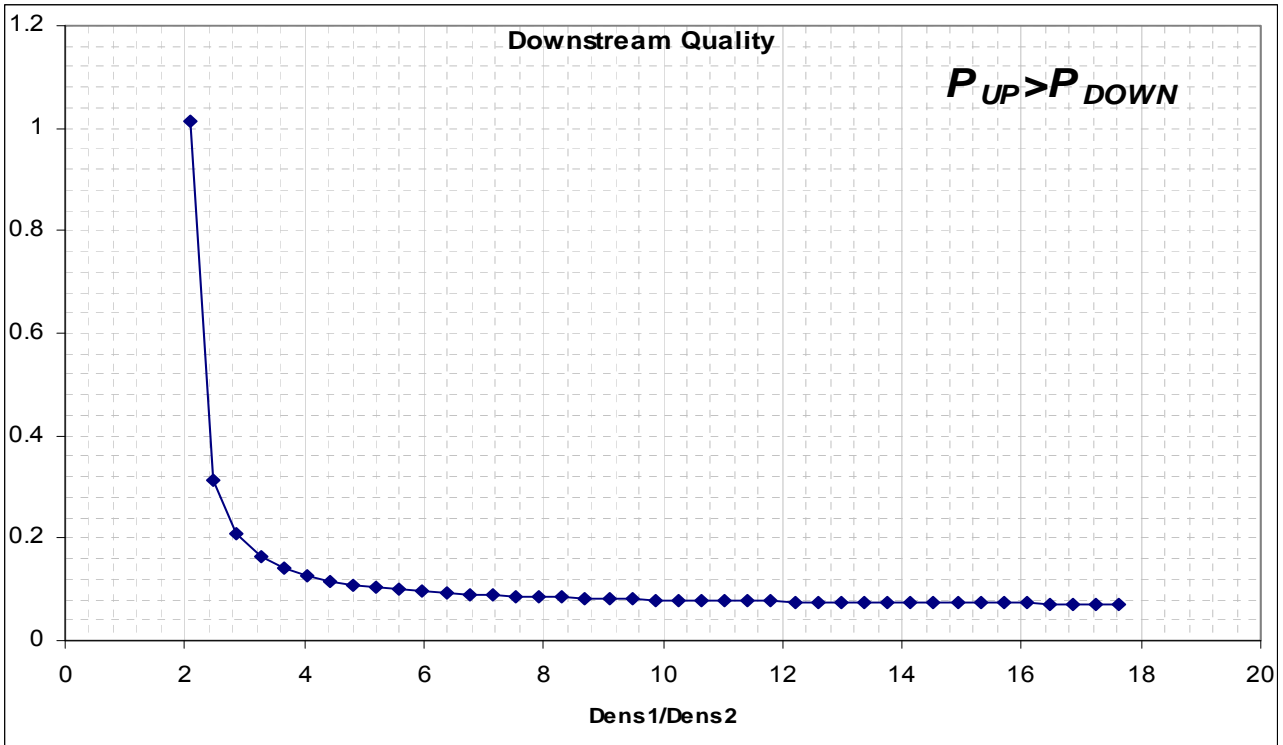


Figure 8.11: Downstream Quality versus the ratio between the upstream and downstream mixture density in CASE 2.

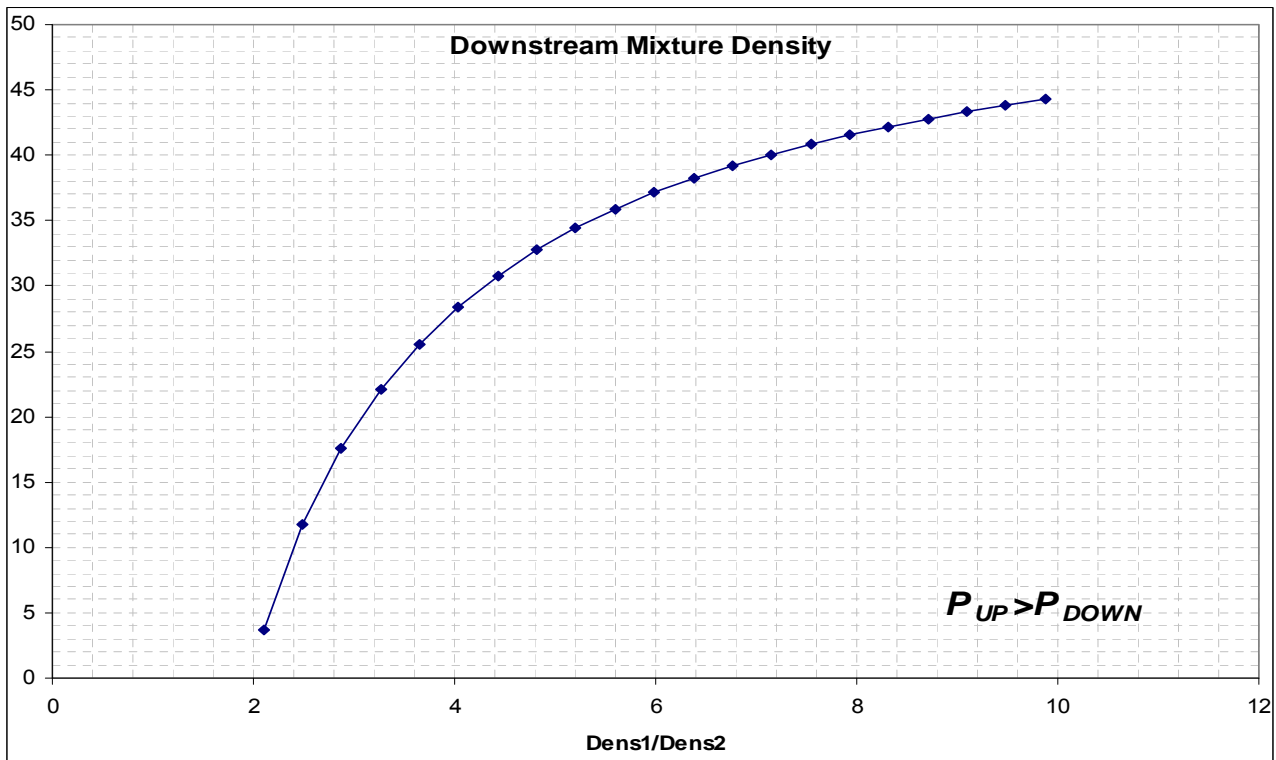


Figure 8.12: Downstream Mixture Density versus the ratio between the upstream and downstream mixture density in CASE 2.

In the two cases, all the figures demonstrate that there is a biunivocal correspondence between the density ratio and each of the involved thermal-hydraulic variables. This consideration should permits to use these relationships to derive the various quantities in the analysed transients.

The previous cases do not consider the situation of upstream pressure lower than downstream pressure, because this condition is practically absent in our transients.

This method has been tested with the RELAP5 data taken from [4]; in particular, for each instant, the upstream and downstream pressures have been extracted in order to find the gas and liquid densities and the gas and liquid enthalpies. Moreover, RELAP5 data have been used to find the ratio between the upstream and downstream mixture densities, in order to simulate the Venturi meter signals. This ratio is called Q .

At any time step, the numeric program creates a dummy vector for the upstream void fraction and derives all the other quantities, as shown above. The various curves, representing the upstream and downstream void fraction, quality and mixture density versus the density ratios, are plotted and interpolated by polynomials of degree 4, as follows:

$$\alpha_{UP} = f\left(\frac{\rho_{UP}(p_{UP})}{\rho_{DOWN}(p_{DOWN})}\right) = a_1 Q^4 + b_1 Q^3 + c_1 Q^2 + d_1 Q + e_1 \quad (8.16)$$

$$x_{UP} = f\left(\frac{\rho_{UP}(p_{UP})}{\rho_{DOWN}(p_{DOWN})}\right) = a_2 Q^4 + b_2 Q^3 + c_2 Q^2 + d_2 Q + e_2 \quad (8.17)$$

$$\rho_{UP} = f\left(\frac{\rho_{UP}(p_{UP})}{\rho_{DOWN}(p_{DOWN})}\right) = a_3 Q^4 + b_3 Q^3 + c_3 Q^2 + d_3 Q + e_3 \quad (8.18)$$

$$\alpha_{DOWN} = f\left(\frac{\rho_{UP}(p_{UP})}{\rho_{DOWN}(p_{DOWN})}\right) = a_4 Q^4 + b_4 Q^3 + c_4 Q^2 + d_4 Q + e_4 \quad (8.19)$$

$$x_{DOWN} = f\left(\frac{\rho_{UP}(p_{UP})}{\rho_{DOWN}(p_{DOWN})}\right) = a_5 Q^4 + b_5 Q^3 + c_5 Q^2 + d_5 Q + e_5 \quad (8.20)$$

$$\rho_{DOWN} = f\left(\frac{\rho_{UP}(p_{UP})}{\rho_{DOWN}(p_{DOWN})}\right) = a_6 Q^4 + b_6 Q^3 + c_6 Q^2 + d_6 Q + e_6 \quad (8.21)$$

The quotient Q , which theoretically simulates the ratio between the outputs of the two Venturi meters, is then substituted into the various polynomials in order to find the downstream quality and the mixture density.

This procedure is not affected by errors if the slip ratio, upstream and downstream of the break, is equal to the unity.

To demonstrate the feasibility of this method and to evaluate the errors deriving from the use of the homogenous model, the program results have been compared to the RELAP5 ones related to the

DVI SPLIT line and the EBT SPLIT line.. The results are shown in Figure 8.14, Figure 8.15, Figure 8.17 and Figure 8.18.

The RELAP5 data derived by [4] provided just the pressure and the mixture density upstream and downstream of the break. Pressures are necessary to determine the gas and liquid densities and the enthalpies, and the mixture densities are essential to simulate the two Venturi meter responses.

For the DVI SPLIT break line, the pressures upstream and downstream of the break and the mass flow rate during the first 3000 seconds of the transient are shown in Figure 8.13. The upstream pressure is higher than the downstream pressure till 2300 seconds and the mass flow diminishes sensibly (< 0.1 kg/s) around 1400 seconds.

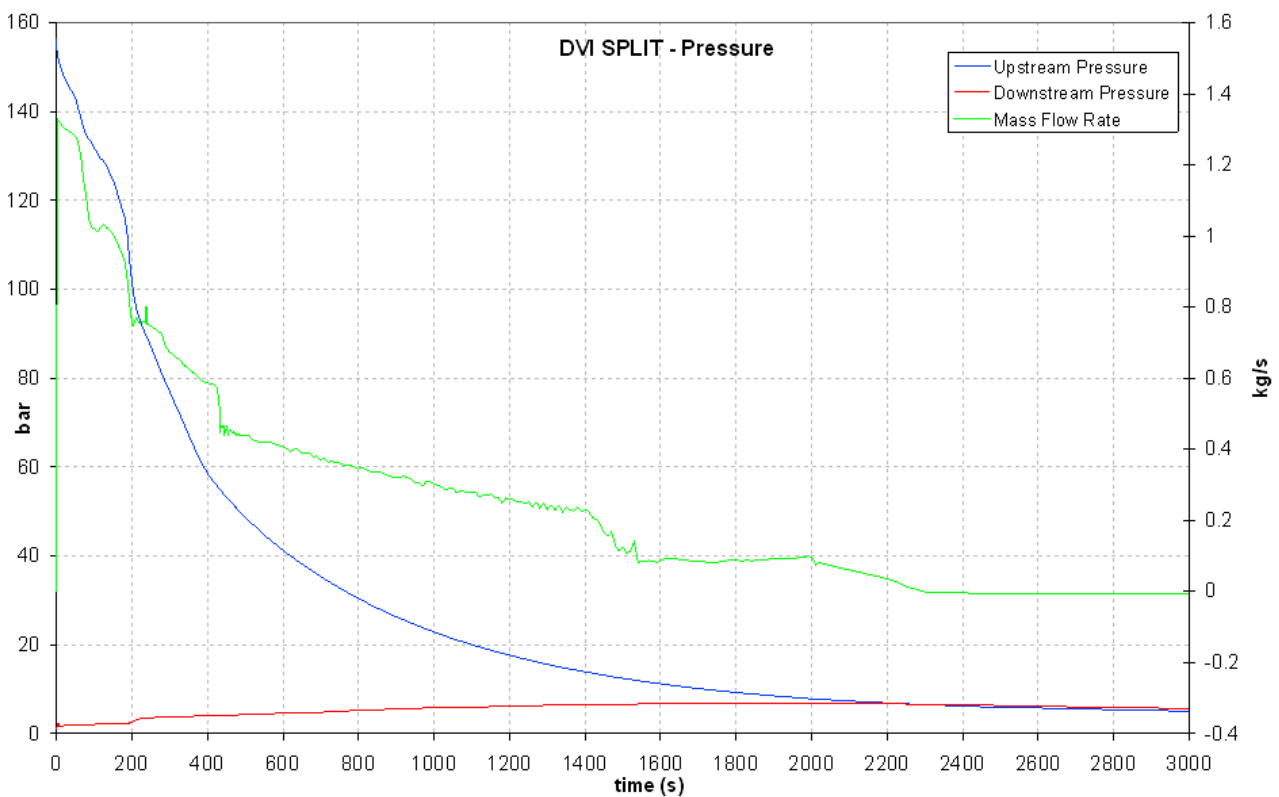


Figure 8.13: Upstream and downstream pressure and mass flow in the DVI SPLIT break line, DVI break test.

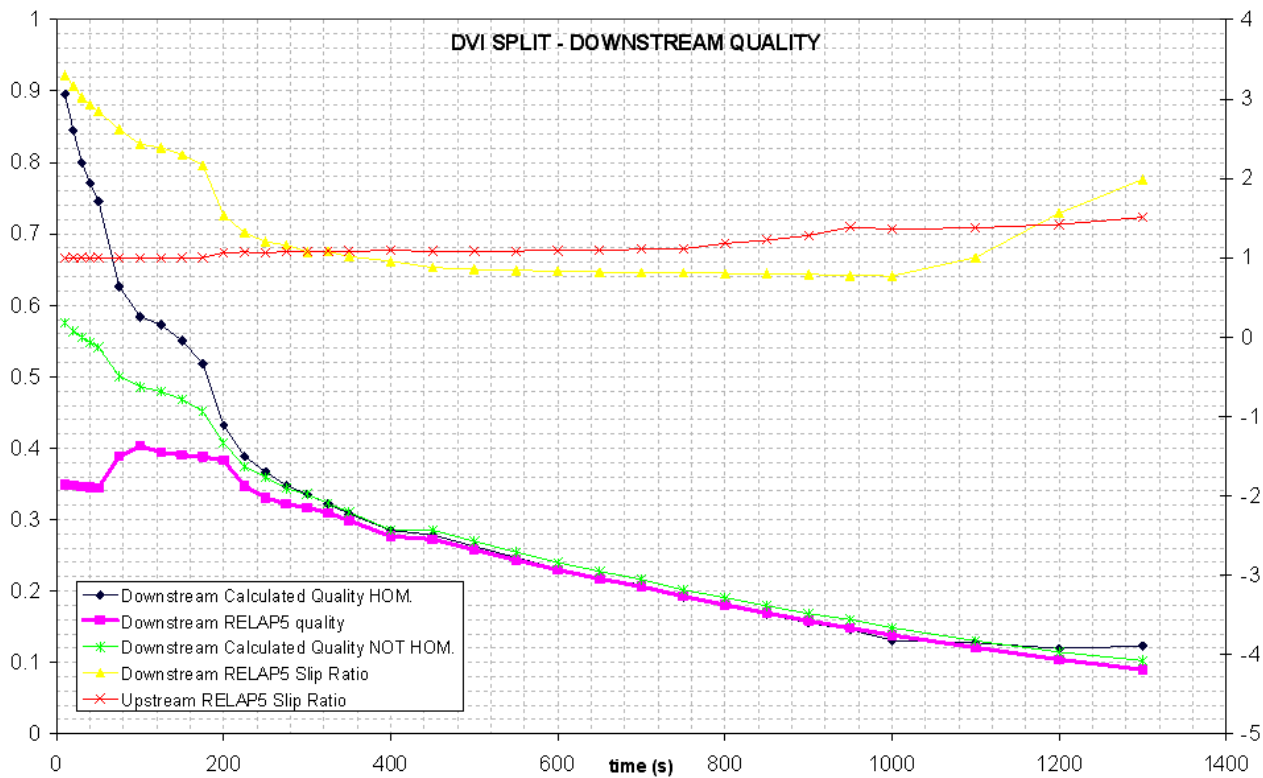


Figure 8.14: Comparison between the RELAP5 quality and the calculated quality downstream of the break during the DVI break test in the DVI SPLIT line.

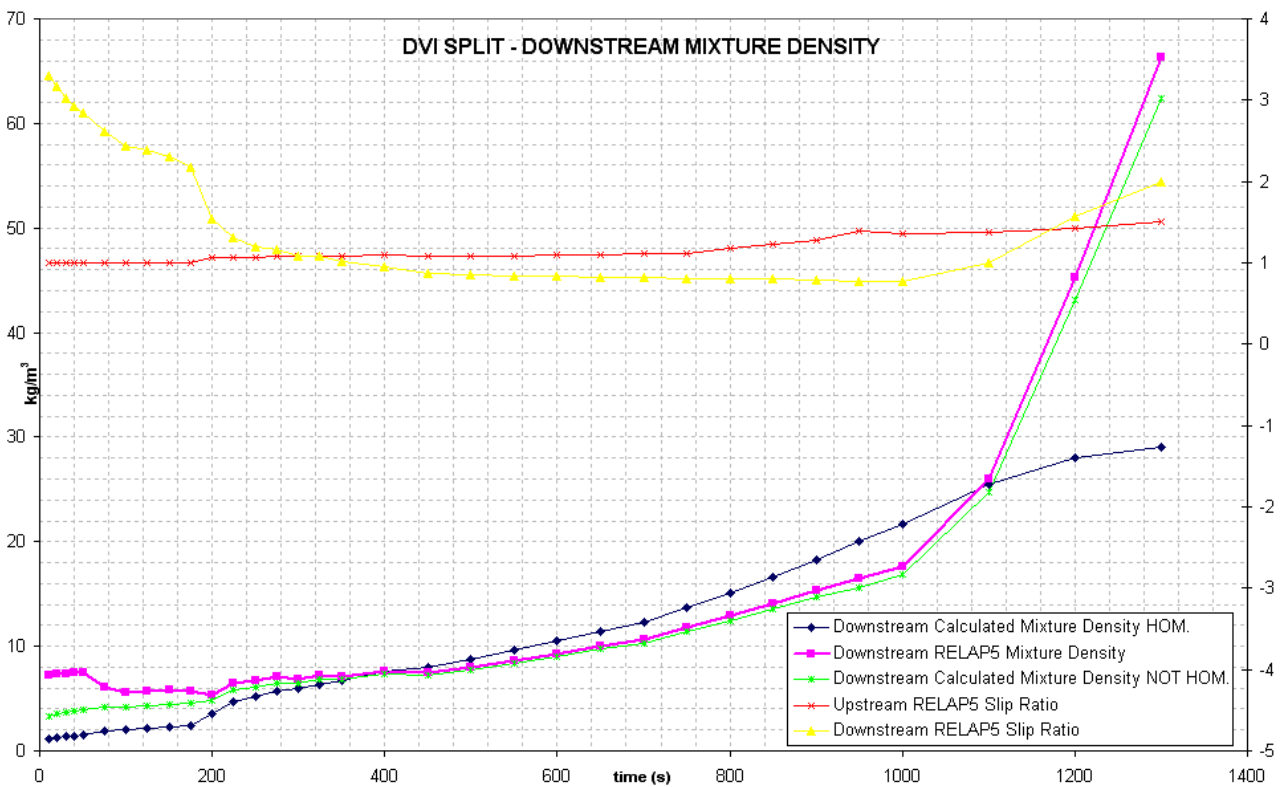


Figure 8.15: Comparison between the RELAP5 quality and the calculated quality downstream of the break during the DVI break test in the DVI SPLIT line.

Figure 8.14 and Figure 8.15 illustrate the outputs of the numeric program for the quality and the mixture density in the case of homogenous model and inhomogenous model for the DVI break test. The homogenous model requires just the use of two Venturi meters, while the lack of information about the slip ratio before and after the break need to be solved with other instrument values to complete the inhomogenous model analytical expressions.

In the present study, the slip ratio values during the transients have been taken by the RELAP5 data [4]. The practice of experimental determination of the slip ratio upstream and downstream of the break is not easily applicable.

The numeric program has been developed also for the inhomogenous model. The physical equations are the same, except for the determination of the upstream quality and the downstream void fraction, in which the slip ratio appears, while for the homogeneous model, they are dependant just on the upstream void fraction and the downstream quality, and pressure.

The formulas (8.9) and (8.14), with the slip ratio, turn into:

$$x_{UP} = \frac{1}{1 + \frac{1 - \alpha_{UP}}{\alpha_{UP}} \frac{\rho_L^{UP}}{\rho_G^{UP}} \frac{1}{S_{UP}}} \quad (8.22)$$

$$\alpha_{DOWN} = \frac{1}{1 + \frac{1 - x_{DOWN}}{x_{DOWN}} \frac{\rho_G^{DOWN}}{\rho_L^{DOWN}} S_{DOWN}} \quad (8.23)$$

The analysis of the plots allows to reveal which model is better for the SPES3 testing campaign. To understand the influence of the slip ratio, its upstream and downstream trends are shown in each graph. The transient is studied up to 1400 seconds because, as shown in [5], after that time the mass flow is very little.

The slip ratio upstream of the break is close the unity value between 200 and 1000 seconds, while it is slightly lower before 200 seconds and it increases after 1000 seconds. The slip ratio downstream of the break is much higher than 1, around 2.5, before 250 seconds, then it decreases slowly towards 1 and around 1100 seconds it starts to increase quickly. The Figure 8.14 shows that the quality is perfectly described by the homogenous model between 200 and 1200 seconds. This fact is due to the closeness of the slip ratios to the unity value. In fact, in this gap, the use of the inhomogenous model, does not improve the results, while, before 200 seconds and after 1200 seconds, when the slip ratios are far from the unity, the homogenous model worse simulates the real values. As regard to the conditions before the break, the slip ratio can be set to unity and the homogenous model can be applied, while, after the break, the knowledge of the slip ratio appears to be necessary. This value can be achieved using at least other two instruments, as described in sections {5} and {6}.

The same considerations can be done for Figure 8.15. The agreement is satisfactory, but the influence of the slip ratio downstream of the break is very important, in particular after 1100 seconds.

In conclusion, for the DVI SPLIT break line, the determination of the mixture density and quality downstream of the valve can be done even using the homogeneous model, because the complications of the use of other instruments are not counterbalanced by the improvement in the results.

This method has been tested also for the EBT SPLIT break line during the EBT transient. The pressures upstream and downstream of the break and the mass flow during the first 3000 seconds are shown in Figure 8.16. The upstream pressure is higher than the downstream pressure up to 1700 seconds and the mass flow rate decreases sensibly (< 0.1 kg/s) around 1500 seconds.

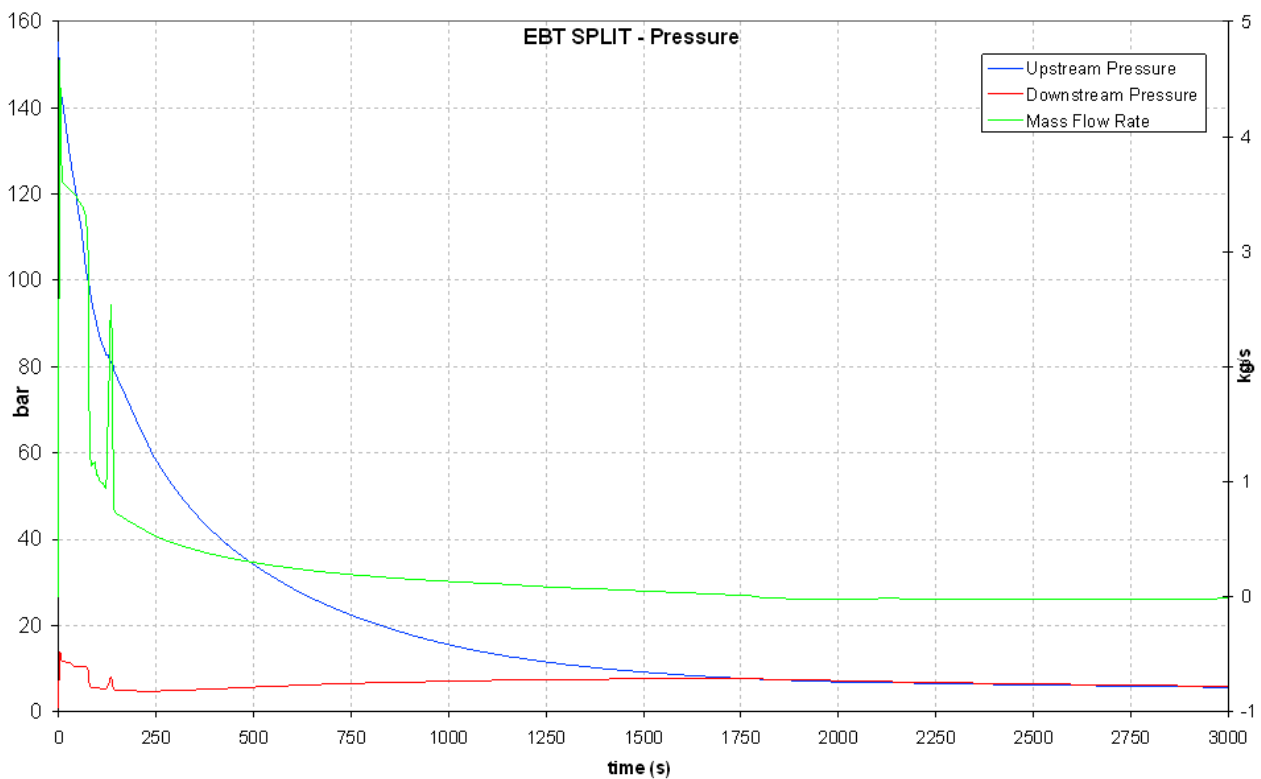


Figure 8.16: Upstream and downstream pressure and mass flow in the EBT SPLIT break line, EBT break test.

The results are shown in Figure 8.17 and Figure 8.18.

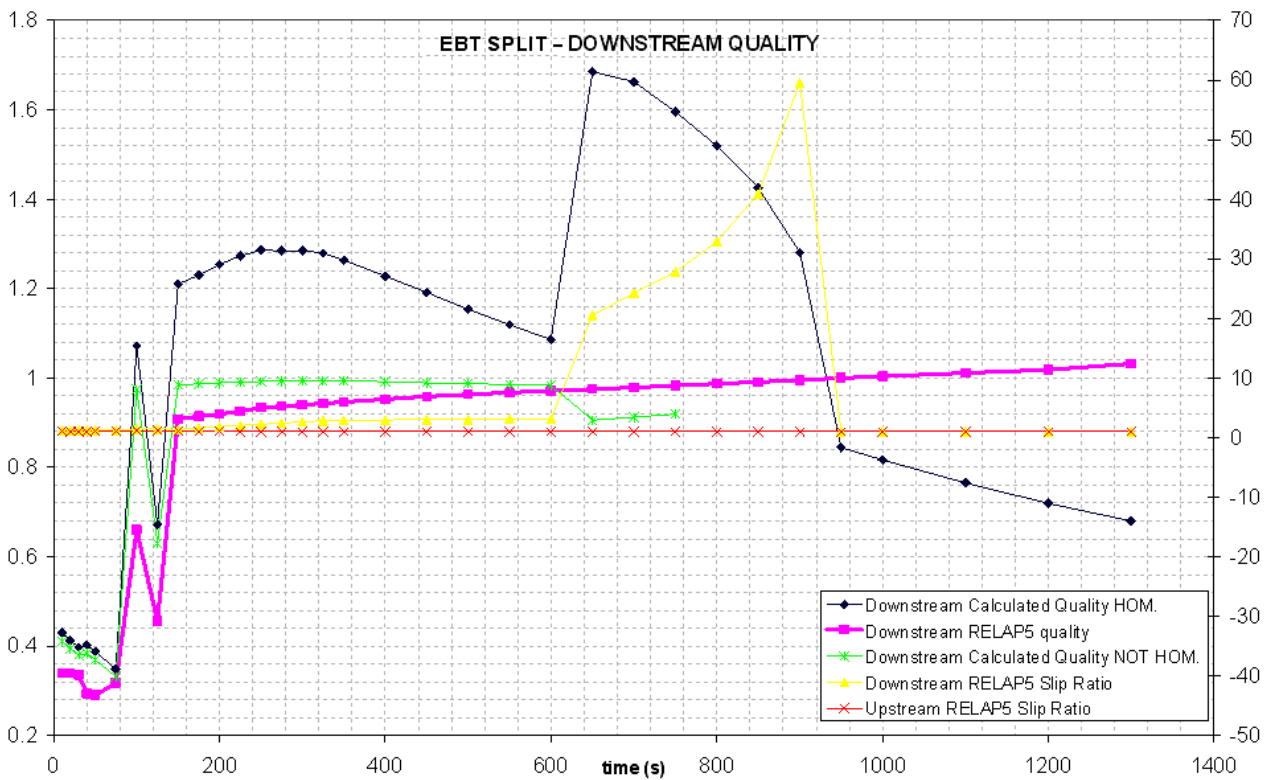


Figure 8.17: Comparison between the RELAP5 quality and the calculated quality downstream of the break during the EBT break test in the EBT SPLIT line.

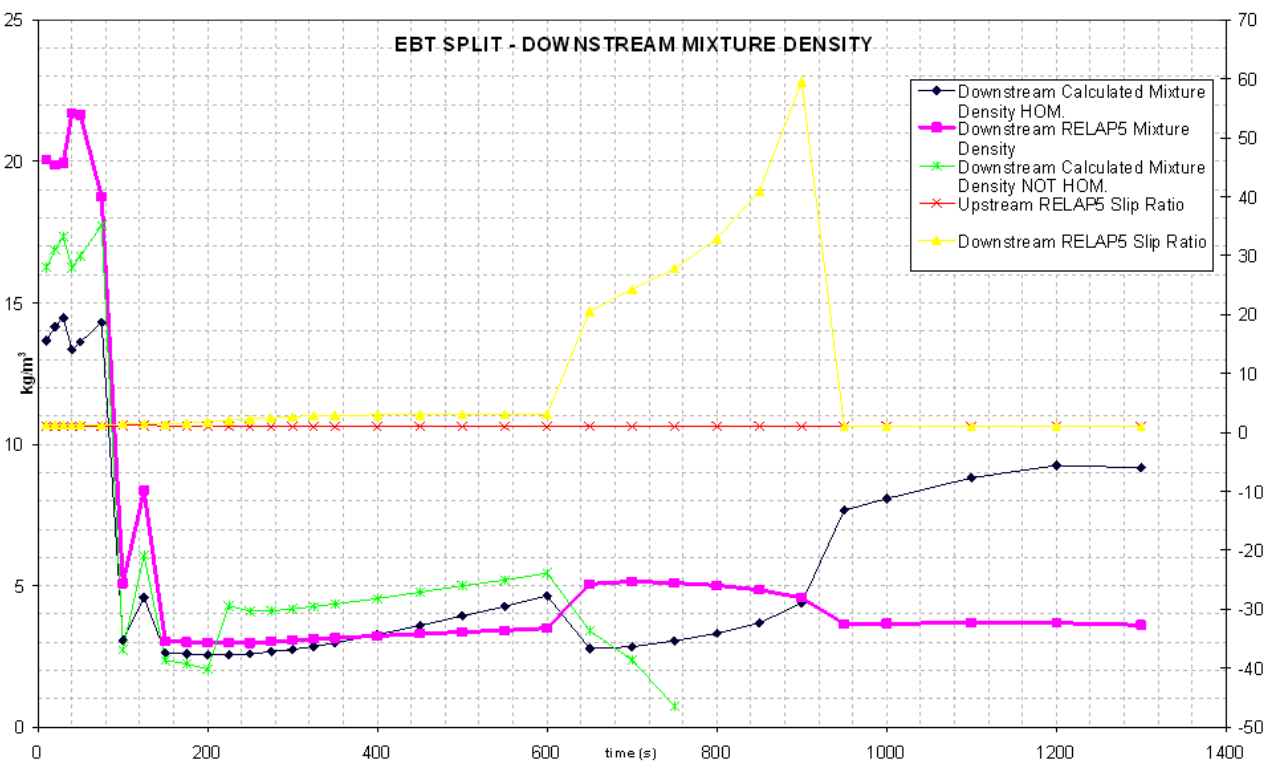


Figure 8.18: Comparison between the RELAP5 quality and the calculated quality downstream of the break during the EBT break test in the EBT SPLIT line.

In the EBT transient the slip ratio calculated before the break is always around one, therefore the homogenous equations can be used, while the slip ratio after the break is around 1.2 up to 600 seconds, then it reaches the value of 60 at 900 seconds, finally it decreases again to 1. For the previous considerations, it is necessary to determine the slip ratio downstream of the break, using other devices.

As shown in [5], the mass flow rate of the EBT SPLIT break line is close to zero after 1000 seconds, therefore the two Venturi meter method has been tested in this range. Figure 8.17 shows the comparison of the quality calculated using the homogenous model, the inhomogenous model and the RELAP5 data. The homogenous model is not useful for this measurement, in particular when the downstream slip ratio is very far from the unity. The inhomogenous model, with the slip ratio values taken by the RELAP5 data, seems to be compatible. The same considerations can be done for Figure 8.18, in which the analytical and numeric mixture density is presented. The agreement is generally better and there is no improvement using the inhomogenous model.

For the EBT transient, the use of this analytical method to derive the downstream quality and mixture density is not suggested. The problems derive by the high values of the void fraction upstream of the break, which, as shown in [5], is always around the unity, unlike the DVI SPLIT break line, where the void fraction is zero up to 200 seconds and reaches the values of 0.994 at 1100 seconds, when the mass flow rate is insignificant. The same situation occurs in the ADS ST (stage I) and ADS DT (stage I) during all the transients and in the ADS SPLIT break line.

In conclusion, the two-Venturi meter method shows limited possibilities of applications (only DVI SPLIT break line) and it does not result a viable instrument for mass flow measurement in the SPES3 testing campaign.

The application of the homogeneous model with two-Venturi meters could be pursued after proper calibration and validation versus experimental data. Anyway, the advantages on the mass flow measures would be lower than the system set-up for data recording.

9 CONCLUSIONS

The theoretical possibility to determine the two-phase mass flow rate at high temperature and high pressure using a spool piece, consisting of a Drag Disk, a Turbine Flowmeter, and a Void Fraction Detector has been investigated in support to the experimental campaign to be executed in the SPES3-IRIS facility.

The data obtained by the SPES3 facility simulation with the RELAP5 thermal-hydraulic code have provided the reference conditions for the analytical analyses.

The theoretical outputs of the instruments, the Turbine Flowmeter, the Drag Disk and the Void Fraction Detector have been combined and simulated by an appropriate numerical program in order to get information about the mass flow, the quality value and the slip ratio in the lines where two-phase conditions are foreseen.

According to literature, the Turbine Flowmeter has been described by three different models for mixture velocity: Rouhani, Aya and volumetric model.

The combinations of two instruments, instead of three, have been investigated in the attempt of simplifying the spool piece and generally it does not return the exact mass flow; the coupling of a Drag Disk and a Turbine Flowmeter provides the most accurate results for the mass flow, in particular applying the Rouhani model. The coupling of a Turbine Flowmeter and a Void Fraction Detector returns unattainable results. There is no way to determine the quality value and the slip ratio by these configurations.

An appropriate numerical program shows that the spool piece consisting of the three instruments returns the exact values of the mass flow, quality and slip ratio, demonstrating the feasibility of the method.

The effectiveness of the homogenous model has also been studied and compared to the other models. It is not applicable for the SPES3-IRIS transients, due to the elevated slip ratio and fast transient responses.

The possibility to obtain information on the two-phase mass flows and the other thermal-hydraulic parameters with two Venturi meters, upstream and downstream of the rupture, has been considered and compared to the other solutions. The method would be applicable in homogeneous conditions, but the presence of high slip ratios and the impossibility to know the velocity of the phases without the other two devices, make this technique impracticable.

A specific test campaign is needed to verify the spool piece performance in the conditions foreseen for SPES3 to obtain all the "calibration coefficients" which have been arbitrarily set in the theoretical study described in this document.

REFERENCES

- [1] G. D. Storricks: IRIS integral system test specification. Westinghouse Electric Company STD-AR-08-01 Rev.1, November 2008.
- [2] SIET document 01 334 RT 07 Rev.1: Conceptual design of SPES3-IRIS facility Rev.1, September 2008
- [3] SIET document 01 423 RT 08 Rev.0: SPES3-IRIS facility nodalization for RELAP5 Mod.3.3 code and steady state qualification, January 2009.
- [4] SIET document 01 489 RT 09 Rev.0: SPES3-IRIS facility RELAP5 base case transient analyses for design support, April 2009.
- [5] SIET document 01 525 ST 09 Rev.0: SPES3 - Two-phase Mass Flow Measurements: Technical Specifications, July 2010.
- [6] Izuo Aya: A Model to Calculate Mass Flowrate and Other Quantities of Two-Phase Flow in a Pipe with a Densitometer, a Drag Disk, and a Turbine Meter. ORNL/TM-4759 November 1975.
- [7] S. Z. Rouhani: Application of the Turbine Type Flowmeters in the Measurements of Steam Quality and Void. Symposium of in-core Instrumentation, Oslo, Norway, June 1974.
- [8] K. G. Turnage, C. E. Davis: Advanced spool piece development. Presented at the 7th Water Reactor Safety Research Information Meeting, Gaithersburg, Maryland, November 1979.
- [9] K. G. Turnage, C. E. Davis: Two-phase flow measurements with advanced instrumented spool piece and local conductivity probes. Presented at Reactor Safety Instrumentation Review Group Meeting, Silver Spring, Md., 25 Jul. 1979
- [10] SIET document: M. Pezzani, O. Vescovi: Misura della portata bifase con spool pieces: calibrazione e qualificazione dell'apparato sperimentale
- [11] N.C.J. Chen, D.K. Felde: Two phase flux uncertainty analysis for thermal-hydraulic test facility instrumented spool pieces. Prepared for the U.S. Nuclear Regulatory Commission, Office of Nuclear Regulatory Research, under interagency agreements DOE 40-551-75 and 40-552-75 ; prepared by the Oak Ridge National Laboratory
- [12] L. Maroti, H.-M Prasser, P. Windberg: Investigation of two-phase flow phenomena at integral test facilities using needle conductivity probes. Lecture (Conference): 8th International Conference on Thermal Engineering and Thermogrammetry, Budapest, 2.-4.6.93 p. 275 - 280
- [13] Huang, Z. Y. et al. (2003): Application of electrical capacitance tomography to the void fraction measurement of two-phase flow. IEEE Trans. Instrum. Meas., 52, pp.7-12.
- [14] V. V. Kontelev, V. I. Melnikov: An Ultrasonic Mesh Sensor For Two-Phase Flow Visualisation. Technical State University of Nishny Novgorod, Russian Federation
- [15] H. Pietruskea, H.-M Prasser: Wire-mesh sensors for high-resolving two-phase flow studies at high pressures and temperatures. Forschungszentrum Rossendorf e.V., Institute of Safety Research, P.O. Box 510119, Dresden, Germany